SIXTH FRAMEWORK PROGRAMME

Project contract no. 043363

ManMade

Diagnosing vulnerability, emergent phenomena and volatility in man-made networks

SPECIFIC TARGETED PROJECT

NEST PATHFINDER

Sub-Priority Tackling Complexity in Science

Work Package 6 – 6.3

A report on a GIS-based method to assess fragility curves for interconnected systems

Revision 1

Due date of delivery: M30

Actual submission date: 3rd of December 2009

Start date of project: 1st of January 2007   Duration: 36 months

Lead authors for this deliverable:

[Karmen Poljansek, Flavio Bono, Eugenio Gutiérrez, JRC]

Project co-funded by the European Commission within the Sixth Framework Programme (2002-2006)		
Dissemination Level		
PU	Public	
PP	Restricted to other programme participants (including the Commission Services)	
RE	Restricted to a group specified by the consortium (including the Commission Services)	X
CO	Confidential, only for members of the consortium (including the Commission Services)	

Table of Contents

List of Figures

List of Tables

1 Summary

The issue of vulnerability of critical infrastructures has attracted considerable attention from both the academic and policy-making spheres. It is rare that the findings in a purely mathematical subject matter (combinatorics and graph theory) spills over into the realm of politics and social policy in — what appears to be— such a short period; however, it is ironic that modern graph theory has its origins in an urban planning problem solved by Euler nearly three-hundred years ago (the Seven Bridges of Köningberg).

The mathematical field of graph theory has, for the major part of the intervening period since its inception, been the subject of much theoretical dissertation; however, over the last decade it has been adopted by the mathematical-physics research community as one of the main mathematical methods in the armoury of, so-called, complex systems analysis.

It is not surprising that, in view of the complex behaviour of modern-day infrastructure systems, many researches considered that the study of the topology of the connections that make up such infrastructures be represented in terms of graphs. It was soon realised that although graph theory had developed a broad range of interesting results for certain classes of graphs, real-world networks were characterised by interconnection topologies that had, hitherto, not been studied or considered. Important steps were taken by extending the concepts of the topology of random graphs proposed by Erdös-Renyi to, so-called, Small-World (Watts and Strogatz) and Scale-Free graphs (Barabassi).

In particular, in view of the similarities by these pseudo-random graphs and the graphs of real-world systems, considerable attention was paid to understanding how these reacted to certain kinds of 'attacks'. By 'attack' we mean the generic elimination of part of the real-networks' constituent elements (which for its corresponding graph are represented by its nodes and connecting edges), which could either the result of an intentional plan, a random process or, as is done here, due to the actions of some natural process (earthquake, storm, ageing, etc).

Research on the nature of attack vulnerability was successfully conducted on many types or real-world networks; however, it was obvious that this was not the whole picture. Real-world networks are interconnected to other critical infrastructures, either by physical, operational or social ties. So, in reality, critical infrastructures are not many but actually only one: that mega-infrastructure that encompasses all our daily activities. Clearly, developing an analysis for this all-enveloping mega-infrastructure is not feasible, but we can take some steps into understanding how, at least, two types

of infrastructure depend on each other, and how their interdependence affects their aggregate vulnerability. More specifically, what we address in this document is how a natural hazard (here an earthquake) not only explicitly generates vulnerabilities in a given network (here the European Electricity transmission grid), but how the vulnerability of another network on which it is partially dependent (here the European Gas Transmission network) induces a second, implicit, vulnerability by virtue of their interconnections.

We study two important issues of modern interdependent critical infrastructure systems: first we assess the network response under seismic hazard; then we analyse the increased vulnerability due to coupling between networks. The probability reliability model we develop here encompasses the spatial distribution of the network structures using a Geographic Information System (GIS) and provides a probabilistic assessment of the damage performance of a network subject to earthquake hazard when coupled to a second network (also vulnerable to earthquake attack). We employ the seismic risk assessment of individual network facilities (based on seismic hazard maps and structural-mechanical fragility curves) and present the result in the form of the *system* fragility curves of the (independent and dependant) network in terms of performance measures.

In order to evaluate the impact of seismic disruption of the coupled networks on the electricity supply to the population, various parameters for measuring network performance are defined; these parameters, based upon topological properties taken from graph theory, are computed for different hazard levels and then visualised on a GIS. We characterize the coupling behaviour among networks as a physical dependency of the electricity grid on the gas network through gas power plants. Dependence of one network on the other is modelled with an interoperability matrix, which is defined in term of the strength of coupling, and with additional mechanical-structural fragility curves of the gas source supply stream.

2 Introduction

Transportation and lifeline utility systems, like water management (waste and potable) energy (oil, natural gas, electric power) and communication systems, are essential infrastructures for society to operate and the economy to function. Here, the elements of infrastructure are facilities regarded as engineering structures, which are physically connected to each other. Thus, infrastructures are spatial structures that happen to extend over large geographical area and often exceed not only within the communities (municipality, county, and region) borders but also across country borders.

As engineering structures, they are vulnerable to natural hazards like earthquake, wind, or flood and manmade hazards derived from unintentional (human error) and intentional (terrorist attacks) causes. If the infrastructure's elements were to undergo significant damage, or even failure, social and economical welfare of society could be jeopardized. In spite of their fundamental importance, most people take them for granted in everyday life. However, at a corporate and governmental level, their importance has triggered worries about their vulnerability to any number and type of malfunctions that could trigger catastrophic operational collapse. Therefore a new term has been adopted for such important structures, critical infrastructure facilities, and consequently the concept of critical infrastructure vulnerability (T.D. O'Rouorke [17]) has increased in importance over the last decade.

Individual critical infrastructure elements are a part of the whole interconnected system. The system functionality changes when one of the components does not work properly, much in the same way as organs in the human body and the consequences of the failure of one facility may spread through the whole system. All of a sudden we are not talking only about the vulnerability of one facility, but also about the vulnerability of the system. Furthermore, it is clear that systems do not work in isolation. On the contrary, they are interdependent with other critical infrastructure systems. What does this mean? The propagation of the failure in one system can spread among systems; therefore such behaviour introduces extra vulnerability into the functioning of each particular system by virtue of its dependence on others.

However, society expects that the infrastructure service will continue with minimal disruptions, even during and after the emergency situation. Such expectations have probably been reinforced by reliable availability of the infrastructure service in the past where small disturbances have been successfully locally absorbed by the system. This perception may be eroded as large-scale accidents (such as electricity blackouts) may become more frequent and the repercussions more complicated.

The most likely triggering factors are probably due to increasing demands combined with constant growth, imposed upon aging processes and equipment, and stressed by unusual environmental and operating conditions. These are probably only the symptoms of the fact that the management of critical infrastructure systems are not completely controllable for any contingency. Compounding this view, as a result of increased international terrorism, the concept of critical infrastructure has become important in terms of national security. Whereas, critical systems have existed for long enough to have been exposed several times to the disruptive potential of natural disasters, new operating conditions under which they work (e.g. deregulation and unbundling) may possibly introduce new vulnerabilities that were not present before: the internationalisation of critical infrastructures may generate new impacts over large geographical areas as a result of one localised failure event. These factors have prompted new studies concerning the vulnerability of critical infrastructures at a continental level.

In this study, critical infrastructure systems are modelled as complex networks presented by the set of vertices (physical assets) connected by edge links amongst each other. The way these connections are formed not only dictates the complexity of the networks behaviour, but also how the vulnerability of each element influences on the vulnerability of the network as a whole. In general, we diagnose three levels of failure propagation. First, where the failure of one element is independent of the failure of the others, but which might impair the functionality of the whole network. The second level of failure propagation is when the failure of one element is dependent on the failure of another element/s in the system. For this purpose, we must consider the network as dynamical system that carries the load flows. The mechanism of load redistribution can be triggered whenever the load exceeds the element capacity due to increasing demand on the network or due to decreasing resistance of the damaged network. The later is recognized as a cascading failure mechanism where cascades represents the time between the successive failures, and which depends on the speed of increasing demand on the still-working elements as well as how much of the capacity has remained in the elements at the first place. Such phenomena have caused the memorable electricity blackouts in Italy, the USA and Canada). The third level of failure propagation considers the interconnection between the systems where the failure propagates through the coupling links between two functionally different infrastructures systems (e.g. gas and electricity transmission). Such dependencies introduce an extra vulnerability of the dependent network due to the failures in the independent network.

Whereas society is becoming more aware of the vulnerabilities of the critical infrastructures, new questions are emerging. The most crucial one is the question of the resilience of the critical

infrastructures; so what is the difference between vulnerability and resilience? In the concept of critical infrastructures explained in [17], vulnerability is a broad measure of susceptibility to suffer loss or damage, whereas resilience is the capacity to withstand loss or damage or to recover from the impact of emergency or disaster. So, the higher the resilience, the less likely damage may occur, and the faster and more effective is the recovery likely to be. Conversely, the higher the vulnerability, the more exposure there is to loss and damage. However, resilience and vulnerability are interactive. Understanding resilience and vulnerability is a key element of effective disaster management (the discipline dealing with risk-avoidance whereby risk is associated to an event with a harmful outcome). Therefore, risk management becomes a necessity when a system failure may cause detrimental consequences.

A systematic method for addressing risk assessment and risk management is, so-called, Probabilistic Risk Analysis (PRA), which concerns the performance of a complex system in order to understand likely outcomes and its areas of importance. PRA has historically been developed for situations in which measured data about the overall reliability of a system are limited and expert knowledge is the next best source of information available. It is valuable because it does not only quantify the probabilities of potential outcomes and losses, but it also delivers reproducible and objective results. There are many obstacles for the implementation PRA. One of the main reasons is lack of input data. It is also a very expensive method because it is time-consuming and computationally demanding; it is very difficult to formulate the problem and the interpretation of the results is not trivial.

Infrastructure systems are of large scale, complex and geographically distributed, so it is not surprising that, lately, the use of GIS for the integration and manipulation of all available data has become more popular. Moreover, GIS plays a double role: in the first instance GIS software is a vital tool for encompassing the spatial characteristics of infrastructure systems; and as such, it provides the topology of the network accompanied by additional information that, once parsed into a graph, can be analyzed with graph-theoretic methods. Finally, having numerically processed the graphs, GIS can again be used for the effective visualization of results of the analysis in terms of various forms of mapping that allow users to examine spatial characteristics.

The services provided or carried by critical infrastructure are in great demand, and their demands are constantly increasing. We are confronted with evolving systems whose constant growth increases their complexity and consequently reduces the mathematical tractability of the dynamical processes they carry or generate. This complexity motivates the need to develop and use techniques

from complex systems analysis in order to, first understand, and then enhance such systems' operability.

If we turn our attention to the hazards to which these infrastructures are exposed to, a widely-used method to assess the vulnerability of individual assets to a given type of hazard is the use of, so-called, fragility curves. Fragility curves are used in tandem with probabilistic numerical approaches such as Monte Carlo simulations; this combination of methods —which is the basis of our method here—was, for example, applied for the assessment of seismic vulnerability recently by [2], [21] and [24].

Descriptions of how the manner and magnitude of interdependency among different infrastructure can potentially affect network performance, have been thoroughly defined by Rinaldi [21].Whereas Dueñas Osorio et al. [8] extended the specific case of seismic vulnerability to include interdependency of the electricity and water distribution networks. The main source of the input data in [8] was based on the HAZUS approach. HAZUS-MH [11] is a risk assessment methodology for analyzing potential losses from floods, hurricane and earthquakes distributed by FEMA. HAZUS couples scientific and engineering knowledge with geographic information systems (GIS) technology to produce estimates of hazard-related damage before, or after, a disaster occurs. However, HAZUS was proposed and has continued with its development for application in the United States. Because the HAZUS data sets are, in most cases, geographically dependent; it is evident that we are bound to encounter difficulties when applying the same strategy to Europe; in particular the unavailability of certain hazard maps of different natural hazards and the vulnerability under particular hazards of facilities which are designed for USA standards. The probabilistic approach requires two types of extensive databases: fragility curves grouped by structural class and geographic hazard distributions. Bearing in mind that at the European level there has been little effort to compile and collate these two key components, it is at present not feasible to run similar analysis at a European level comparable to that performed for the USA.

2.1 Research goal and objectives

A key question is how to calculate the impact of natural hazards on interdependent critical infrastructure systems. A natural hazard is a type of unintentional attack with a known occurrence potential that directly affects a given network's assets (e.g. structural damage), whereas interdependency introduces mew modes of failure propagation through which a hazard can cause indirect damage to the functionality of a system that perhaps has not been damaged directly by the

hazard. So our approach is to first assess the potential physical damage to individual network assets and then examine how the topological connectivity is eroded as a result of losing said assets from the primary network and the impact of disconnection of structurally damaged assets from a depending network (whereas the system failure analysis pertinent to cascading failures, for example, has not been considered). However, we do employ PRA in order to assess the topological vulnerability of the combined (interconnected) systems but do not examine the problems of long-term maintenance and planning. However, the results of our analysis should have a perspective of its application in further risk management procedures.

The objectives to are thus:

- Employment of the GIS tool into probability risk analysis of critical infrastructure system.

- Development of probabilistic reliability model to understand the sensitivity of interconnected networks to seismic hazards.

2.2 The outline of the report

The report is divided into three main parts. The first part (Chapter 3) describes the assembly of GIS information to compile the interconnected graph of the European electricity and gas network. The second part (Chapters 4, 5, 6 and 7) deals with the mathematical formulation of the probabilistic reliability model, the seismic response of the networks and their interdependency behaviour (where we also explain the probabilistic background of all input data and the definition of network performance measures). Finally, in the third part (Chapter 8) we present the results of the PRA of our case study: the European Interconnected Gas and Electricity Transmission systems from two perspectives of global measures of network fragility and their geographical distribution.

3 Assembly of GIS information

This chapter describes the GIS-based methods that have been used in order to create the first Volume of an Atlas for the vulnerability assessment of networked infrastructures that are subjected to spatially distributed natural hazards (floods, landslides, wind storms and heat waves). This first Volume concerns the vulnerability of the European Electricity and Gas networks exposed to seismic hazards. We present an overview of the results obtained through the application of GIS-based probabilistic vulnerability assessment methods for the Europe and how this type of information can be of use in for decision-making for mitigation, preparedness and emergency resource deployment.

3.1 GIS processing

Geographical Information Systems have proved to be effective tools in the analysis of large-scale infrastructure and natural and social systems where the spatial or geographical distribution plays an essential role in the manner of the processes that define such systems (e.g. the flow of road traffic through large urban systems). Modern GIS systems are usually associated with maps whereby territorial and urban elements information is collected as the basis of spatial analyses; many applications are being developed in disasters analysis and prevention.
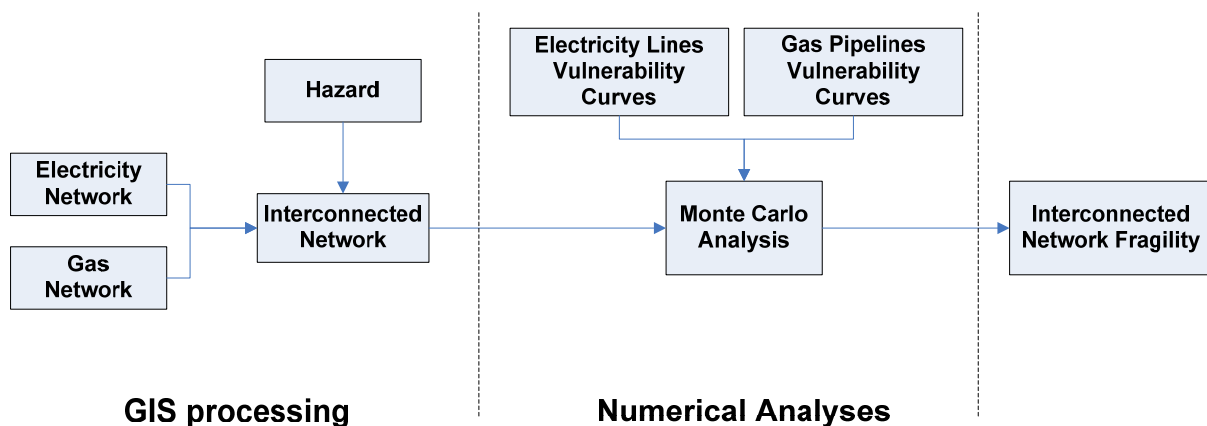
Figure 1: GIS-based method to assess fragility curves for interconnected systems.

However, infrastructural systems are not only related to their geographical distribution and position, but their characteristics are strictly related to their topology and interdependency with other networks.

The GIS method presented here is not limited solely to the GIS environment but was adapted to combine elements of network topology and statistical fragility analysis: the European energy network is considered as a whole combining the gas and electricity networks and the mutual induced fragilities due to their interconnectivity.

For our analysis different GIS data were considered as specified in the table below. These data were then parsed using spatial and network analysis to generate mathematical objects to precisely quantify topological (i.e. the interconnections) and physical (i.e. hazard levels) and social parameters (i.e. the potential populations affected). The main details are described in detail in the following paragraphs.

Data (year)	Type	Source	Description
Gas pipelines (2005)	polyline	Platts	The Platts Natural Gas Pipelines geospatial data layer contains polyline features representing natural gas transmission pipelines in Europe. These pipelines represent the "midstream" transportation routes of natural gas after it has left the gathering systems and before it reaches the local distribution systems.
LNG terminals (2007)	point	Platts	The Platts LNG Terminals geospatial data layer contains point features representing the location of LNG import and export terminals in Europe and the Mediterranean. Detailed attribute data includes storage capacity, regasification capacity, and supply source.
Electricity lines (2007)	polyline	Platts	The Platts Transmission Lines geospatial data layer contains polyline features representing electric power lines of transmission voltages covering Europe. Transmission lines can carry alternating current or direct current with voltages typically ranging from 110 kV to 765 kV. Transmission lines can be overhead and underground; underground transmission lines are more often found in urban areas.
Substations (2007)	point	Platts	This data layer contains point features representing electric transmission, sub transmission, and some distribution substations in Europe. These substations are fed by electric transmission and sub transmission lines and are used to step up and step down the voltage of electricity being carried by the lines, or simply to connect various lines and maintain reliability of

			supply. These substations can be located on the surface within fenced enclosures, within special-purpose buildings, on rooftops (in urban environments), or underground. A substation feature is also used to represent a location where one transmission line "taps" into another.
Power plants (2007)	point	Platts	The Platts Generating Stations geospatial data layer contains point features representing power generating facilities in Europe. Although a power plant may have multiple generators, or units, the power plant layer represents all units at a plant as one feature. Detailed attribute information associated with the power plant layer includes fuel types, prime movers, and operational and financial statistics.
Countries (2007)	polygon	Platts	Countries administrative borders
Urban Areas	polygon	Platts	European Urban Areas
Population (2008)	raster	Landscan	This Dataset comprises a worldwide population database compiled on a 30" X 30" latitude/longitude grid. Census counts (at sub-national level) were apportioned to each grid cell based on likelihood coefficients, which are based on proximity to roads, slope, land cover, night-time lights, and other information.
Seismic EU PGA	raster	GSHAP	The seismic hazard map of the larger Europe-Africa-Middle East region has been generated as part of the global GSHAP hazard map. The hazard, expressing Peak Ground Acceleration expected at 10% probability of exceedance in 50 years, is obtained by combining the results of 16 independent regional and national projects; among these is the hazard assessment for Libya and for the wide sub-Saharan Western African region, specifically produced for this regional compilation and here discussed to some length. Features of enhanced seismic hazard are observed along the African Rift zone and in the Alpine-Himalayan belt, where there is a general eastward increase in hazard with peak levels in Greece, Turkey, Caucasus and Iran.

3.2 European Interconnected Energy Network

The interconnected Energy network of Europe was compiled from the original electricity transmission electricity lines and gas pipeline datasets [4].

The analysis focused on the main transmission lines of these two networks; namely the electricity lines with a voltage greater or equal to 220 kV, and gas pipelines with a diameter greater or equal to 15 inches (Figure 2).

After the elimination of the minor lines, network analysis was performed to detect isolated network regions and corrections were made in order to have a fully connected network.
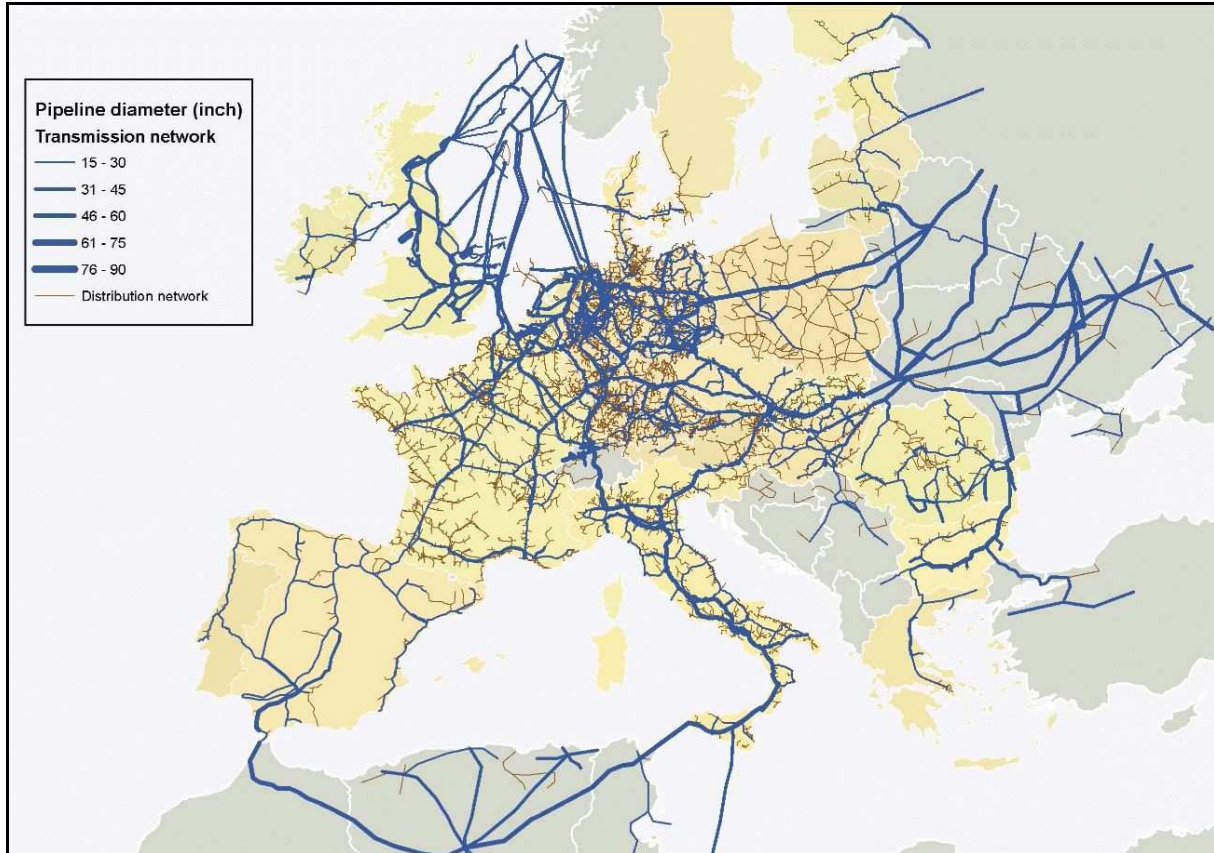
Figure 2: European gas pipeline network. Transmission pipelines overlaid with the distribution network. Link thickness is proportional to the pipeline diameter.

1. Original dataset
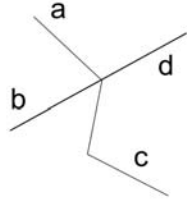
LineID	Diameter
a	15
b	24
c	18
d	20

2. Coordinates definition

LineID	Diameter	Xfrom	Yfrom	Xto	Yto
a	15	8.5	15.2	11.7	12.3
b	24	7.2	8.4	11.7	12.3
c	18	11.7	12.3	18.9	4.3
d	20	11.7	12.3	23.8	14.7
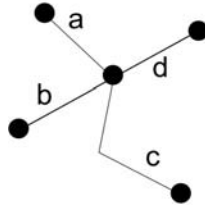
3. Nodes feature set creation

NodeID	X	Y
1	8.5	15.2
2	11.7	12.3
3	23.8	14.7
4	7.2	8.4
5	18.9	4.3
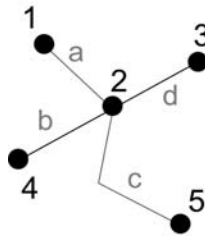
4. End nodes ID assignation

NodeID	X	Y
1	8.5	15.2
2	11.7	12.3
3	23.8	14.7
4	7.2	8.4
5	18.9	4.3

NodeID	X	Y
1	8.5	15.2
2	11.7	12.3
3	23.8	14.7
4	7.2	8.4
5	18.9	4.3

Table Join

LineID	Diameter	Xfrom	Yfrom	Xto	Yto
a	15	8.5	15.2	11.7	12.3
b	24	7.2	8.4	11.7	12.3
c	18	11.7	12.3	18.9	4.3
d	20	11.7	12.3	23.8	14.7

LineID	Diameter	Xfrom	Yfrom	Xto	Yto	IDfrom	IDto
a	15	8.5	15.2	11.7	12.3	1	2
b	24	7.2	8.4	11.7	12.3	4	2
c	18	11.7	12.3	18.9	4.3	2	5
d	20	11.7	12.3	23.8	14.7	2	3

Figure 3: Network structure field structure definition in the database table; we show schematically how the GIS data of a gas network is parsed to generate a connectivity list that can be converted into a graph structure. Starting from (1) where each individual line segment is uniquely assigned an identification number (line ID) and its diameter, we then have in (2) the geographical coordinates of the two end points (vertices) of each line. In (3) the end points are assigned an ID number consistent with the end points of the line segment. In (4) the data are condensed into the final tabular structure that can be used to generate a graph.

In order to translate the network dataset suitable for the mathematical analyses, the GIS data must be processed to obtain a structured table, representing the connected pairs, with the following fields:

- *NodeFROM*

- *NodeTO*

- *EdgeValue*

The electricity transmission dataset already contains the structured form needed for the conversion because each single line (network edge) is defined by the two substations (end nodes); on the other hand, the gas pipeline dataset had to be processed in order to create the required structure: i.e. a point feature set was generated from the end nodes of the original pipelines polyline; then, a unique *ID* was assigned. The pipe nodes table were joined to the pipelines' table based on the relationship between columns of the geographical coordinates and the reference fields *FromID* and *ToID* were added to the pipes fields attributes and populated accordingly (see Figure 3).

3.2.1 Networks interconnections

Natural gas is extracted from gas fields and pumped into the transmission pipelines by compressors. Natural gas can also be transported from gas producing countries by LNG ships that are capable of carrying liquefied natural gas (LNG); the gas is compression-cooled to the liquid state and is converted back into its gas state at the destination LNG terminals (Regasification process).

Electricity is generated by power plants at relatively low voltages (some kilovolts), but in order to carry electricity across long distances high voltage (HV) lines are required to minimize power losses; a substation connected to the power plant usually steps up the voltage for the HV transmission lines. For the distribution systems, the HV electricity is stepped down to lower voltages.

The electricity and the gas network are interconnected through the gas fired power plants; these operate on the natural gas provided by the pipelines and generate electricity by means of gas turbines (see Figure 4).
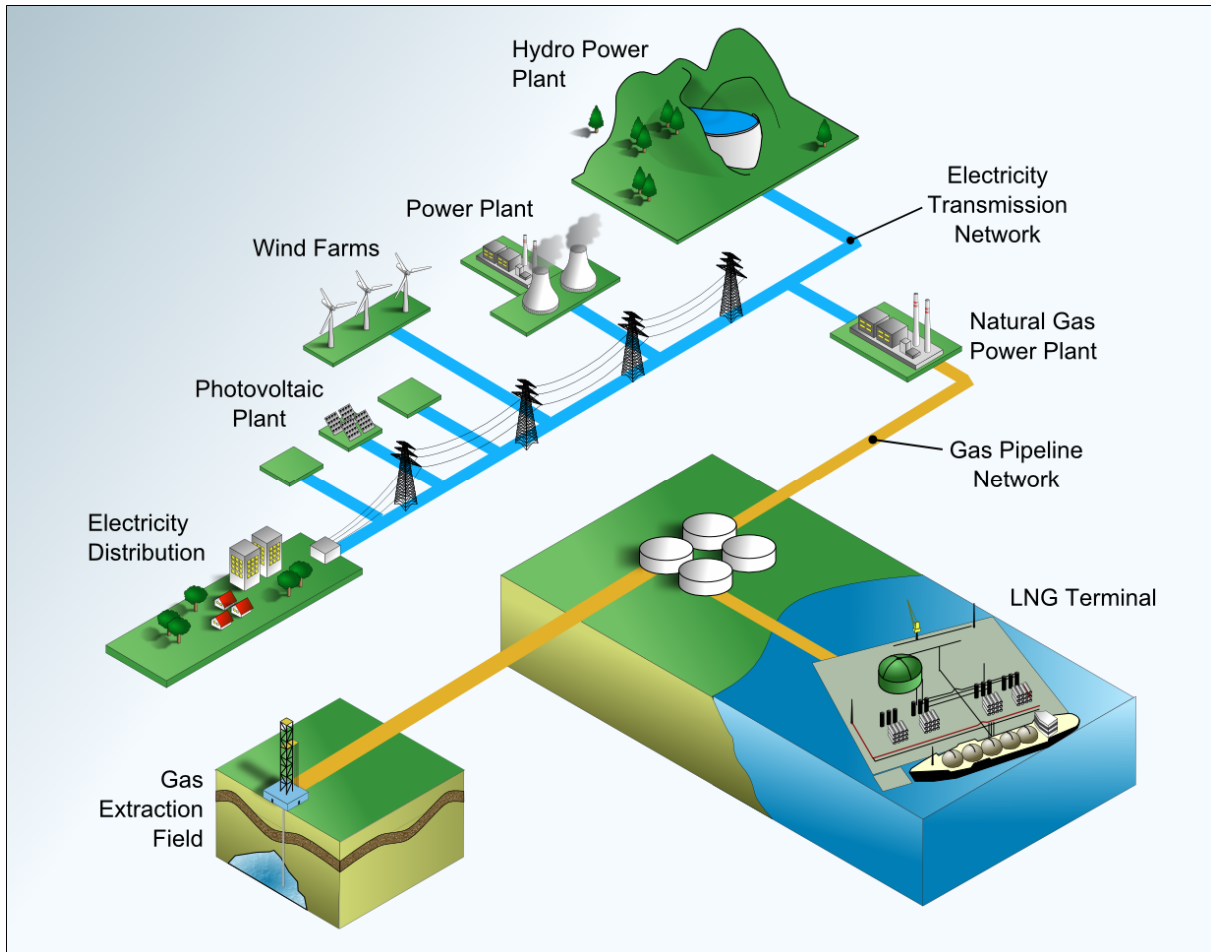
Figure 4: The Energy Interconnected Network.

Given that the interconnections are not provided in the GIS source data, the spatial analysis to define the nearest network nodes for each power plant was performed. However, as the networks considered were limited to the major transmission grids, a further analysis was performed to relate the nodes on the minor electricity grid to the major substations (>=220kV) on the HV grid.

The network analysis of the shortest paths of each minor substation connected to a power plant was performed in order to define the proximity of elements along the interconnected transmission network (Figure 5).
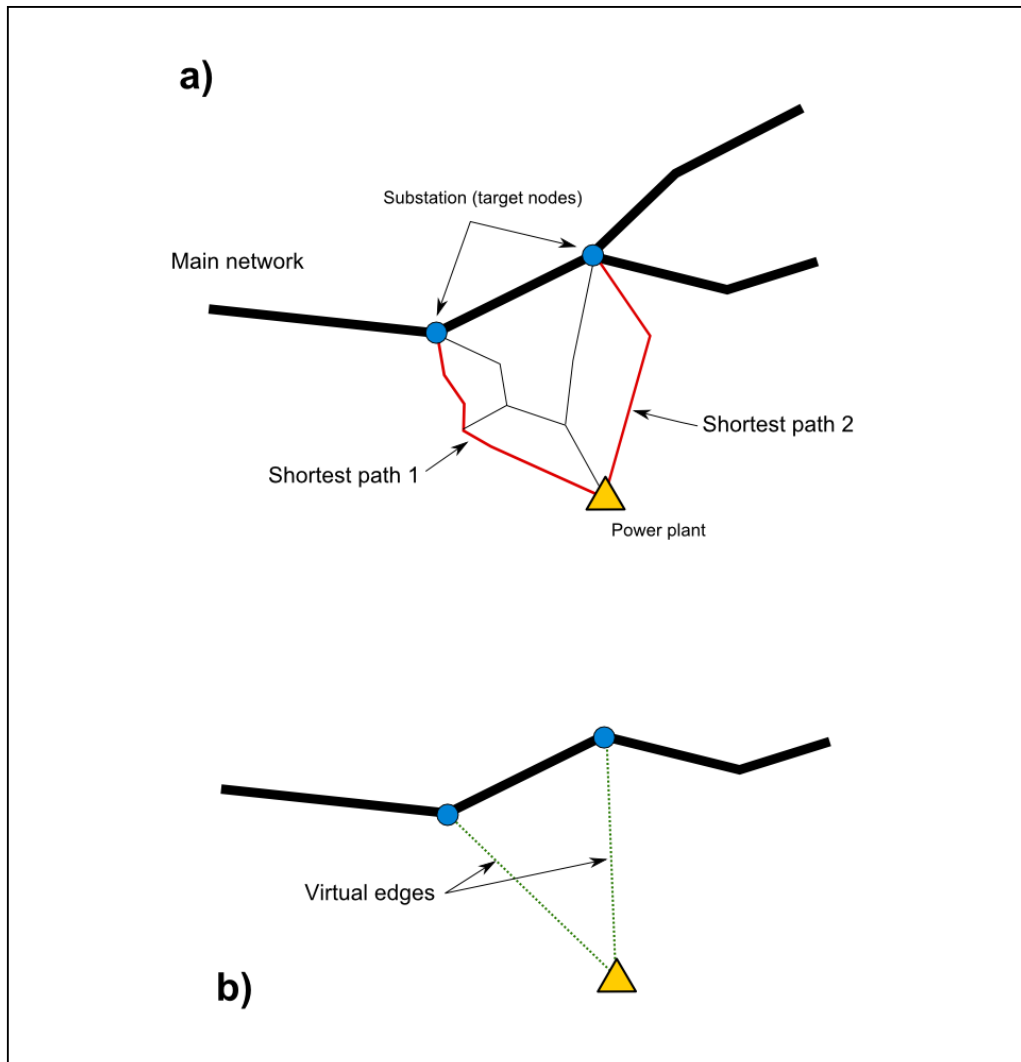
Figure 5: Breadth first search of the shortest paths between a power station and the substations on the main network.
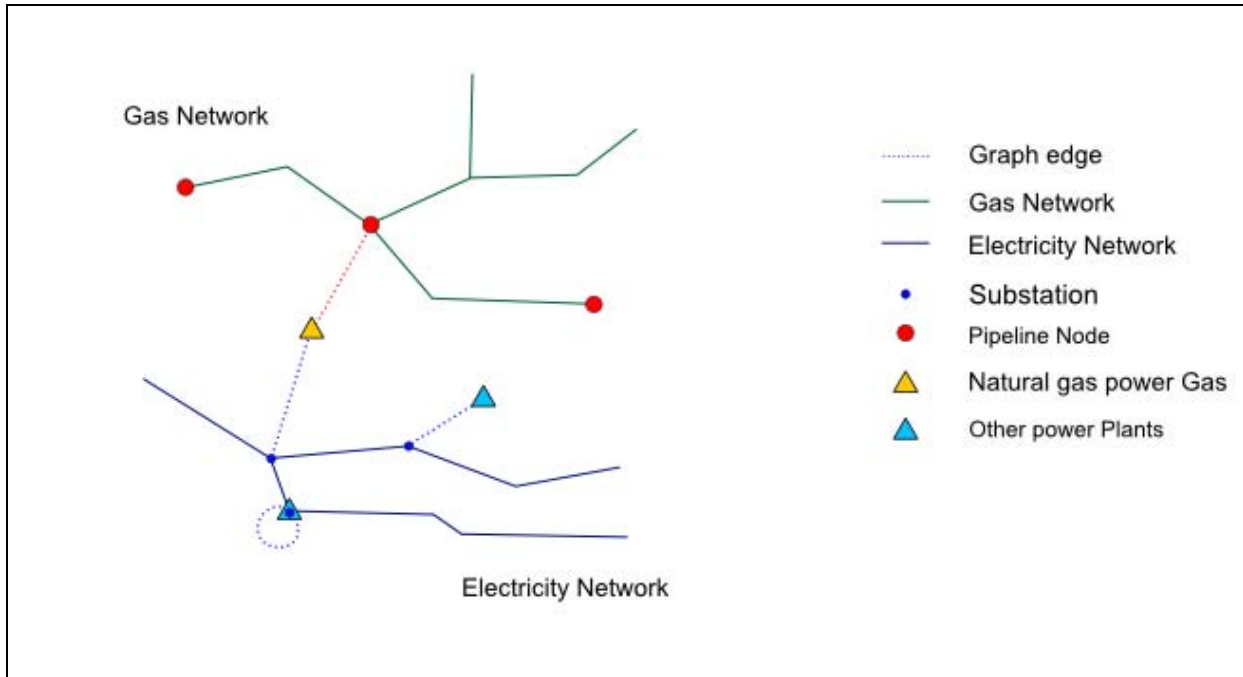
Figure 6: Plants and grids connections.

3.2.2 Substations' Transmission/Distribution definition

The original electricity grid dataset is composed of transmission lines and substation of the whole Europe. The problem now is to distinguish between the nodes serving the distribution network and those that belong to the high voltage transmission lines only; this led to the definition of a set of discrimination rules in the GIS (see Figure 7).

The following rules are selected for the definition of a substation interfacing the high voltage grid to the distribution lines:

- **single degree node**: the HV node is a dangling node.

- **connection to the minor grid**: the node is connected to an electricity line <200 kV

- **location in Urban Areas**: the node is within a urban area. For economic reasons resulting from power losses across long distance transmission, substations tend to be located close to built-up areas whose loads they serve. As observed in [6] the proximity analysis of, the building distribution and the substation distribution is the highly correlated.

23
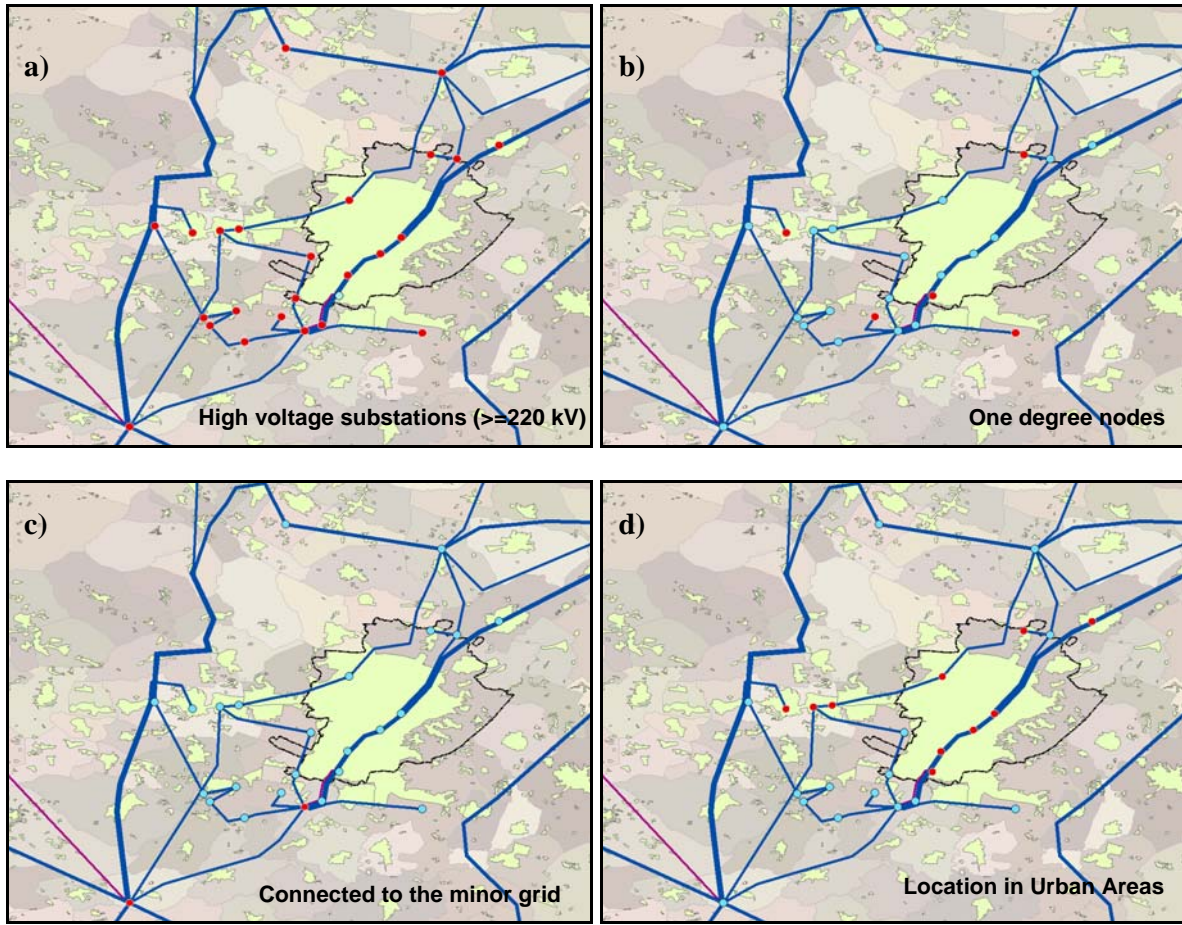
Figure 7: Distributions substation definition criteria
(red points fulfil the single criteria, purple lines belongs to the minor electricity grid).

In Figure 7 we show an example of the electricity distribution system around the city of Turin, where each frame exemplifies one the main discriminating factors of our analysis. If we examine the final parsed data set for the example of (see Figure 8) it can be noted how distribution nodes (in red) are located within in the urban areas. This approach leads to a reasonable identification of the substations connected to the local distribution grids within the limits imposed by the HV only source data availability.

Other nodes were identified as distribution substations by the criterion of having only a single high-voltage transmission line connected to them [1]; however this single criterion (shown in Figure 7b) appears to miss too many distribution points if compared to the one resulting from the actual approach (Figure 8).
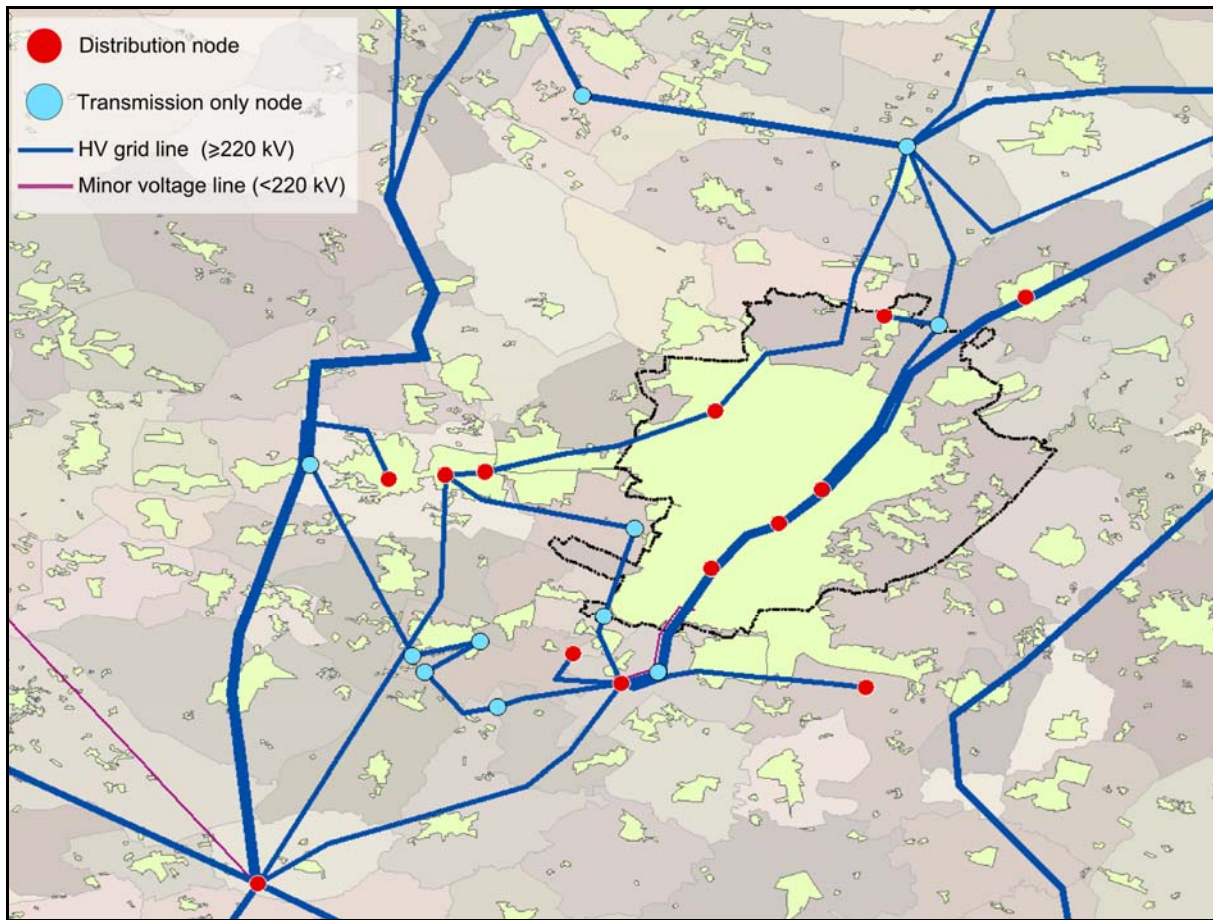
Figure 8: Transmission and Distribution Nodes based on defined criteria.

3.2.3 Population served by substations

In order to evaluate the population affected in case of hazard-induced damages to the electricity network, the served population was computed for each distribution substation. The European population density is based on the Landscan 2008 dataset [14]. this raster data represents the world population density on a grid of 30"x30" (see Figure 9).

The population served is computed generating Thiessen Polygons (also known as Voronoi) for the distribution substations (see Figure 10, step 2). Thiessen polygons define individual areas of influence around each of a set of points whose boundaries define the area that is closest to given point relative to its neighbours; so each single polygon can be considered as area served by each vertex (e.g. of each substation).
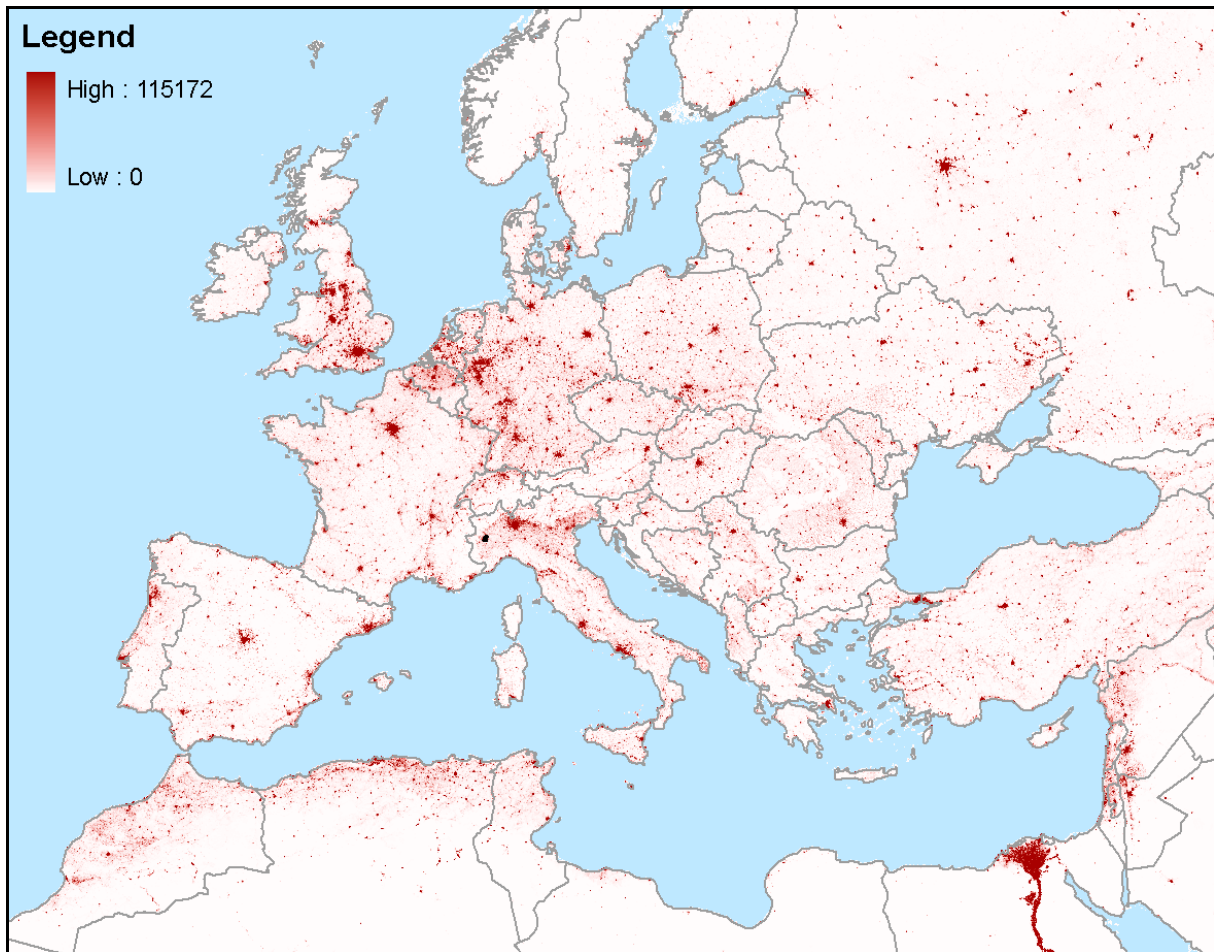
Figure 9: Landscan European population density map.

Computing zonal statistics for each Thiessen polygon on the basis of the Landscan raster dataset (step 4 in see Figure 10) allows every polygon to be assigned with the population resident in the area. Once the Thiessen polygon population is defined, a spatial joining between substations and the intersecting polygons is performed; the population served by each single distribution substation can be defined by the correspondent population in the associated Thiessen polygon.
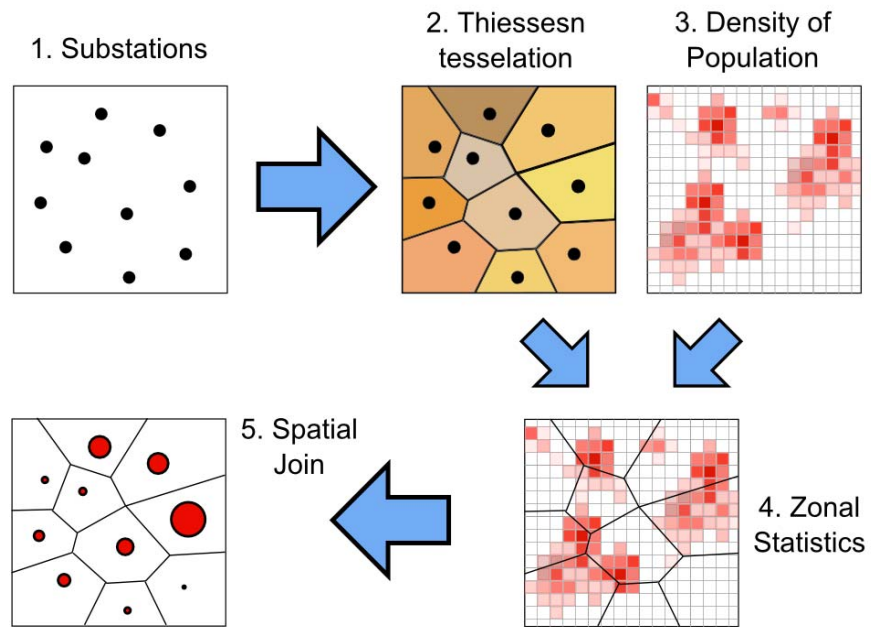
Figure 10: GIS processing for the substations' served population definition.
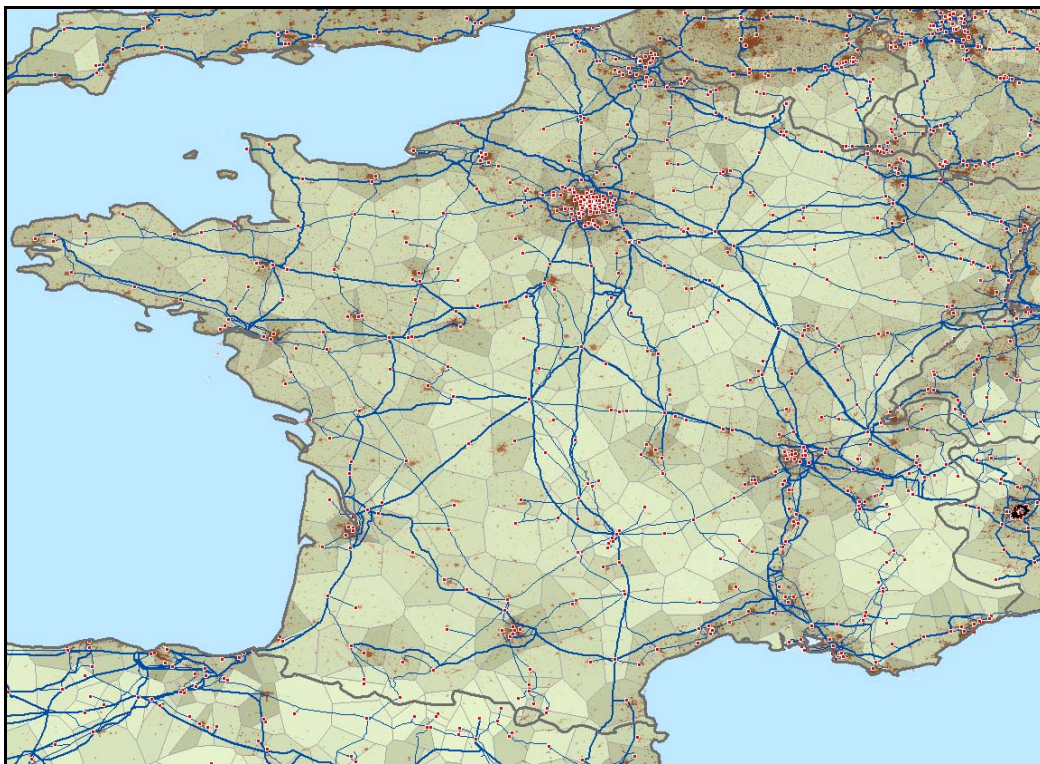
Figure 11: Distribution substation (red dots), population and served areas (greenish polygons) in France.

3.2.4 Hazards level

The mathematical method used to quantify the topological vulnerability of the European energy network elements is independent on the type of hazard provided we associate the corresponding structural fragility curve to the corresponding hazard. In other words, a given element has an associated fragility curve for each hazard. Thus, the fragility curve represent the probability of failure of a certain element of the system (e.g. power plant, substations or gas pipeline) when subject to a given species of hazard. The same structure can then behave differently depending on its response to a seismic event or a wind storm, with different probabilities of failure and, consequently, different fragility curves and damage scenarios. Hence, this approach may be implemented as well for different threats.
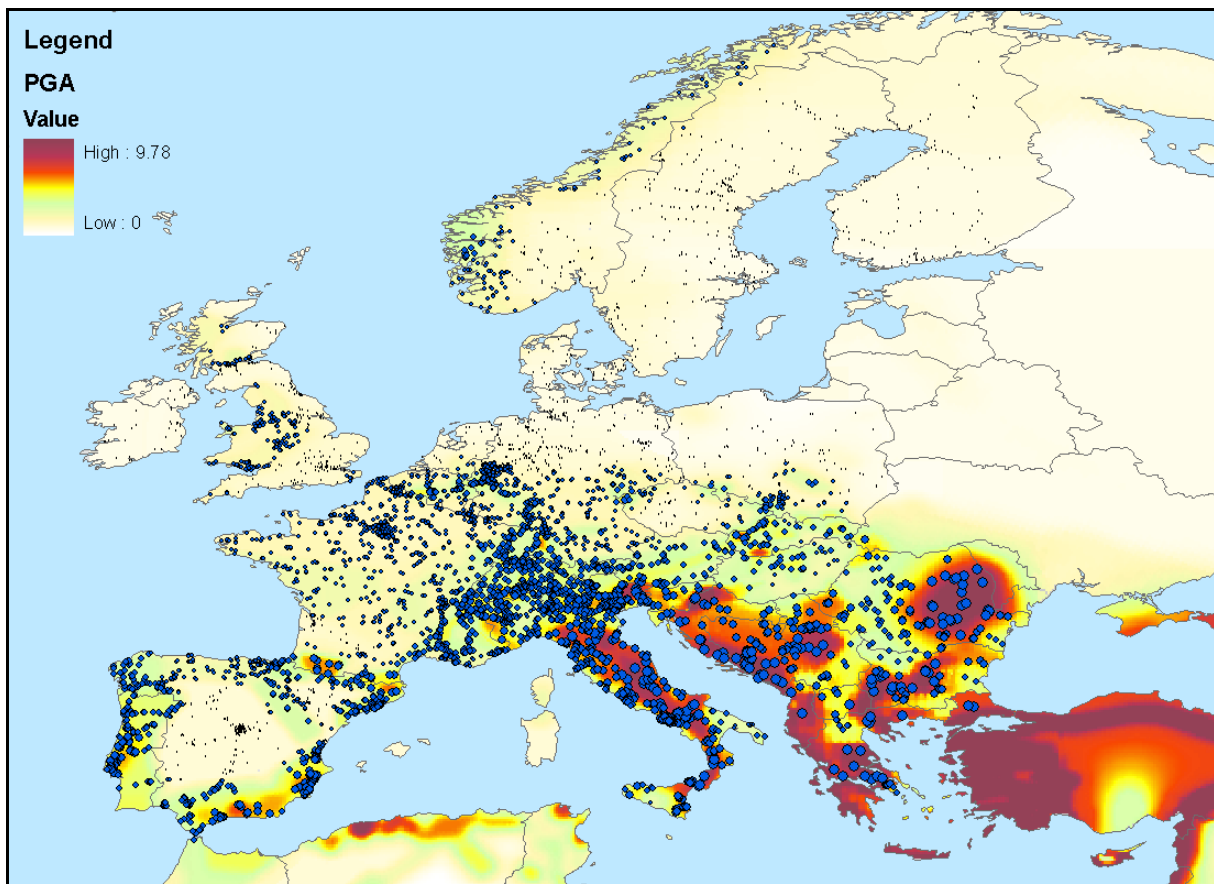
Figure 12: Seismic hazard Map of Europe and electricity substations scaled according to the PGA value - 10% Probability of exceedance in 50 Years, 475-Year Return Period.

For the analysis presented here, the response of the EU Energy network was considered with respect to its seismic vulnerability, and in order to ascribe the seismic hazard level to each network element, the peak ground acceleration (PGA) map of Europe was retrieved from the GSHAP Global Seismic Hazard Map [13] and overlaid on the GIS to the geographic distribution of network assets.

The original dataset is in the form of a list of Lat/Long coordinates with the associated PGA value. This was imported into the geodatabase and a point feature set was generated. The points were then interpolated and the PGA value was assigned to each node of the interconnected network based on its geographical location. Doing this the probabilistic amount of hazard impacting each element was defined.

4   Topology of network datasets

Our case study is the interconnected system of Gas and Electricity European transmission networks that are spatially co-located structures connected through the gas power plants, and the operability of the gas power plants is dependent on the gas fuel supplied by the gas network. The network analysis is executed on each of the networks separately but the vertices of gas power plants are shared. The networks are considered, in the first instance, as multiple edge, undirected and unweighted; i.e., with neither real flows nor the capacities of flow.
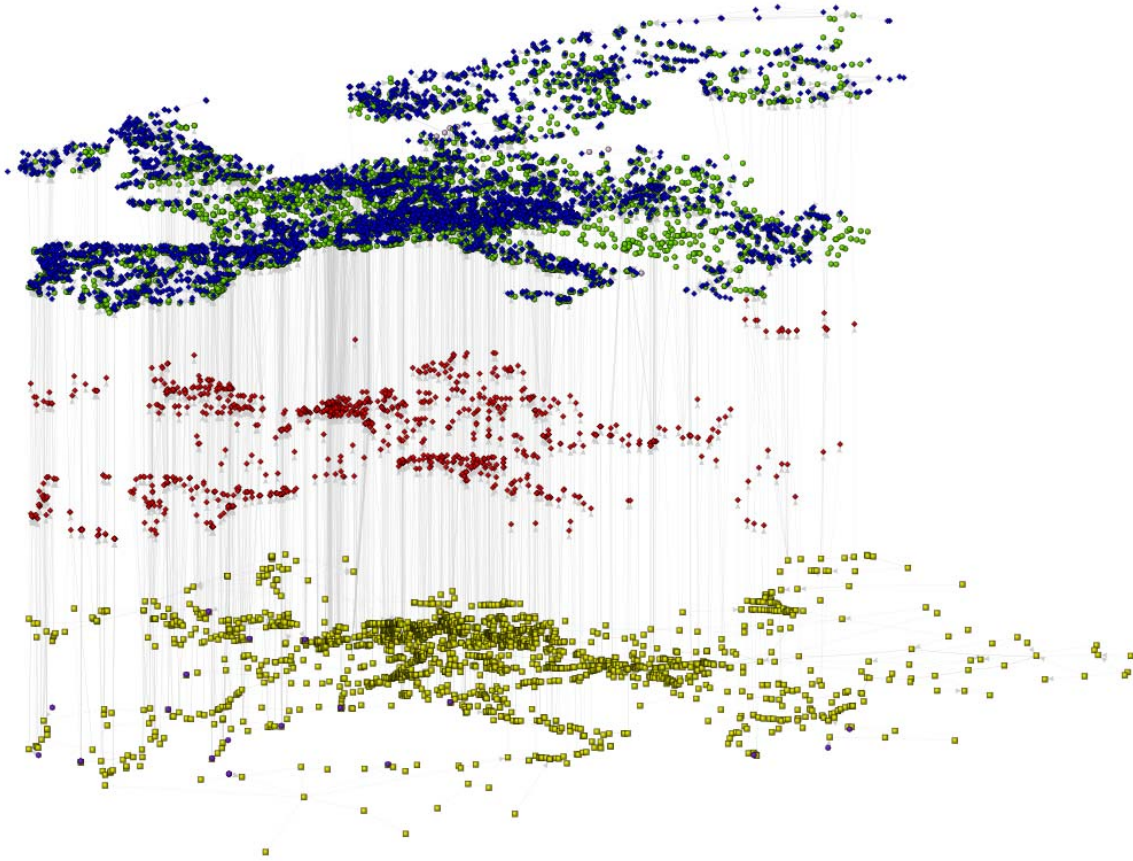
Figure 13: Interconnected system of the gas network (bellow) and electricity network (above) with gas power plants as the common vertices (in the middle).

Because we wish to treat infrastructures as complex networks it is appropriate to first compare their topology with existing theoretical network types, i.e. Erdos-Reyni graphs, Scale-Free networks and

networks with the Small Wolrd characetristics. Dorogotsev and Mendes [7] suggested an empirical method for comparing real world complex networks to theoretical network types. For the case of undirected graphs this method checks for certain topological measures, such as degree distribution, the average clustering coefficient and the characteristic path length defined as average shortest path.

From the analysis of the vertex degree distributions, it appears that the Energy network has a high number of one-degree vertices. Probably the majority of the one-degree vertices in the networks are power plants and LNG terminals which are connected a single edge to the closest vertex in the main network. However, the complementary cumulative functions of vertex distribution are more similar to the Exponential than Scale Free form (Figure 14).

Table 1: Topological characteristics of the interconnected system and its component networks.

	INTERCONNECTED SYSTEM	ER_{12741}	GAS NETWORK	ER_{3231}	ELECTRICITY NETWORK	ER_{10508}
Number of edges	17798		3738		14060	
Number of vertices	12741		3231		10508	
Average degree of the vertex (maximum degree of the vertex)	2.79 (67)		2.3 (25)		2.68 (67)	
Diameter (Characteristic path length)	80 (30)	21 (9)	101 (33)	22 (9)	94 (27)	22 (9)
Average clustering coefficient	0.028	0.0002	0.020	0.0005	0.030	0.0002

The topological characteristics of the Gas and Electricity networks are compared with topological characteristic of random graphs with the same number of vertices and average degree of vertex calculated as the average of the 50 random (Erdos-Reyni graphs) network models (Table 1). The characteristic path length and the average clustering coefficient of the Energy networks are always higher than their counterpart average random model. The key feature of the Small World graphs is their small characteristic path length which is like random graphs but with much higher average cluster coefficient ([25]). High average cluster coefficients could be a sign of redundancy in the Energy networks in order to improve its resistance to local failures. As far as Scale Free model is concerned, we need to check the simultaneous existence of growth and preferential attachment mechanism ([3]). The fact is that current structure of the Energy networks is the result of structural evolution over many years, but the exponential cumulative distribution of the degree of vertex indicates the absence of preferential attachment. Presumably, the new vertices have been connected to the existing vertices biased by their adequate geographical location and the length of the transmission line needed, rather than their connectivity.
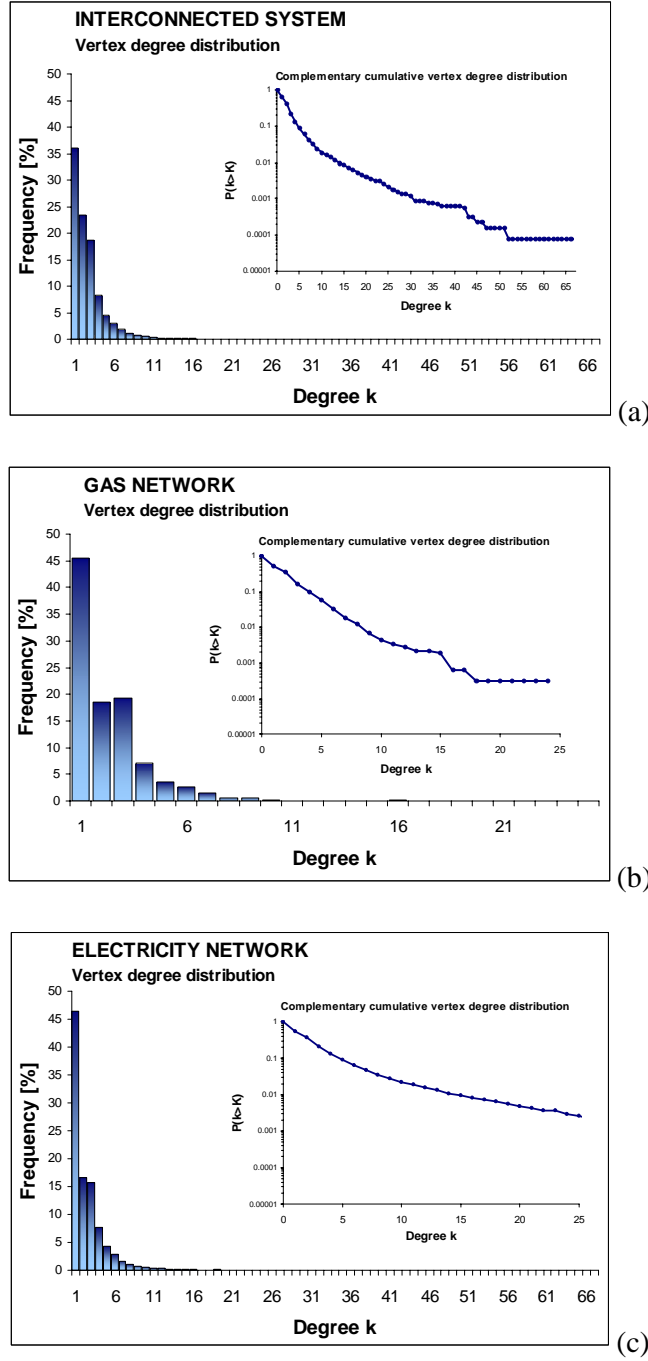
Figure 14: Vertex degree frequency distributions and their complementary cumulative distribution of the interconnected system, (a), and its networks,(b) and (c), regarded as undirected networks.

Having made the comparison between true random and scale-free networks and the Gas and Electricity networks and noted their dissimilarities, it would appear that we can discard these generic types of networks as descriptive of these two real-world networks. In conclusion, we can

say that our real complex networks have some topological characteristics in common with all three types of existing model networks but none of the models would fit them completely.

4.1 Sources and sinks

In order to define the networks' performance measures (Chapter 6.1) we have to designate which vertices in the networks are sources, and which are sinks. All the vertices that do not belong to either of these two classifications are transmission vertices. Directions of the flows (electricity power or natural gas) are presumably always from sources to sinks. Therefore we introduce into the networks topology an extra information field: the directedness of those links, which are adjacent to sources and sinks. Introducing directedness as a key functionality of the network, eliminates some shortest paths because they are not expected to occur in real situations. For example, the shortest path from source to sink that goes through another source is, in our case, not admissible because the power plants do not have a transmission function. But with no links directed to the power plant such situation cannot appear.

Table 2: Division of vertices according to their functionality.

	source vertices	transmission vertices	sink vertices
GAS NETWORK	163	2070	998
ELECTRICITY NETWORK	5381	1419	3708

In the case of the gas network, the source vertices are vertices located in the immediate vicinity of exploitable gas fields (142 vertices) and the LNG terminals (21 vertices). Gas storages should be treated as the source vertices as well; however, at present they are not considered part of the network because we do not know how quick their intermediate response to the shortage of the gas in the system is. Furthermore, there are two types of the gas-consumption vertices that could be treated as sinks: first, there are vertices that transport gas through the distribution network to consumers which use gas directly for heating and cooking. Secondly, there are gas power plants that use natural gas as a fuel for the generation of electricity. However, for the purpose of expressing the interdependency effect of the electricity network on the gas network, the gas power plants play the

primary connection role. Therefore, the sink vertices of the Gas network are designated to be only the gas power plants.
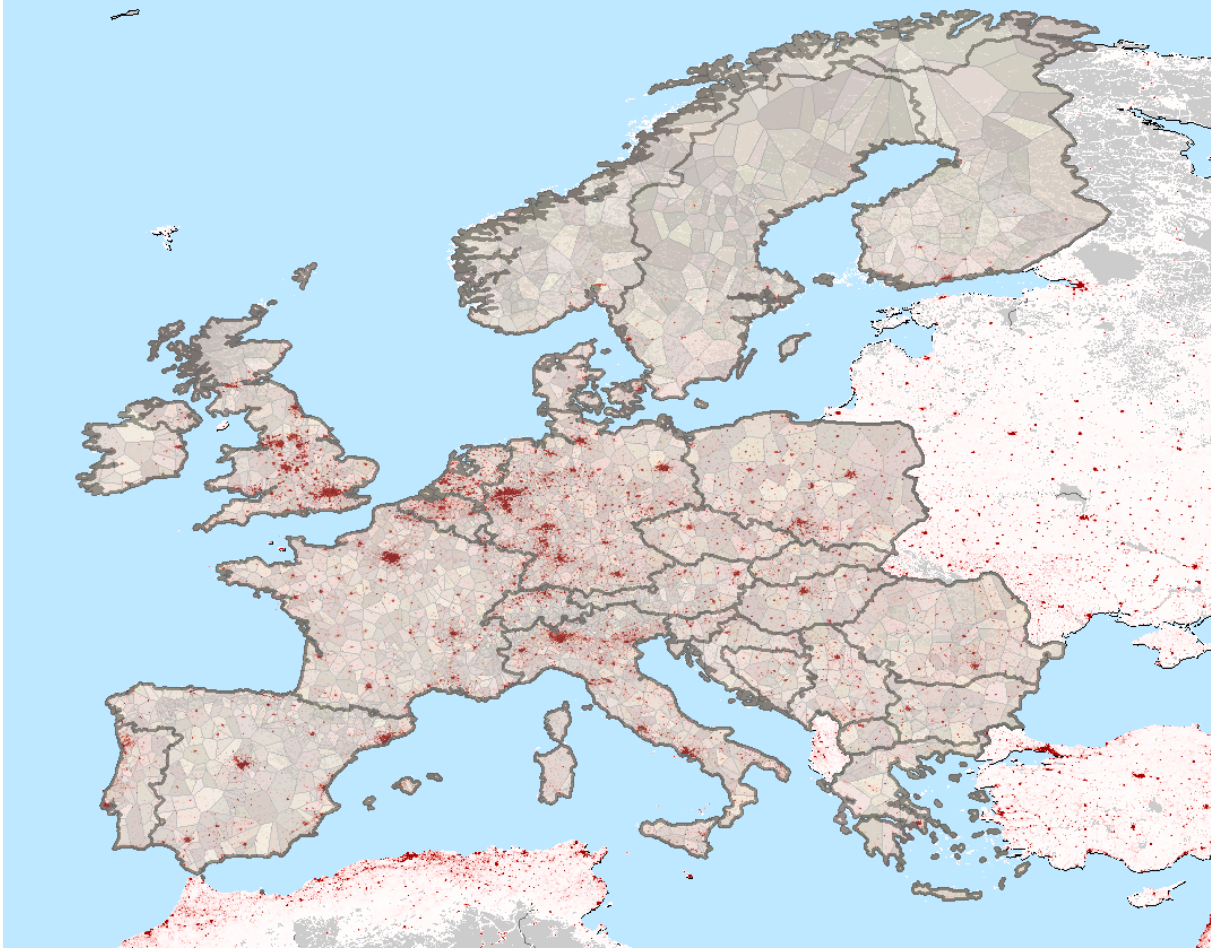
Figure 15: European map for population density covered with Thiessen polygons.

For the Electricity network, on the other hand, all power plants are source vertices; but, in addition to the 998 gas power plants compiled for our analysis, there are also 4383 power plants sourced by other types of fuel. Conversely the sink vertices are defined as substations that deliver the power into the electricity distribution network. Such high voltage substations we call distribution substations (Chapter 3.2.2). These are all substations which either have degree one or substations which may have higher degree but which are located inside urban areas or have at least one edge leading to the lower voltage substation on the distribution network(we have found 3708 distribution substations and identified them as the sink vertices). One characteristic of such electricity sink vertices is that they can form bidirectional connections with the other vertices; however, this is not

the case with the sinks in gas network. Furthermore, if electricity sink vertices are regarded as the entrance point into the electricity distribution network, it is justifiable to define an area that is covered by each distribution substation. We have therefore divided Europe into small patches, each of which is associated with one distribution substation (Chapter 3.2.3). For this purpose we have applied the tool from the ArcGIS software called Thiessen Polygons, which encloses the space around each point using an algorithm to calculate the location of a boundary mid-way between the available points. In this manner, using the geographical distribution of the population (Figure 15), we can calculate the population assigned to the distribution substations as additional information which can be used for evaluation of the performance measures (we refer to this as the Impact Factor on Population).

5 Hazard and risk assessment

A hazard is a situation, which possesses a level of threat to life, health, property, or environment caused by natural phenomena or human behaviour (unintentional or intentional). Here we will focus on natural hazards that could potentially be harmful to people's life, property or environment. It is important to make a distinction between the risk and the hazard because one can change the risk without changing the hazard. In general, the concept of risk combines the probability of occurrence of phenomena and the probabilistic evaluation of the economic and life loss associated with the phenomena. It is often expressed with the following mathematical relationship:

$$Risk = (likelihood\ of\ event) \times (consequences\ of\ the\ event) \tag{1}$$

As such, a risk is often expressed in measurable quantities such as the expected number of fatalities, injuries, extent of damage, failures, or economic loss. The whole process of measuring is called risk assessment, which must measure both the probability and consequences of all of the potential events that comprise the hazard. Risk assessments normally involve examining the factors or variables that combine to create the whole risk picture. Some of these variables are eventually incorporated in the risk model that serves as a measurement tool.

We can mitigate the effects of hazards by preparing for them. For example, seismic standards help to engineer earthquake-resistant buildings. Besides, the effectiveness of applied provisions can be improved with more accurate prediction of time, location, or intensity of the hazard occurrence. A set of provisions to control the risk is called *risk management*. Without risk assessment, we cannot make decisions related to managing those risks. Because the additional provisions need extra financial investment, the risk management must deal with the judgment of the accepted risk and mitigation costs (cost-risk modelling)

If we return back to the basic understanding of the risk, three questions must be answered:

What can go wrong?

Answering this question begins with a general definition of failure. Strictly speaking, failure is an event when manmade structures are unable to perform their intended function. In general, this can be understood as the collection of (all) possible damage mechanisms encountered in the event where structures, equipment or environment can affect the population of the affected area.

How likely is it?

By the commonly accepted definition of risk, it is apparent that probability is a critical aspect of all risk assessments; so, some estimate of the probability of failure will be required in order to assess risks. A probability (chance or likelihood) expresses a degree of belief. While dealing with a very simple situation (one variable with a long history of observations) we can say that probability estimates arise from the statistical analyses that rely on measured data or observed occurrences. In the past, complex systems (like chaotic systems) tended to be regarded as unobservable due to the apparently aberrant nature of their performance; i.e. their behaviour not easily be described using standard mathematical cannons. Thus, although they have always been scrutinised, such observations were not amenable to a systematic analysis with the mathematical tools of the day. However, with the advent of recent mathematical techniques to study non-linear chaotic systems, we have improved our knowledge of how their behaviour is generated. In particular, it is now known that non-linear processes generate probability distributions that are not well represented by standard Poisson distributions. Thus the standard statistical analysis, which often disregarded certain data as outliers or errors in measurement, provides an incomplete estimate of probability of extreme events occurring; therefore the data must incorporate other types of information such as, for example, the power-law distribution of failures of blackouts or the return period of earthquakes.

What are the consequences?

The main part of risk analysis is to judge the potential consequences. Consequence implies a loss of some kind referring to undesirable affect of the hazard event on the populated environment and the population itself. Many of the aspects of potential losses are readily quantified. For some types of damage the most straightforward approach is to quantify the consequences with the monetary value of losses (repair costs, production loss, health insurance cost, property cost): it is a very appropriate common denominator when considering different types of consequences together. For other types of damage, such as loss of life or social disruption (and even environmental impacts), this approach is more difficult to apply.

5.1 Seismic hazard and risk

The case study of this report is focused on vulnerability of manmade networks to seismic hazards. Seismic hazard is defined as the probable level of ground shaking associated with the recurrence of earthquakes. The assessment of seismic hazard is only the first part in the evaluation of seismic risk, which is referred to as the likelihood of the event in the Equation (1). Seismic hazard is presented in seismic hazard maps with the expected earthquake ground motion at a given geographical location. When considering the local soil conditions and the other vulnerability factors of the affected infrastructures (i.e., the type and consideration of seismic design implicitly represented by the fragility curves) or population, we progress to the second step in the evaluation of seismic risk, referred to as consequences of the event in Equation (1).

It is possible that large earthquakes in remote areas result in high seismic hazard but show no risk; on the contrary, moderate earthquakes in densely populated areas result in small hazard but high risk.
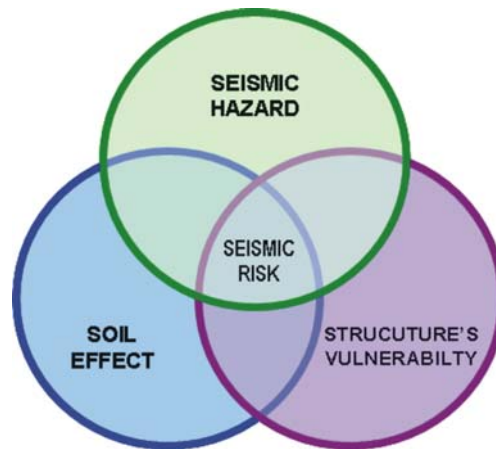
Figure 16: Seismic risk.

5.1.1 Seismic hazard maps

A probabilistic seismic hazard map is a map that shows the earthquake-hazard exposure that geologists and seismologists agree could occur in area covered. It is probabilistic in the sense that the analyses take into consideration the uncertainties in the size and location of earthquakes and the resulting ground motions that can affect a particular site. The basic elements of modern probabilistic seismic hazard assessment consider the following [12]:

- An earthquake catalogue presented as the database with the data of seismicity from different periods (historical, early instrumentally recorded, and recently instrumentally recorded)

- An earthquake source model that integrates the earthquake history with evidence from seismotectonics, paleoseismology, mapping of active faults, geodesy and geodynamic modelling,

- Strong seismic ground motion that evaluates ground shaking as a function of earthquake size and distance, taking into account propagation effects in different tectonic and structural environments and finally

- Computation of probability of occurrence of ground shaking at a given time period to produce seismic hazard maps.

The maps are typically expressed in terms of probability of exceeding a certain ground motion. The ground motion parameter usually used is Peak Ground Acceleration (PGA); i.e., the maximum acceleration experienced during the course of the earthquake motion. It can be measured with respect to *g* (the acceleration due to gravity), in % of *g* or m/s² (PGA is one of the most important input parameters for earthquake engineering design, since it can be related to the horizontal force that a structure must resist). Other ground motion parameters used to characterize earthquake ground motion include Peak Ground Velocity (PGV) and Permanent Ground Displacement (PGD). The later two are not only used for description of the ground motion, but more rather for the detection of possible ground failures such as fault rupture, land sliding or liquefaction.

T [years]	R [%]
100	40
475	10
975	5
2475	2
10000	0.5
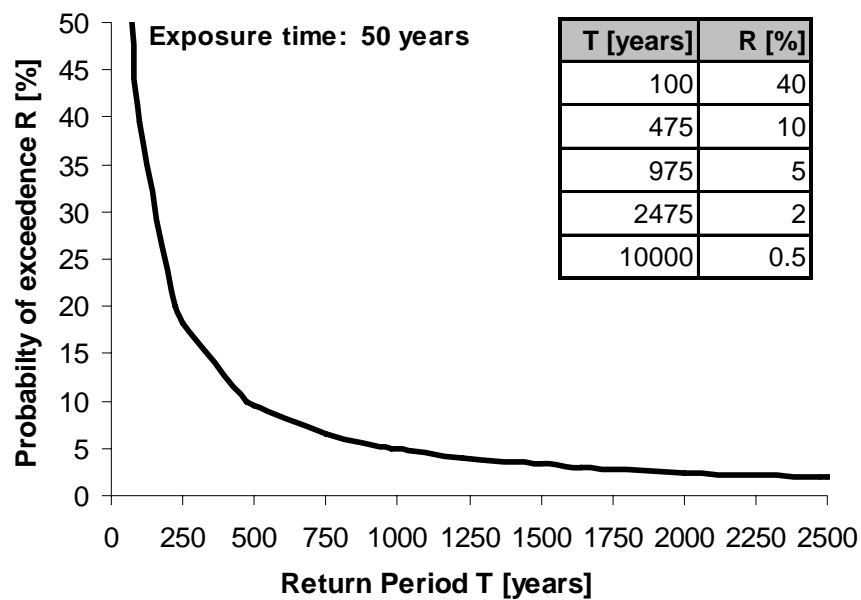
Figure 17: Relation between the return period, exposure time and the probability of exceedence of the event of given magnitude.

The description of the seismic hazard map is a monotonic function with the return period T and the exposure time n. The return period (or recurrence interval) is the average time span between two events of a given magnitude at a particular site. The exposure time usually equals the expected life of the structure. In order to calculate the design life expectation of the structure, both these parameters as well as the return period of the event must be employed when calculating the risk of the structure with respect to a given event. The risk assessment is thus the likelihood of at least one event that exceeds design limits of the structure in its expected life. It is obtained from

$$R = 1 - \left(1 - \frac{1}{T}\right)^{n},$$ (2)

where $1/T$ refers to the annual probability of occurrence of exceeding a given ground motion. For example, seismic hazard maps calculated for 475 return period and 50 years of exposure time corresponds to 10% probability of exceedence (Figure 17). In fact, there is 90% chance that these ground motions will not be exceeded. This level of ground shaking has been used for designing ordinary buildings in high seismic areas.

The higher return period (lower annual probability of occurrence) defines the event of the higher magnitude. Therefore, buildings of higher importance must be designed for hazard events with higher return period than 475 years. For example typical design hazard level for hospitals and schools is 1000 years return period while design hazard level for nuclear power plants is 10 000 year of return period. From that point of view the return period as the parameter of the seismic hazard map defines seismic hazard level. A high return period corresponds to a higher seismic hazard level. Similarly, we can deduct form Figure 17 that low probability of exceedence corresponds to the high seismic hazard level. Figure 18 clarifies this statement for the area covered by Slovenia. This example was shown because of the availability of the data, which are not so easily obtained for the other European countries. But we must bear in mind in this paragraph that that we did not vary the time of exposure.

Furthermore, for presenting the correlation between the annual probability of exceedence and ground motion parameter at one site we use hazard curves. For example, the PGA for certain location on 475-year return period seismic hazard map is one point in a hazard curve. Then the values are read directly from the seismic hazard maps for different hazard levels. In such a manner, the hazard curve for the capital of Slovenia, Ljubljana, (Figure 19) was obtained. The hazard curves are important not only for comparing the hazard at different sites, but also for determination of the expected consequences or even loss when using the fragility curves (Chapter 5.1.2).

Seismic hazard maps data are always calculated for the rock sites, so an additional adjustment must be made to take into the account the effect of local characteristics of ground layers on the PGA. EUROCODE 8 [10] introduced soil factors for the PGA amplification. Soil factors are dependant on the soil type that is characterized in the majority of cases with average shear wave velocity in the upper 30m of layers.
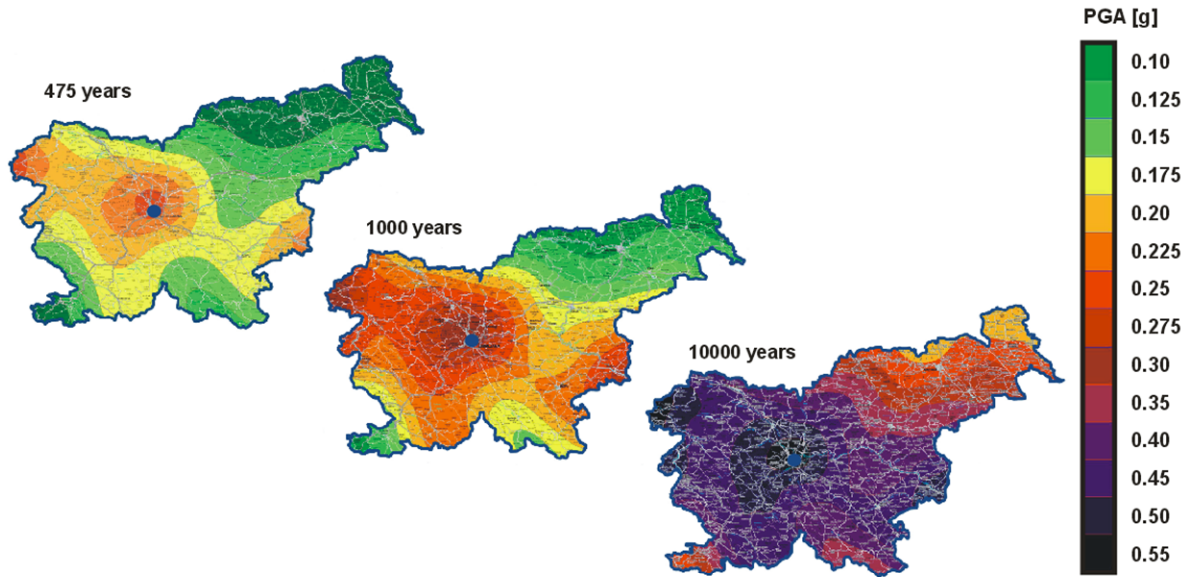
Figure 18: Example of seismic hazard maps for different hazard levels for Slovenia.
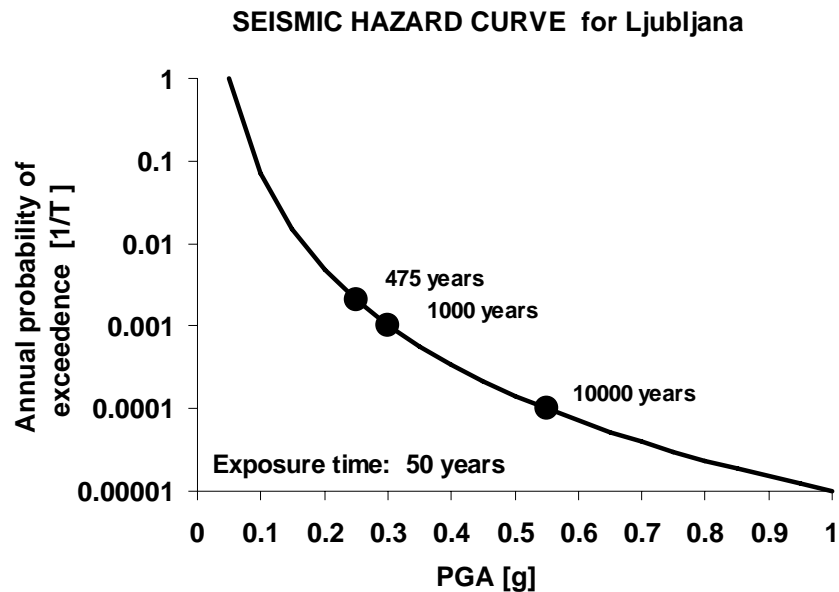
Figure 19: Example of hazard curve for Ljubljana, the capital of Slovenia.

5.1.2 Fragility curves

In the previous chapter we examined how to deal with the likelihood of the event characterized as a seismic hazard. Now we show how to evaluate the seismic vulnerability of each element of the network and how it fits in with the assessment of seismic vulnerability of the infrastructure network as a whole. For example, a substation is an element of the electricity network presented as a vertex; but from an engineering point of view, the same substation is a structure that can be damaged in the event of an earthquake. The seismic vulnerability of the structure is expressed by its associated fragility curves. In general, a fragility curve (also called damage functions) is a just the graphical representation of the conditional probability of exceeding a certain damage limit state at a given level of seismic hazard, which is dependant on the type of structure. Based on fragility curves, the functionality of the structure can be assessed whenever functionality is correlated to the damage state.

Our source for the fragility curves used in our analysis is taken from HAZUS ([11]) programme, which contains definitions of fragility curves for important elements of the utility systems. HAZUS has been introduced in the United States as a nationally applicable standardized methodology for multi hazard potential loss estimation. The data for the calibration of these fragility curves are collected from the statistical analysis of damage of the critical infrastructure on the west coast of the United States. They are modelled as lognormally distributed functions defined by a median ground motion parameter ($median$) and a standard deviation (σ) as a measure of dispersion. The final shape of the fragility curve is defined by the cumulative distribution of the lognormally distributed function and shows the probability of exceeding certain damage states (DS) at a given ground motion parameter (a.e.PGA):

$$P\left(DS > ds \mid PGA\right) = \frac{1}{2} + \frac{1}{2}\operatorname{erf}\left(\frac{\ln(PGA) - \ln(median_{PGA})}{\sigma\sqrt{2}}\right). \tag{3}$$

5.1.2.1 Electricity power system

In the case of electricity power system, we use the fragility curves for the substations and power plants. The shape of the fragility curve for the given element is dependant on the damage state. When the structure is defined as the vertex in the network five damage states are defined: none (ds_1), slight/minor (ds_2), moderate (ds_3), extensive (ds_4) and complete (ds_5). More severe damage states correspond to the lower probability of exceedence at the same PGA. Damage states as defined in HAZUS are dependant on the type of element and the level of the damage of its subcomponents.

Substations

Fragility curves of the substations are classified according to the voltages assigned to the substation and according to whether all subcomponents of the substations are anchored or not. Substation are classified according to their voltage rating: from low voltage (<150 kV), medium voltage (150 – 350 kV) and high voltage (>350kV). Furthermore, we have to define the subcomponents of the substation. First, the substation can be entirely enclosed in the building where all the equipment is assembled in one metal-clad unit and is treated as one anchored component. Other substations are usually compounded of subcomponents (transformers, disconnect switches, circuit breakers, lightning arrestors) that are located outside the substation's building. An anchored subcomponent in this classification refers to equipment that has been engineered to meet modern seismic design criteria.

In order to estimate the probability of exceeding a certain damage state of the substation, the following items are required as input:

- Geographic location of the substation (longitude and latitude).
- PGA,
- Properties of the substation (voltage and design) for the classification.

Damage states of low voltage substation									
	Anchored/Seismic component				UnAnchored/Standard component				
	minor	moderate	extensive	complete	minor	moderate	extensive	complete	
Median [g]	0.15	0.29	0.45	0.90	0.13	0.26	0.34	0.74	Median [g]
Standard deviation	0.70	0.55	0.45	0.45	0.65	0.50	0.40	0.40	Standard deviation
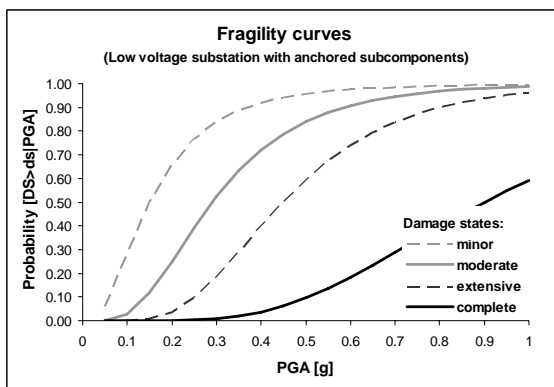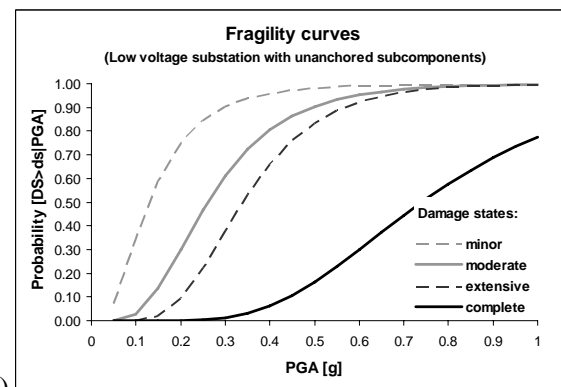
(a) (b)

Figure 20: Fragility curves for low voltage substations with (a) anchored subcomponents and (b) unanchored subcomponents.

Damage states of medium voltage substation								
	Anchored/Seismic component				*UnAnchored/Standard component*			
	minor	moderate	extensive	complete	minor	moderate	extensive	complete	
Median [g]	0.15	0.25	0.35	0.70	0.10	0.20	0.30	0.50	**Median [g]**
Standard deviation	0.60	0.50	0.40	0.40	0.60	0.50	0.40	0.40	**Standard deviation**
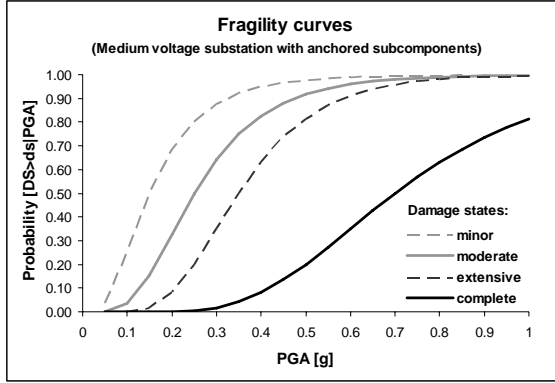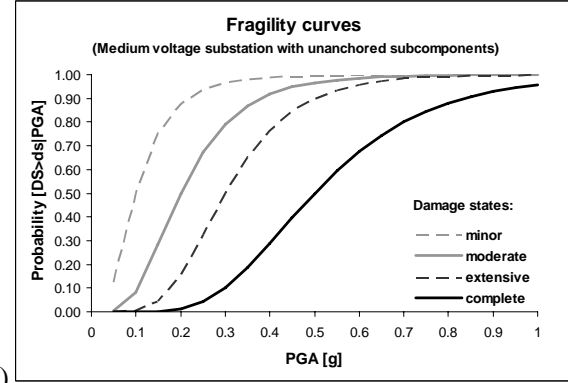
Figure 21: Fragility curves for medium voltage substations with (a) anchored subcomponents and (b) unanchored subcomponents.

Damage states of high voltage substation								
	Anchored/Seismic component				*UnAnchored/Standard component*			
	minor	moderate	extensive	complete	minor	moderate	extensive	complete	
Median [g]	0.11	0.15	0.20	0.47	0.09	0.13	0.17	0.38	**Median [g]**
Standard deviation	0.50	0.45	0.35	0.40	0.50	0.40	0.35	0.35	**Standard deviation**
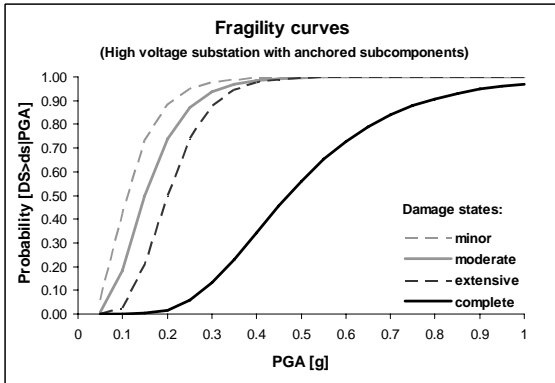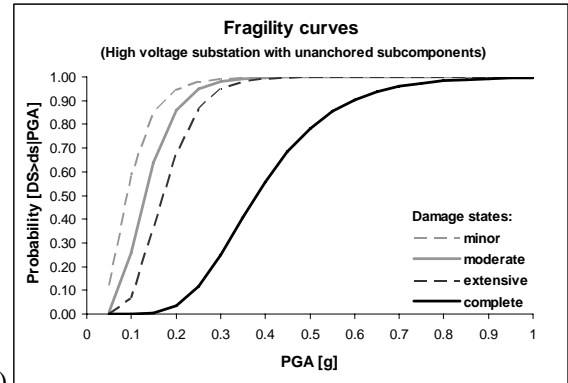
Figure 22: Fragility curves for high voltage substations with (a) anchored subcomponents and (b) unanchored subcomponents.

Power plants

Fragility curves of the power plants are classified according to the power rating in MegaWatts under normal operations. Small power plants have a capacity of less than 200 MW, whreas medium/large power plants have capacity greater than 200 MW. Again, the classification is also a function of whether the subcomponents (generators, turbines, racks, boilers, pressure vessels) are anchored or not, noting that the fuel type of the power plant is not important.

In order to estimate the probability of exceedence of certain damage state of the power plant the following items are required as input:

- Geographic location of the power plants (longitude and latitude).
- PGA,
- Properties of the power plant (power and design) for the classification.

Damage states of small generation plant									
	Anchored/Seismic component				*UnAnchored/Standard component*				
	minor	moderate	extensive	complete	minor	moderate	extensive	complete	
Median [g]	0.10	0.21	0.48	0.78	0.10	0.17	0.42	0.58	**Median [g]**
Standard deviation	0.55	0.55	0.50	0.50	0.50	0.50	0.50	0.55	**Standard deviation**
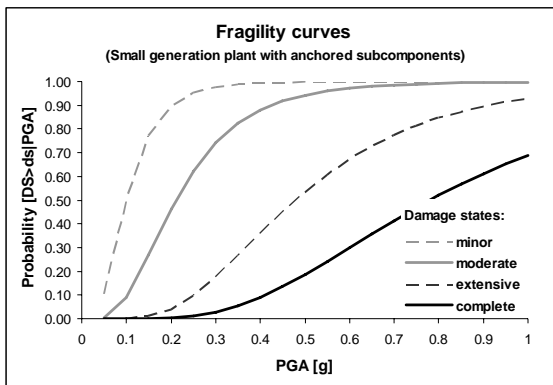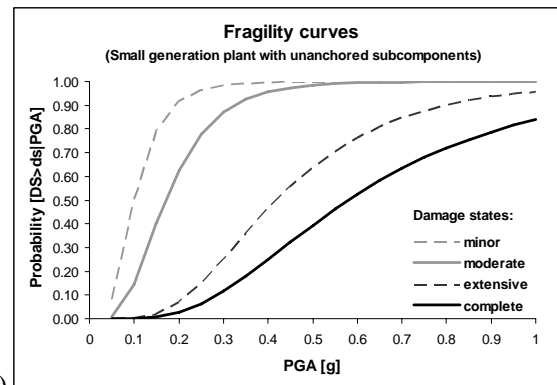
Figure 23: Fragility curves for small power plants with (a) anchored subcomponents and (b) unanchored subcomponents.

Damage states of medium/large generation plant								
	Anchored/Seismic component				UnAnchored/Standard component			
	minor	moderate	extensive	complete	minor	moderate	extensive	complete	
Median [g]	0.10	0.25	0.52	0.92	0.10	0.22	0.49	0.79	Median [g]
Standard deviation	0.60	0.60	0.55	0.55	0.60	0.55	0.50	0.50	Standard deviation
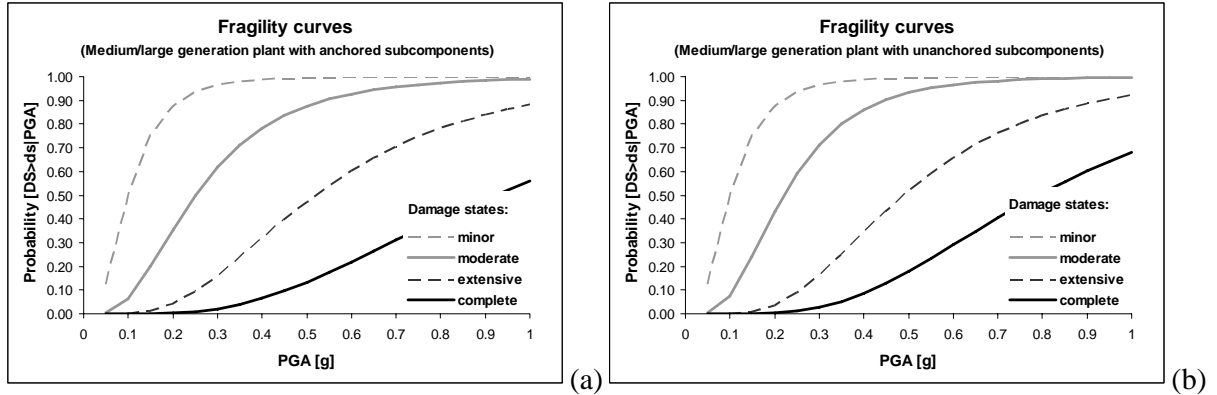
Figure 24: Fragility curves for medium/large power plants with (a) anchored subcomponents and (b) unanchored subcomponents.

5.1.2.2 Natural gas system

In the case of natural gas system, we use the fragility curves of the compressor stations, gas power plants, and pipelines. Fragility curves for the power plants are already presented in chapter 5.1.2.1. The same can be used here because the fragility curves for the power plants are not fuel-dependent.

Compressor stations

Compressor stations serve to maintain the flow of gas in the transmission pipelines. In the analysis of natural gas network no differentiation is made between the types of the compressors (centrifugal or reciprocating). Compressor stations are categorized as having either anchored or unanchored subcomponents. Compressor stations are mostly vulnerable to PGA. As for the electricity network the fragility curves are lognormally distributed functions that give the probability of exceeding 5 different damage states for a given level of ground motion characterized by PGA.

In order to estimate he probability of exceedence of certain damage state of compressor station the following items are required as input:

- Geographic location of the compressor station (longitude and latitude).
- PGA.

Damage states of compressor substation								
	Anchored/Seismic component				*UnAnchored/Standard component*			
	minor	moderate	extensive	complete	minor	moderate	extensive	complete	
Median [g]	0.15	0.34	0.77	1.50	0.12	0.24	0.77	1.50	**Median [g]**
Standard deviation	0.75	0.65	0.65	0.80	0.60	0.60	0.65	0.80	**Standard deviation**
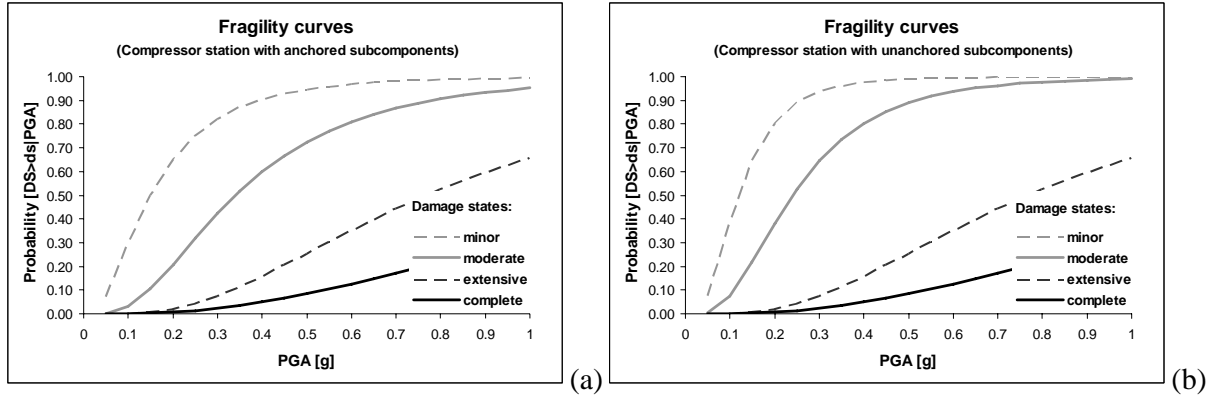
Figure 25: Fragility curves for compressor stations with (a) anchored subcomponents and (b) unanchored subcomponents.

Natural gas pipeline

For pipelines two damage states must be considered: namely, leaks and breaks. Generally, when a pipeline is damaged due to the ground failure the type of damage is likely to be a break. This type of damage is correlated to the permanent ground displacement (PGD). When the pipe is damaged due to the seismic wave propagation, the type of damage is likely to be due to leakage. It has been reported in [16], that the earthquake damage statistics give close correlation of pipeline leaks with the peak ground velocity (PGV). In earthquake risk assessment the use of these two parameters of ground motion are not as widespread as PGA. Therefore, it would be very useful to have PGA-related fragility curves. Wald et al. [23] suggest a conversion from PGA to PGV presented in Table 3. We use it to construct the fragility curves of pipeline due to the seismic wave propagation related to PGA. However, we had to factor out damage caused directly by ground failure because seismic hazard maps for PGD values (or relations of PGD with PGA) are not available.

In [15] and [22] different fragility curves of pipelines are presented, while the HAZUS methodology incorporates the fragility relationship of O'Rourke and Ayala [16]. The pipe diameter is not considered as an influential factor. Their function (Equation (4)) estimates expected number of repairs per unit length dependant on the PGV [cm/s]. By the HAZUS definition, this repair rate function covers damage mechanism that results in 20% of breaks and 80% of leaks.

$$RR[repairs/km] = k \times 0.0001 \times PGV^{2.25} \,, \tag{4}$$

where the constant factor $k = 1$ in the case of brittle pipes and $k = 0.3$ in the case of the ductile pipes. Classification of pipes is made according to the material and the joint type. Brittle pipes are asbestos cement, concrete, cast iron, and pre-1935 steel. Ductile pipe types are steel, ductile iron or PVC. Steel pipes with gas-welded joints and those where information on the joining process are considered brittle, whereas steel pipes with arc-welded joints are considered ductile. Although most pipelines are typically made of ductile steel, we classify all the pipelines as brittle because in our database there is no information on the type of joining between pipe lengths (i.e. a pipe system made of two ductile pipe sections joined by brittle joints, comprehensively inherits the brittleness of the joint)

Table 3: Correlations between different ground motion parameters for description of an earthquake event.

PERCEIVED SHAKING	Not felt	Weak	Light	Moderate	Strong	Very strong	Severe	Violent	Extreme
POTENTIAL DAMAGE	none	none	none	Very light	Light	Moderate	Moderate/Heavy	Heavy	Very Heavy
PEAK ACC.(%g)	<17	.17-1.4	1.4-3.9	3.9-9.2	9.2-18	18-34	34-65	65-124	>124
PEAK VEL.(cm/s)	<0.1	0.1-1.1	1.1-3.4	3.4-8.1	8.1-16	16-31	31-60	60-116	>116
INSTRUMENTAL INTENSITY	I	II-III	IV	V	VI	VII	VIII	IX	X+

Repair rate function is a useful indicator to characterize the probability of having pipeline ruptures since it allows estimation of the mean occurrence rate of the break. Supposing that the ruptures occur continuously and independently of one another, the Poisson process can be introduced as follows:

$$P(R = r) = \frac{(RR \times L)^r}{r!} e^{(-RR \times L)} \tag{5}$$

Equation (5) presents the probability that the number of ruptures R equals r within a given pipeline segment of length L. Moreover, the probability of at least one pipeline rupture occurrence of the pipeline is:

$$P(R > 0) = 1 - P(R = 0) = 1 - e^{(-RR \times L)} \,. \tag{6}$$

At this point we assume that the occurrence of one rupture impairs the pipeline functionality. So Equation (6) can be used as a fragility curve for the pipeline malfunction or simply failure.

In order to estimate the probability of pipeline's failure the following items are required as input:

- Geographic location of the end node of the pipeline (longitude and latitude).
- PGA (preferably PGV and PGD),
- Properties of the pipelines for the classification (material and type of welding).

(a) (b)
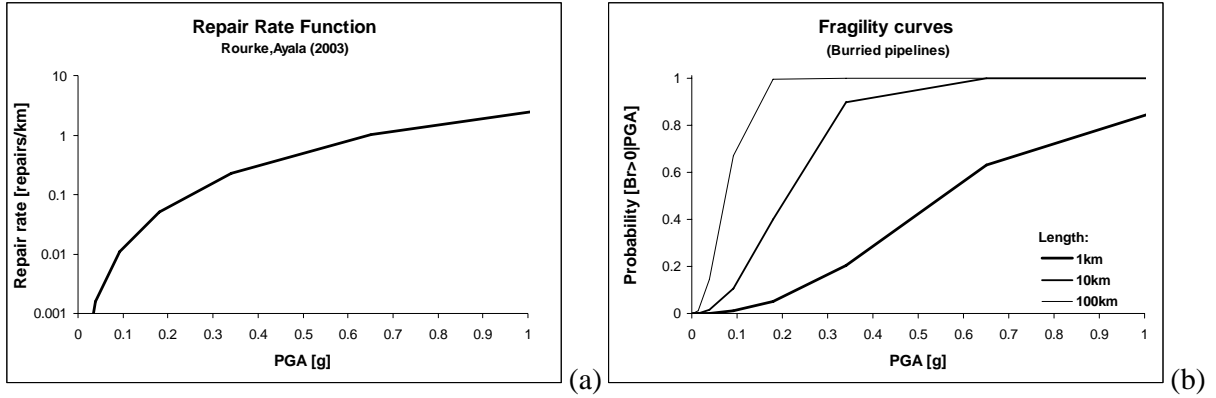
Figure 26: Repair rate for the pipelines (a) and fragility curves (b) for the different length of the pipeline.

6 Probabilistic reliability model

Every element of a network experiences different seismic demand depending on its geographical location and its dynamical characteristics. Our main interest is how the seismic damage of each of the vulnerable network's elements affect the overall network performance. In our model only seismic damage that causes evident mechanical element failure which could be detrimental to the operability of the other elements in the network is considered. It is presumed that, eventually, the topological deterioration of the overall connectivity due to the failure of any of the element/s compromises the functionality of the entire network.
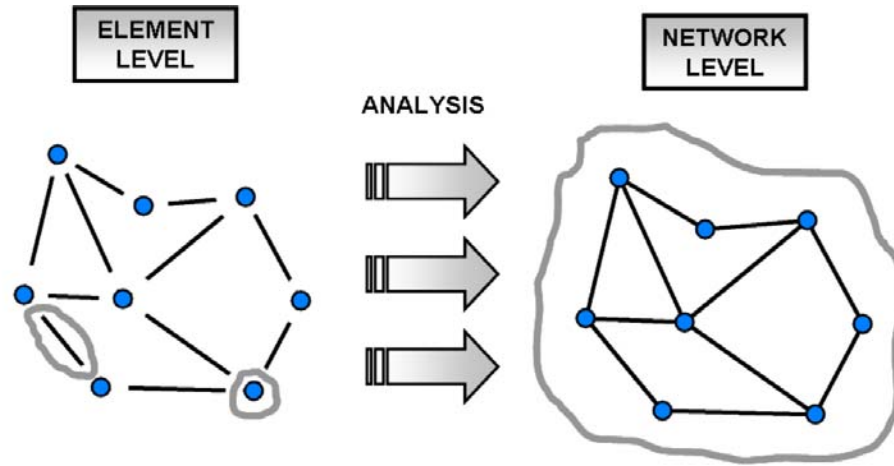
Figure 27: Propagation of probabilities of elements failure through the analysis.

Therefore, determination of element failure implies the generation of a damaged network. In principle, the connectivity analysis of the damaged network assesses the extent to which it is capable of operating functionally, but our analysis does not consider dynamic processes like simulation of cascading failure. Detection and development of cascading failures is possible to track down using power flow analyses; however, such an analysis requires an extensive dataset of possible flows and existent capacities outside the scope of our analysis.

Earlier we introduced the probability of failure for each element, so now our model must be able to propagate all these singular probabilities of failure through the network and present the result as the probability of failure or probability of exceeding any other defined damage state of the whole

network. This transformation from element level to the network level was performed using Monte Carlo simulations.

Monte Carlo simulation is one of the most widely used techniques in simulating the behaviour of physical systems. Its advantage lie in the simplicity of modelling systems with a large number of uncertain parameters (random variables) with imprecisely known (or in many cases even assumed) characteristics of their probability distributions. It will be presented in more details in chapter 6.2.2.

6.1 Performance measures

So far, we have shown how the input data has been collated. In addition to the network datasets, we have presented the seismic hazard (seismic hazard map) and seismic risk (fragility curves of the elements) of the networks elements in terms of probability distributions. Before proceeding with the network analysis we must introduce network performance measures. If we are to compare the robustness of the network to the quality of the network's performance we need various parameters that quantify the network's performance regardless of the hazard type.

Such measures must have two important attributes. First, they should be a representative characteristic of the whole network, and secondly they should be able to quantifiable. Consequently, the definition of damage states can be introduced in relation to the various descriptive parameters chosen to quantify damage (i.e. the undelivered power or the population affected). Finally when the performance measures are presented as the probability estimation in the form of network fragility curves, they can be used as surrogate measures for risk indicators. However, they also directly reflect the response of the network under the chosen hazard. In the following chapters, connectivity loss, power loss and impact on population are presented. They are based upon the topological properties taken from graph theory, but the last two measures, power loss and impact factor on population, can be exported to GIS database in order to evaluate actual impact of the seismic disruption of the (dependant) electricity network on the electricity supply to the population.

6.1.1 Connectivity loss

For this purpose, we employ the concept of connectivity loss defined in [1]. Connectivity loss $CL\,[\%]$ measures the decrease of the ability of every sink vertex to receive flow from the source vertices. It requires division of vertices into sources, transmission vertices, and sinks (chapter 4.1).

N_{source} is the number of the sources in undamaged network, and N^i_{source} is the number of the sources connected to the i-th sink vertex in the damaged network.

$$CL = 1 - \left\langle \frac{N^i_{source,dam}}{N_{source}} \right\rangle_i \qquad (7)$$

Values of connectivity loss range from 0-1 (or 0-100%) where the undamaged state is characterized by $CL = 0$. Since the original electricity network is considered one single strong component, each sink vertex is connected to all the sources. Nevertheless, in real networks we cannot always assume the strong component condition. For that very reason, we modified Equation (7) in order to apply it on disconnected networks as well.

$$CL_{mod} = 1 - \left\langle \frac{N^i_{source,dam}}{N^i_{source,orig}} \right\rangle_i \qquad (8)$$

In the case of disconnected networks, the connectivity analysis starts from the undamaged network in order to count the number of the sources connected to the i-th sink vertex in the undamaged network $N^i_{source,orig}$.

The basic process in the procedure of calculating the connectivity loss is checking the existence of the path between the sources and sink vertex. For this purpose, the breadth first search algorithm (reference: BGL library) is employed. The results of the breadth first search are the trees (of the shortest path) with all the vertices with the root in each of the source vertices. However, it can happen, that the shortest path between the source and the sink run through another source vertex. The breadth first search algorithm cannot distinguish among the types of the vertices. In order to avoid this undesired solution we made the networks directed (Chapter 4.1). So the connections can carry directional or undirectional flow. In our case, most of the connections can still carry undirectional flow except that the flows from the sources to their adjacent vertices are always defined and directed towards the transmission vertices. When the analyzed network is directed, it is important that the roots of breadth first search trees are source vertices. The final calculation of the connectivity loss measure goes through the counting process of the relevant shortest paths.

Since connectivity loss is a network characteristic, it can be used for definition of network damage states. Dueñas-Osorio et al. (2007) used the following network damage states:

- Minor: $DS_2 = 20\% \, CL$,
- Moderate: $DS_3 = 50\% \, CL$,
- Extensive: $DS_4 = 80\% \, CL$,

6.1.2 Power loss

We employ the size of the power plants in terms of operating power [MW] and define the power loss PL [%] as the next performance measure. It follows a similar concept to connectivity loss:

$$PL = 1 - \left\langle \frac{P_{dam}^i}{P_{orig}^i} \right\rangle_i \tag{9}$$

P_{orig}^i and P_{dam}^i are the sums of the power of all the power plants connected to i-th distribution substation in the undamaged and damaged network, respectively. Undamaged state has $PL = 0$.

6.1.3 Impact factor on population

Considering that each distribution substation supplies electricity to an assigned population area, we can evaluate the impact of the disruption of the electricity network under seismic hazard on the population. So, we know the number of people POP_i that are assigned to each distribution substation (chapter 4.1). Besides, in the previous chapter we have already calculated the decreased electricity power supply P_{dam}^i / P_{orig}^i for each distribution station. We can assume that part of the population is still supplied by electricity while another part undergoes shortage. The division between supplied and affected population is executed in the ratio of still-disposable to lost electricity power. Therefore the part of supplied population covered by the i-th distribution substation equals the normalized power supply of the i-th distribution substation in the damaged network (chapter 6.1.2). Finally, the overall impact factor IP [%] is calculated as the normalized value of affected population. It equals 0 in the case of undamaged network.

$$IP = 1 - \frac{\sum_{i=1..N_D} \frac{P_{dam}^i}{P_{orig}^i} POP_i}{POP_{all}} \tag{10}$$

Like connectivity loss, power loss and impact factor on the population are also network characteristic ranging from 0 to 100%, and they can be used for the definition of network damage states.

6.2 Seismic performance network analysis

6.2.1 Applied terms

Due to the lack of data needed for the whole analysis and the complexity of the problem, the following items are taken into account with the simplified approach or are not considered at all:

- Electricity and gas networks are spatially distributed structures. So each element is exposed to a different magnitude of a given seismic event (in terms of magnitude of PGA) by virtue of its location on the seismic hazard map even when we consider the same hazard level. Consequently, the fragility curves of the whole network are dependent on the hazard level or the return period. The larger the geographical area covered by the network, the larger the range of the PGA applied to the elements of the network. In spite of this, the fragility curves of the networks are presented as a function of the maximum expected PGA to which the network, as a whole, is subjected to.

- For the network fragility curves, we need to consider more hazard levels because a single hazard level explains only one point in the desired fragility curve of the network. The ideal situation would be to have a hazard curve for each element whose vulnerability is questioned. Unfortunately, the seismic hazard map [12] for the whole Europe exists only for 475 return period with 10% of probability of the exceedence at the 50 years of exposure time. But if we assume that trends of all hazard curves (Figure 19) are the same, we can multiply the values of PGA from the existent seismic hazard map with the general factor. This PGA factor should be less than 1 if we would like to have lower hazard levels, and more than 1 if we would need the ground motion parameter for the higher hazard levels. This way we do not know exactly which hazard level is under consideration. Nevertheless, we have already determined that the only relevant information in the final network fragility curves is the maximum expected PGA applied to the network.

- The soil type associated to the facilities of the network is not generally known. To take advantage of the GIS tools the geological map of the area defining the soil types would be very useful, but unfortunately this is not available in our analysis. Therefore, in this study the influence of the local soil type on the seismic risk is not considered.

- The seismic response of the pipelines due to ground failure could not be considered. For this purpose we would need the seismic hazard maps describing permanent ground motion that were also not available.

Furthermore, the following assumptions were considered in the analysis:

- In order to define the functional state of an element exposed to seismic hazard we must define which damage state is considered to meet the failure criterion. Failure criterion implies at least damage beyond the short-term repair for the facility to become a functional part of the network system immediately (or shortly) after the event. In the case of the power plants, substation, and

compressor stations the failure is considered as the extensive damage state. In HAZUS this damage state is referred to as ds_4 (Chapter 5.1.2.1). In the case of pipelines, malfunction of the connection is considered for the occurrence of at least one rupture on the segment between two adjacent vertices.

- The analysis considers that the designs of facilities fulfil all seismic criteria. Nevertheless, information of this type is not available in the database

- In the case of the electricity network, the power plants and substations are considered as the vulnerable part. Evaluation of the seismic response of these elements defines vertices that fail. Elimination of failed vertices will generate the damaged electricity network. In the case of the gas network the pipelines, compressor stations, and gas power plants are considered as vulnerable elements. Evaluation of their seismic response defines vertices and edges that fail. Elimination of failed edges and vertices will generate the damaged gas network.

- The data of the compressor stations in the Platts database [19] were not always consistent with the situation derived from other data (e.g. satellite images). Therefore, only the source vertices of the gas network were defined to function also as compressor stations.

- When defining damaged pipelines in the gas network, multiple lines are taken into account; but when there is more than one pipeline between two adjacent vertices, the evaluation of the seismic response (including the random part of the Monte Carlo smulations) is executed for each of them.

- We deal with directed network whenever analyzing the connectivity (Chapter 6.1.1). So, in order to simulate the flow in both directions we also provide the arc for both directions. This is not the case when we examine the failure of the pipeline. The rupture of the pipeline segment that carries bidirectional flow stops the flow in both directions. So, in this situation the network is regarded as undirected.

- The pipeline itself is the spatial structure. Namely, one segment (the part between two adjacent vertices) geographically lies on the points with different values of PGA. In order to determine the probability of failure from the fragility curves we apply the maximum of the PGA values assigned to the end vertices of the segment.

- Fragility curves of the pipelines are length-dependent. If we fix the parameter of PGA value in the fragility curve's equation, longer pipelines are exposed to higher probability of occurrence of at least one damage along the pipeline. Therefore, the pipeline vulnerability increases with its length, but because the compilation of the gas network from the GIS data included the merging of long segments in order to reduce the topological size of the network (number of vertices and number of edges), artificially long segments of pipeline were generated. In reality, edges (pipeline lengths) are sectioned by many crossings with the distribution pipelines of smaller diameter. When eliminating the distribution network from the gross data set, the remaining pipeline segments were assembled together from those short segments. Consequently, the lengths of many edges in analysed network are longer compared to reality and their vulnerability turns out to be higher (because longer stretches of pipeline are more

vulnerable). In order to mitigate undesirable consequences of artificially long merged pipelines we consider only $1/\left(N_{CR}+1\right)$ of their length for calculation of their fragility curves; where N_{CR} stands for the number of crossings on each gas pipeline.

6.2.2 Monte Carlo simulations

The uncertainties due to randomness --not only in the magnitude of the seismic event but also in the seismic response of the facilities—are propagated through the network analysis when using Monte Carlo simulations. We refer to this model as the seismic performance network analysis. Despite the random input values, the model analysis itself is solved as a deterministic calculation. For example all the probabilities of exceeding a certain damage state of the networks elements can be converted into an absolute damage state; this is the advantage of Monte Carlo simulation.
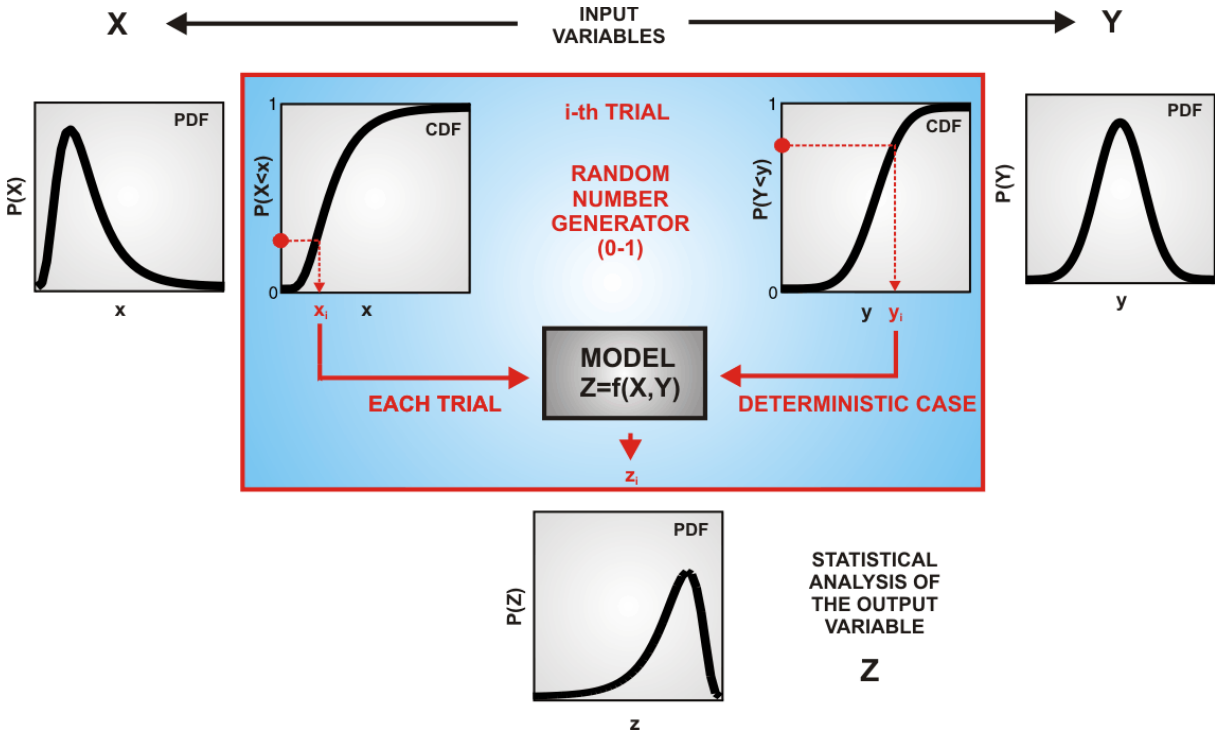

Figure 28: Monte Carlo simulations scheme.

Monte Carlo simulation is a numerical approach. It performs trials, and each trial is one deterministic solution of the phenomena. The input variables for the model for each trial are defined from a cumulative distribution function of the random variable (Figure 28) with random number

56

generator. In our case, a random number between 0 and 1 selects a damage state for each element. We compared the random number with the probabilities of exceedence of a certain damage state obtained from fragility curve of each element. The mathematical realisation of a trial of 'dice-throwing' vis-avis the occurrence of a seismic event of a certain magnitude results in one frame representing a damaged network, and the outputs of the model in one trial represent one of the possible results. The increasing number of trials N_{trials} decreases the error in the ratio $1/\sqrt{N_{trials}}$.

For the presentation of the final simulation results, we perform a statistical analysis of the outcomes of all the trials. Thus the statistical approach allows one to asses the probabilities of all possible outcomes by looking at only a few outcomes.

6.2.3 Algorithm

So far we explained the fundamental role of the probability reliability model, then we showed how we can apply network analysis for the calculation of the networks' performance, and we integrated the data of seismic hazard and vulnerability of infrastructure into the network definition. Finally, we can say that our probabilistic reliability model consists of seismic-performance network analysis enriched with the Monte Carlo simulations. The desired results of the probabilistic reliability model is the presentation of the outputs of seismic performance network analysis as the network fragility curves in terms of the performance measures (connectivity loss, power loss, or impact on population).

The basic steps of seismic performance analysis of the whole network are:

1. Choose the seismic hazard level.
2. Identify the location of all the vertices of the network and assign the PGA value to this location.
3. Find the probability of exceeding the limit damage state for all the vulnerable elements of the network from the relevant fragility curves.
4. Execute the random number generator with the uniform distribution between 0 and 1 for all the elements. An element is damaged when its random number is smaller than the probability attained in the step 2.
5. Define the damaged network.

    At this stage, the elimination of each considered element is dependent merely on its location (PGA), dynamical characteristics that reflect the seismic response (fragility curves) and random number generator but it is independent from the other elements. Afterwards, the edges with at least one end-vertex eliminated are deleted from the network by virtue of the fact that

they are disconnected from the main network core and not because of statistical dependence among the elements.

6. Perform the network analysis (model analysis) to obtain the connectivity characteristics of the damaged network.

7. Determine the performance measures (connectivity loss, power loss, and impact on population).
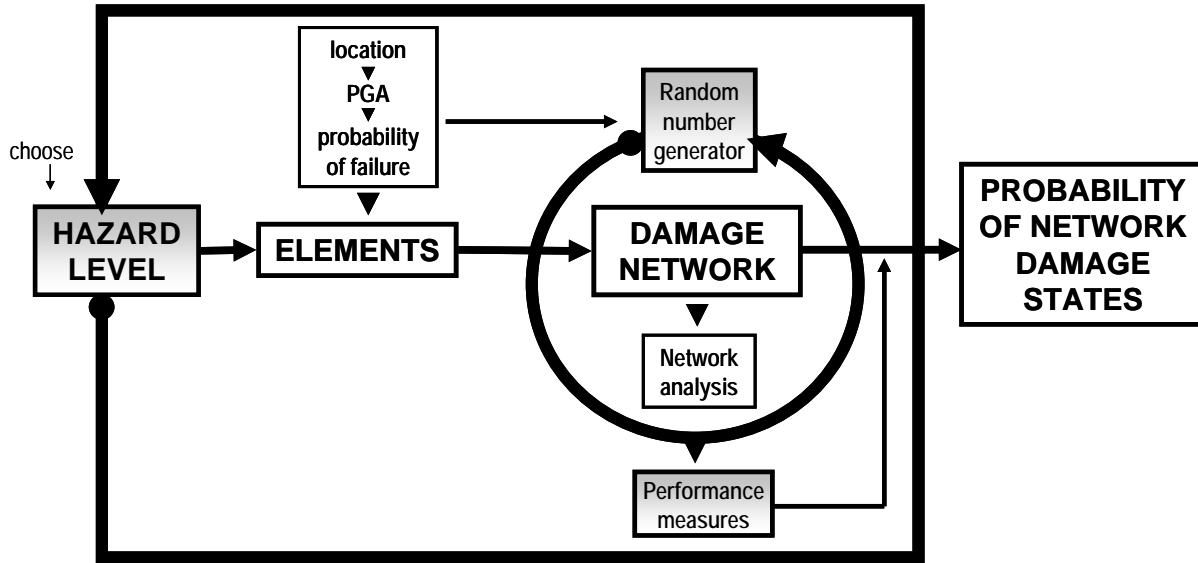
Figure 29: The algorithm applied in the MatLab procedure.

Steps from 4-7 perform one trial in Monte Carlo simulation; repeating these steps we are executing more trials and afterwards we determine the distribution of the networks performance measure. The best way to present them is the complementary cumulative distribution function which defines the probability of exceeding the given value of the performance measure. For a better understanding, the probability of exceeding a chosen performance measure is the ratio of number of trials where the performance measure exceeds this value according to number of all the trials. Thus, one curve of the complementary cumulative distribution function of the performance measure corresponds to one hazard level.

In order to execute the entire mapping out of the probability distribution of performance measures this process is performed at several PGA factors (reflecting different hazard levels). Only then, does the response data capture satisfactorily the phenomenon behaviour allowing construction of the network fragility curves.

After all the series of trials are completed we introduce the notion of network damage states. The probabilities of exceedence of certain damage states at each hazard level characterized with PGA become the input for the calculation of network fragility curves. The description of the given network damage state corresponds to one fragility curve whereas the Monte Carlo simulations executed at one hazard level contribute only one point to the fragility curve at a given limit damage state. Finally, the network fragility curves can be established by fitting the results of the probabilities of exceeding a given network damage state to a cumulative lognormal distribution function (see for example in [8])

7 Probabilistic model for network interdependency

Interdependence among infrastructure systems is a nontrivial problem because factors of different nature contribute to their coupling characteristics. Rinaldi et al. [20] define interdependency as "a bidirectional relationship between two infrastructures through which the state of each infrastructure influences or is correlated to the state of the other"'. They presented a, so-called, six dimensional framework to explore the complexity of interdependency. The following dimensions could be considered as interdependent coupling terms: type of interdependency (physical, cyber, geographic, logical), coupling and response behaviour (degree of coupling, the coupling order, and the complexity of the connections), infrastructure characteristic (organizational, operational, temporal range of infrastructure dynamics, spatial scales), infrastructure environment, type of failure (common cause, cascading, escalating) and network state operation (normal, disruption or restoration mode). Such a thorough quantification of networks interdependency is practically impossible due to insufficient or ill-defined parametric data, therefore, the concept of multidimensional coupling dimensions is currently accepted only for generic description and identification of the interconnectedness behaviour. From this point of view, it can be a useful tool for a qualitative overview of the problem in order to find out representative mechanisms that trigger interconnectedness.

In general, fewer fundamental parameters are necessary to capture the essential mechanisms of coupled networks. The criteria for selecting them depends on how difficult it is to obtain pertinent data and possibility to explore their behaviour in a mathematical sense. Nevertheless, the more prior knowledge of the phenomena of interconnectedness between real complex networks exists the more objective judgment can be used for the simplification of its modelling approach.

7.1 Fundamental interdependence

We selected three aspects for establishing the model of network interdependencies. These are physical interdependence, direction of the interaction, and degree of coupling.

Physical interdependence

Two infrastructures are physically interdependent if the state of each depends upon the material output of the other. For the electricity network we may consider that part of the electricity generated is produced by gas-fired power plants, for example. Of course, there are other examples implicitly related to the flow of gas; for example, if no gas is available for home heating, end users tend to use electricity appliances. In our analysis we shall only consider the explicit coupling related to major gas-fired electricity power generation.

Direction of the interaction

As defined in ([20]), interdependency refers to the relation when each of the infrastructures is dependant on the other. In our case, the direction of interconnection is one way only: with dependence of electricity network on gas network, whereas the supply of electrical energy to run the compressor stations is not taken into account (many compressor stations run on gas). Therefore, the gas network is independent while the electricity network is partially dependent on the gas network.. For this reason, we sometimes use the term dependency instead of interdependency when we refer to our example of coupled system.

Degree of coupling

Whenever there is interaction between two systems, the question arises: what is the degree of coupling? Borrowing from [18], we classify interactions as either tightly coupled or loosely coupled. Furthermore, degree of coupling is measured with the strength of coupling which quantitatively implies how fast the disturbances propagate from one network to the other: the higher the strength of coupling the tighter the coupling. Tightly coupled interactions are those that do not tolerate delay; i.e., the process of interaction is time-dependant with little slack. So, disturbances in the gas supply would have an almost immediate effect on electrical power generation. On the other hand, loose coupling implies that the infrastructures are relatively independent of each other and the state of one infrastructure is weakly correlated to, or even independent of, the state of another. Slack is present in the system because the propagation of the disturbances from one network to another is very slow. There are even more possibilities of the regulation of the strength of coupling depending on how slow the propagation of the disturbances is; for example, a gas power plant could have the local gas storage or could even switch to alternative fuel. Such situations imply different levels of

loose coupling of the gas power plant to the gas network. In short, tight and loose couplings refer to the relative degree of dependencies among infrastructures.

7.2 Interoperability matrix

We modelled all three aspects of electricity network dependency on the gas network with the interoperability matrix. A similar approach was adopted by [8]. A set of conditional probabilities of failure are compiled and put together in such a way that the interoperability matrix reflects the physical interdependence, direction of interaction and strength of coupling of our dependency behaviour.

Generally, we need two interoperability matrices to capture the bidirectional relationship between two networks. With one interoperability matrix we can simulate only the coupling behaviour in one direction. The size of the interoperability matrix is always $N_{independent} \times N_{dependent}$, where $N_{independent}$ refers to the size of the independent network and $N_{dependent}$ is the size of dependent network. Two possible interoperability matrices arises by switching the roles between dependent and independent networks. For example $I_{E/G}$ is a $N_G \times N_E$ interoperability matrix which captures the effect of gas network on electricity network and $I_{G/E}$ is a $N_E \times N_G$ interoperability matrix which captures the effect of gas network on electricity network (N_G - size of the gas network, N_E - size of the electricity network). In our study we know in advance that $I_{G/E}$ will have only zero entries, therefore the direction of the interaction is immediately defined.

The type of dependency --in our case physical dependence-- helps us to define the adjacency matrix which is a simpler version of interoperability matrix because it contains only 0 and 1. If the vertex i from the gas network and the vertex j from the electricity network are adjacent, the (i, j) element in adjacency matrix receives the value 1 and presents the directed link between two networks. The inter-adjacent vertices are clearly defined because common elements of gas and electricity networks are gas power plants. They play a double role: the role of sinks in the gas network and the role of sources in the electricity network. So the natural gas transported along the pipelines of the gas network is needed as fuel for the gas power plants. On the other hand, the part of electricity energy transported through the substations in the electricity network is generated also in the gas power plants. Therefore the connections of gas power plants with both of the networks are unambiguously defined. While studying the vulnerability of dependant electricity network the gas power plants

belong to the electricity network. On the other hand when studying the vulnerability of the independent gas network, gas power plants are a constituent vertex. Only one (nearest) gas vertex feeds each power plant with the natural gas, whereas each power plant may have more than one connection to the transmission electricity network. Since all nodes in one network usually do not couple to all nodes in the other, the adjacency matrix is very sparse. Furthermore, the interoperability matrix is a weighted adjacency matrix, where weights describe the strength of coupling. The strength of coupling is defined as the conditional probability of failure of the electricity vertex at the given failure of adjacent gas vertex:

$$P\left(Failure\ E_j^{\text{dep}}\ |\ Failure\ G_i \right) = p_{Ej|Gi} \quad \text{for all } i \text{ adjacent to. } j \tag{11}$$

To be more precise, in the equation above, E_j^{dep} represents failure of the j-th element of the electricity network due to its dependency on the gas network and G_i represents failure of the i-th element of the gas network. In our case the failure of vertex G_i (the vertex from the gas network that is adjacent to power plant) conditions the failure of power plant E_j^{dep} with the probability $p_{Ej|Gi}$. In such a manner we can capture the effect of element failure in the gas network on the overall response (seismic hazard and interdependency effect) of the electricity network using the interoperability matrix.

7.3 Strength of coupling application

The seismic performance network analysis always starts at the element level of the network. First, the seismic response of each vulnerable element is calculated, and then the evaluation of the seismic response of the whole network is performed. Simultaneously the probabilities of failure of each element are propagated through the analysis in order to represent the final result with the probabilities of networks' damage states. But we also know that the seismic response of electricity network is partly dependent on the seismic response of the gas network. So, the overall response of the electricity network should reflect the vulnerability of the electricity under seismic hazard and the influence of the damaged gas network on the functionality of the electricity network. In order to introduce this extra vulnerability of the network due to interdependency, we have to return to the element level. Before repeating the seismic performance network analysis, we must first introduce additional information of coupling behaviour into the network definition and, then again, calculate the seismic response of each vulnerable element. In our case we apply the dependency effect

directly on the gas-fired power plants which we also consider to be vertices of the electricity network.

To consider interdependency behaviour with the probabilistic reliability model we need the updated probability of failure of electricity vertex. In general, the failure of the j-th vertex of the electricity network, denoted E_j, can occur due to an earthquake or due to the failure of the gas supply, denoted E_j^{earth} and E_j^{dep}, respectively. Therefore, the event E_j can be defined as the union of the events E_j^{earth} and E_j^{dep}:

$$E_j = E_j^{earth} \cup E_j^{dep} \tag{12}$$

Because $E_j^{earth} \cap E_j^{dep} \neq 0$, these two events are not mutually exclusive (Figure 30a) and the probability of the electricity vertex failure can be formulated as

$$P\left(E_j^{earth} \cup E_j^{dep}\right) = P(E_j^{earth}) + P(E_j^{dep}) - P(E_j^{earth} \cap E_j^{dep}) \tag{13}$$

Since we know that E_j^{earth} and E_j^{dep} are statistically independent the joint probability of E_j^{earth} and E_j^{dep} equals

$$P\left(E_j^{earth} \cap E_j^{dep}\right) = P(E_j^{earth}) P(E_j^{dep}) \tag{14}$$

If we insert Equation (14) into Equation (13) we get:

$$P\left(E_j^{earth} \cup E_j^{dep}\right) = P(E_j^{earth}) + P(E_j^{dep}) - P(E_j^{earth}) P(E_j^{dep}) \tag{15}$$

Do we know all the probabilities in the above equation? $P(E_j^{earth})$ is determined from the fragility curves of the elements' vulnerability under seismic hazard. As far as $P(E_j^{dep})$ is concerned, we know that event E_j^{dep} will occur only after the occurrence of the failure of the adjacent gas vertex denoted as event G_i. So, events E_j^{dep} and G_i are statistically dependent. The relationship among the probabilities of their occurrences is defined with the conditional probability that expresses the probability of event E_j^{dep} given the occurrence of G_i:

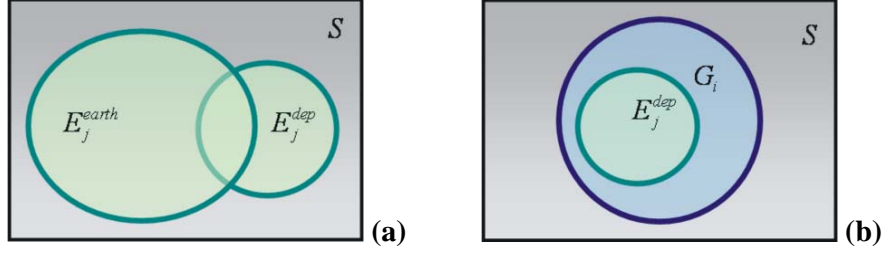$$P(E_j^{dep} \mid G_i) = \frac{P(E_j^{dep} \cap G_i)}{P(G_i)} \tag{16}$$

Figure 30: Venn diagram: (a) failure of the electricity vertex and (b) conditional probability of failure of electricity vertex because of dependency on the gas network due to the failure of the gas vertex.

It is convenient for our analysis that we deal with the extreme case of the dependent events where one set (events G_i) contains the other (events E_j^{dep}). Therefore the intersection of G_i and E_j^{dep} is explicitly defined as $E_j^{dep} \cap G_i = E_j^{dep}$ (Figure 30b). In a similar way, we can express the probabilities of occurrence:

$$P(E_j^{dep} \cap G_i) = P(E_j^{dep}) \tag{17}$$

Now, we can simplify the general Equation (16) for conditional probability. If we consider Equation (16) in Equation (17) we can define $P(E_j^{dep})$ as:

$$P(E_j^{dep}) = P(E_j^{dep} | G_i)P(G_i) \tag{18}$$

Eventually, for the realization of the $P(E_j^{dep})$ we need to know $P(E_j^{dep} | G_i)$ and $P(G_i)$, and $P(E_j^{dep} | G_i)$ is defined as the strength of coupling $p_{Ej|Gi}$ written in the interoperability matrix. Setting the value of the strength of coupling can either be done by setting it to be equal for all the gas power plants, or individually setting coupling strength for each power plant. In the first approach the strength of coupling reflects a general vulnerability of the electricity network to any kind of failures in the gas network. While for the second approach, individual strength of coupling can reflect a vulnerability of each gas power plant to shortage of gas supply. In our analysis we do not have sufficient information to set individual coupling strengths, and so we use a single strength of coupling throughout, but which can be tuned from complete independence $P\left(E_j^{dep} | G_i\right) = 0$, to complete interdependence $P\left(E_j^{dep} | G_i\right) = 1$ (Figure 31).

$$P(E_j^{dep}|G_i)=0.2 \qquad P(E_j^{dep}|G_i)=0.5 \qquad P(E_j^{dep}|G_i)=1$$
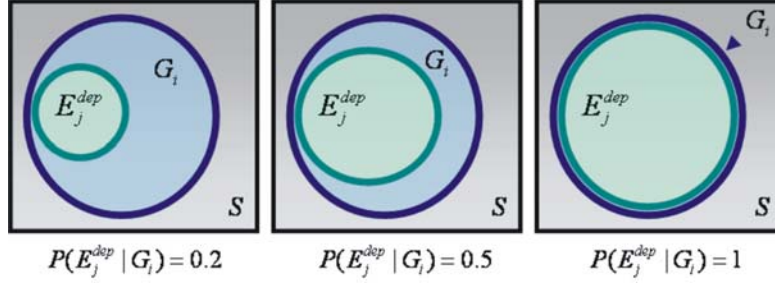
Figure 31: Strength of coupling in Venn's diagrams.

How do we compute $P(G_i)$? The failure of the gas vertex, event G_i, can be induced by an earthquake G_i^{earth} or by the disconnection from the sources $G_i^{connect}$. So, the event G_i is defined as the union of

$$G_i = G_i^{earth} \cup G_i^{connect} \qquad (19)$$

$P(G_i^{earth})$ are determined from the elements' fragility curves for the seismic hazard. While disconnection of gas vertices from the sources $P(G_i^{connect})$ reflects the seismic response of the whole gas network (Figure 32) and can be measured with the connectivity loss.
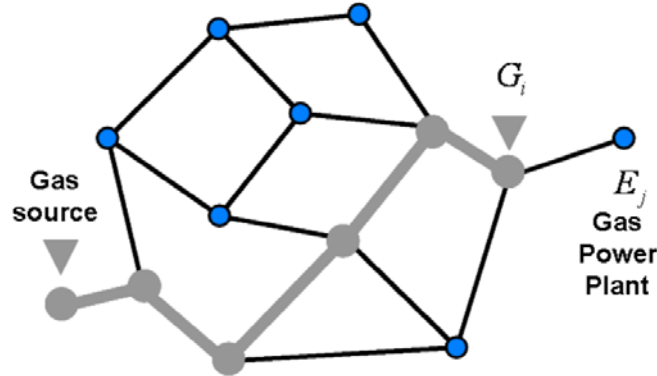

Figure 32: Schema of gas source supply stream of the gas power plant.

It is impossible to compute $P(G_i^{connect})$ analytically because it is associated with the probability of failure of other components in the gas network. But we can determine the probability of failure due to both causes $P(G_i)$ as a part of the seismic response analysis of the gas network using the Monte

Carlo simulation. For each gas vertex adjacent to a power plant the fragility curves are constructed in terms of connectivity loss and PGA. These fragility curves describe the vulnerability of the whole gas source supply stream under seismic hazard while taking into account the whole topology of the gas network as well. The gas source supply stream failure is defined with exceedence of the damage state defined with the 80% of connectivity loss of the gas vertex i that is adjacent to gas power plant.

Whenever the gas vertex i fails because of the earthquake hazard (event G_i^{earth}) the result of the simulation is 100% of connectivity loss for the gas vertex i. When disconnection is the cause of the failure the connectivity loss of i-th gas vertex is defined as

$$CL_{\mathrm{mod}}^i = 1 - \frac{N_{gasPP,dam}^i}{N_{gasPP,orig}^i} \tag{20}$$

$N_{gasPP,orig}^i$ and $N_{gasPP,dam}^i$ is the number of sources connected to the i-th gas vertex adjacent to gas power plant in the original and in the damaged network, respectively. Both events G_i^{earth} and $G_i^{connect}$ can happen simultaneously since they are not mutually exclusive ($G_i^{earth} \cap G_i^{connect} \neq 0$), but must not be considered twice (see Eq. (21)).

$$P\left(G_i^{earth} \cup G_i^{connect}\right) = P(G_i^{earth}) + P(G_i^{connect}) - P(G_i^{earth} \cap G_i^{connect}) \tag{21}$$

Finally, we can evaluate the seismic performance of network taking into account also the effect of the network dependency. The $P(E_j)$ is completely determined with $P(E_j^{earth})$, $P(E_j^{dep} | G_i)$ and $P(G_i)$. With the Monte Carlo simulation of element survivals, we construct the dependent network fragility curves. This time we execute two levels of random number generator in the range 0 to 1 to define the damaged network. In the first level we defined damaged vertices due to the earthquake hazard --checking if the random number is smaller than $P(E_j^{earth})$. In the second level we defined damaged vertices due to the dependency effect --checking if the random number is smaller than $P(E_j^{dep})$. The vertices whose failure arises by at least one of the two, above described, causes are eliminated.

8 Results of simulations

The output from the Monte Carlo simulations consists of network fragility curves expressed in terms of performance measures (Chapter 6.1). Performance measures try to capture two important issues of the interconnected system. First, the response of the system exposed to the seismic hazard and then the influence of interdependency effect. In our case, the gas network plays the role of independent network while the electricity network takes over the role of dependent network where the degree of coupling is regulated with the strength of coupling. In order to develop fragility curves for independent and dependent networks it is necessary to evaluate the network performance under several hazard levels and different strength of coupling.

Table 4: Maximum expected PGA in networks while applying different general PGA factor.

PGA factor	GAS NETWORK (EU) PGA$_{max}$ [g]	ELECTRICITY NETWORK (EU) PGA$_{max}$ [g]	ELECTRICITY NETWORK (IT) PGA$_{max}$ [g]
0.20	0.09	0.10	0.06
0.40	0.17	0.21	0.12
0.60	0.26	0.31	0.17
0.80	0.34	0.42	0.23
1.00	0.43	0.52	0.29
1.25	0.54	0.65	0.36
1.50	0.65	0.78	0.44
2.00	0.86	1.04	0.58
2.50	1.08	1.30	0.73
3.00	1.29	1.56	0.87

We consider 9 hazard levels. Since only one seismic hazard map is available for Europe (Figure 33), different hazard levels are modelled with the general PGA factor. The available seismic hazard map ([12]) is considered to have factor 1 and corresponds to a 475-year return period and 10% probability of exceedence in the 50 years of exposure time. As a rule of thumb the factors 1.25 and 2.5 correspond to 1000 and 10000 year return periods respectively. These estimations ([9]) are based on seismic hazard maps of different hazard levels than those shown for Slovenia (Figure 18).

Therefore, we cannot prove that the rule described is valid for the whole of Europe; even so, we get a feel of the range of the general PGA factor in view of the hazard levels.
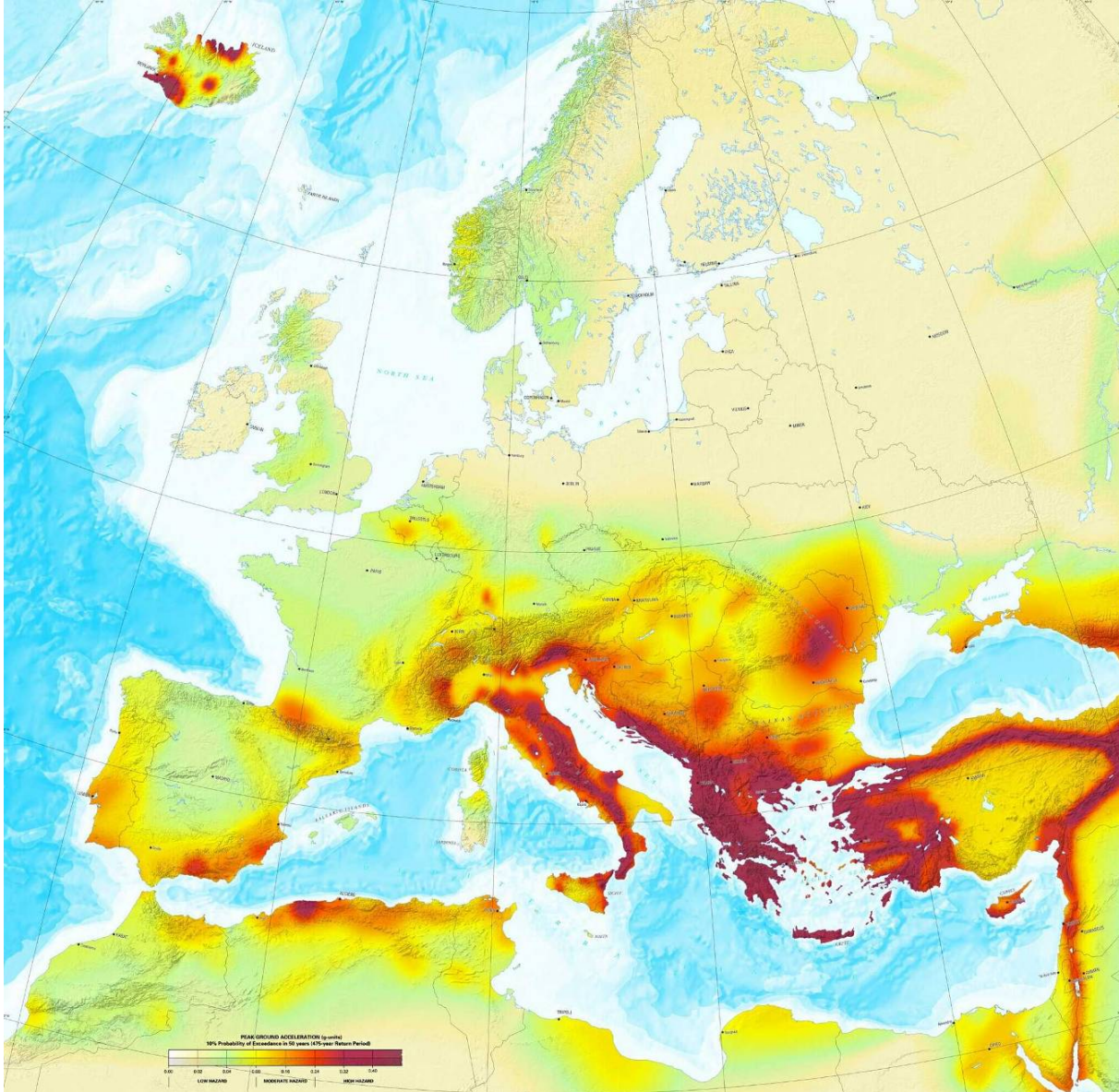

Figure 33: Seismic hazard map of peak ground acceleration for 475 year return period and 10% probability of exceedence in the 50 years of exposure time (Giardini et al., 2003).

General PGA factor used in this study are 0.2, 0.4, 0.6, 0.8, 1, 1.25, 1.5, 2, 2.5 and 0.4, 0.6, 0.8, 1, 1.25, 1.5, 2, 2.5, 3 for gas and electricity network respectively. The results of preliminary analysis

have pointed to the higher vulnerability of the gas network in comparison to vulnerability of the electricity network under the same hazard levels.

Even though we deal with spatially co-located structures, the maximum expected PGA of networks is not the same because of different micro geographical location of the vertices of each of the networks studied. The gas vertex with the maximum expected PGA is located in Turkey (Figure 34), whereas the electricity vertex with the maximum expected PGA is located in Greece (Figure 35).
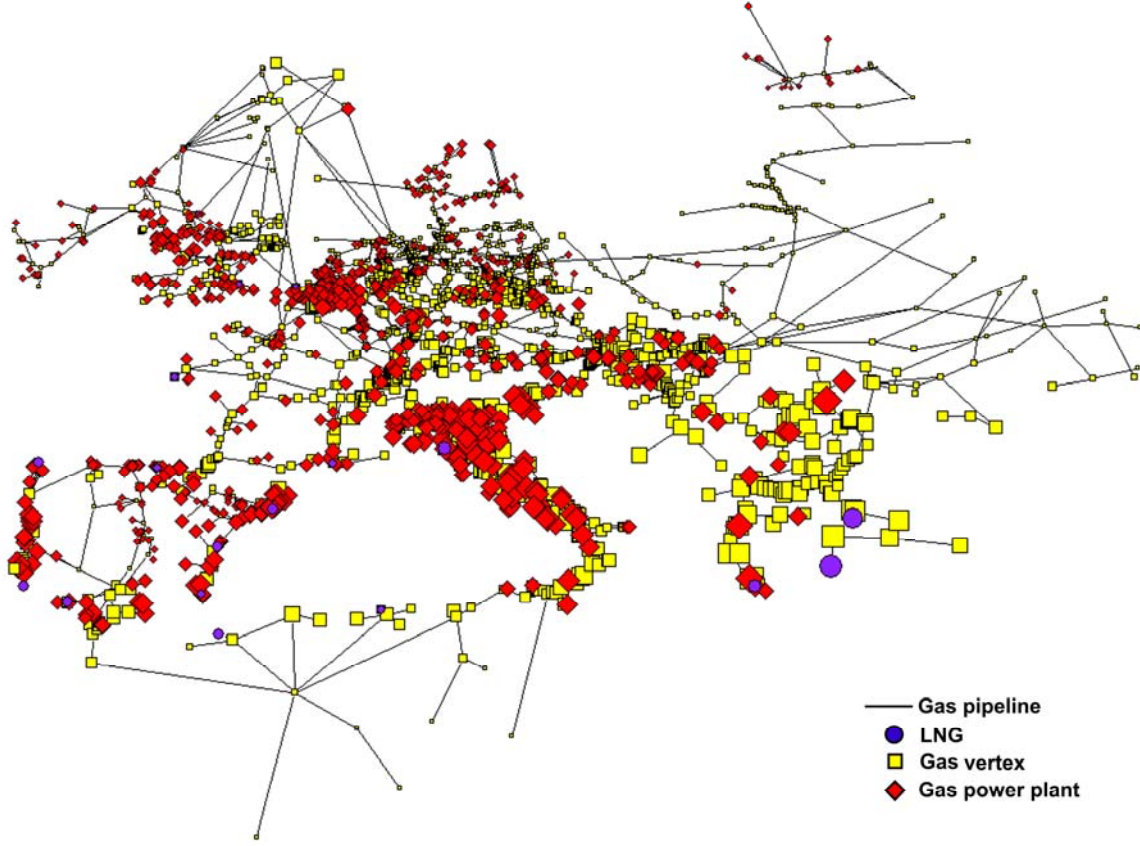

Figure 34: European gas network: The relative sizes of the vertices correspond to the PGA of their location obtained from the 475 return period seismic hazard map.

When interdependency effect is included, one series of trials is characterized not only by the hazard level but also by the strength of coupling. We consider three different values of strength of coupling to model the total independence ($P\left(E_j^{dep} \mid G_i\right) = 0$), the partial dependence ($P\left(E_j^{dep} \mid G_i\right) = 0.5$) and the complete dependence ($P\left(E_j^{dep} \mid G_i\right) = 1$). In order to construct the damaged network the same

strength of coupling is used for all gas power plants. Nevertheless, were we to have more detailed information on the response of each gas power plant to the disturbances of the gas fuel supply, the value of the strength of coupling could performed on a plant by plant basis.
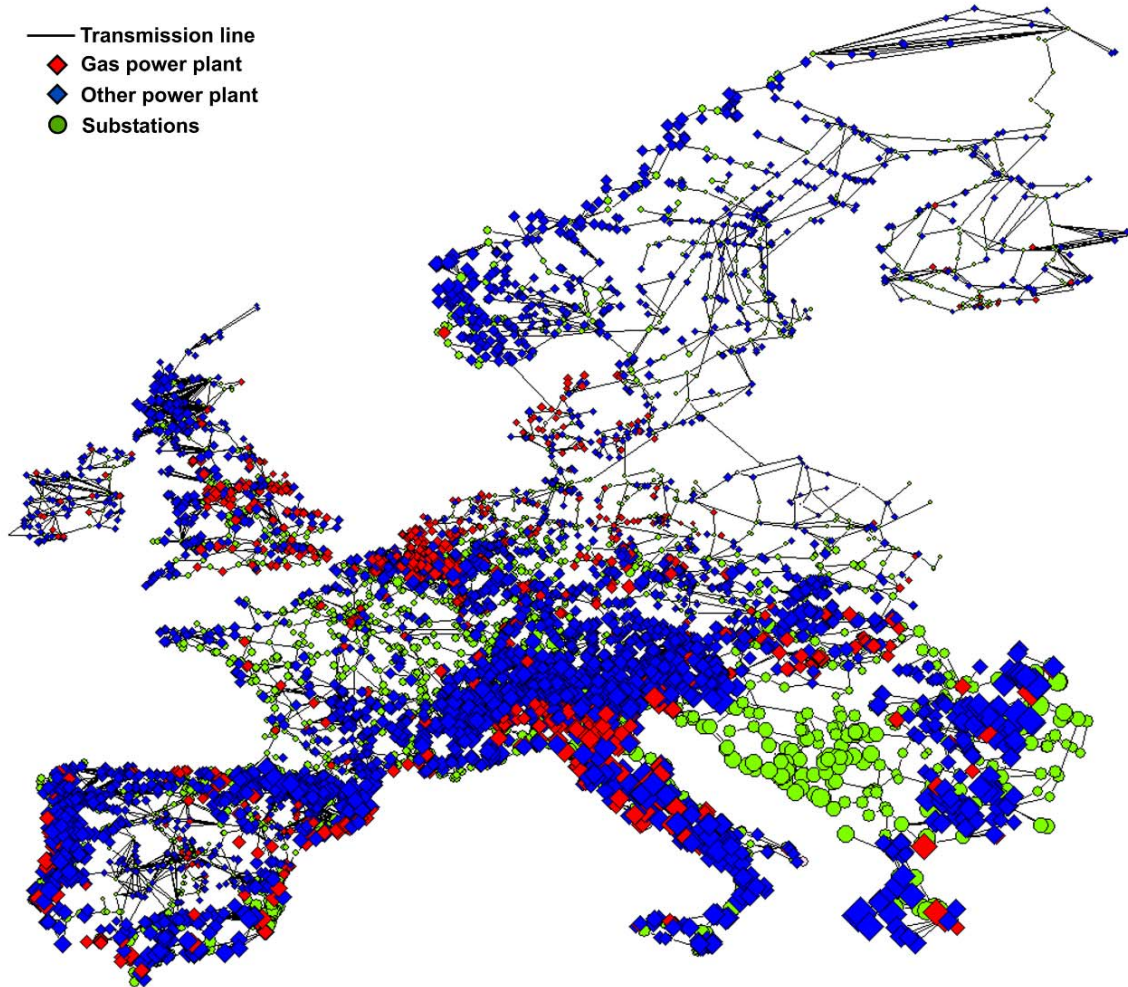

Figure 35: European electricity network: The relative sizes of the vertices correspond to the PGA of their location obtained from the 475 return period seismic hazard map.

The results of the Monte Carlo simulations, i.e. performance measures of the damaged network under one hazard level and one strength of coupling, are presented in statistical terms in the form of complementary cumulative distribution functions. For a certain damage state (Chapter 6.1) we obtain from each complementary cumulative distribution function one probability of exceedence for construction of the network fragility curves. Network fragility curves are presented as the lognormal

distribution function dependent on the maximum PGA in the network as the best fit to collected probabilities. We employ three damage states of network, i.e. minor, moderate and extensive, that are defined with the limiting value of the performance measure: 20%, 50% and 80% of connectivity loss (power loss or impact factor on population), respectively. The probability of occurrence of each damage state is described by one network fragility curve. In the case of the gas network the 10000 Monte Carlo simulations were executed, whereas in the case of electricity network we confined ourselves to 1000 simulations in one series of trials. This is because the electricity network has, not only five times more vertices, but also more than thirty times more source vertices. For this reason, the computational capacity in the case of the analysis of electricity network is in greatly increased.

First, we investigate the seismic response the gas and electricity networks as if they were independent. This is then followed by an additional analysis of the gas network in order to obtain the fragility curves of the gas source supply stream (this introduces the interdependency behaviour). Afterwards, the results of the seismic response of the dependent electricity network (we show the cases for Italy and whole of Europe) are presented. Finally, the geographical spread of damage at a European level is visualized in terms of the power loss and affected population.

8.1 Independent network vulnerability

In order to compare the independent gas and electricity networks, the connectivity loss as performance measure has been chosen to evaluate their response under earthquake load. Figure 36a and Figure 37a show the complementary cumulative distribution functions for different hazard levels. The results follow the trend that the probability of exceedence of certain value of connectivity loss increases with the hazard levels. These results are the basis for the fragility curves of different damage states in Figure 36b and Figure 37b. We observe that the more extensive a damage state the lower is the probability of its occurrence at any given PGA. This is very evident with the shift of the fragility curves of more extensive damage state to the right. Furthermore, these results show that gas network is more vulnerable to earthquake hazard than the electricity network. Notice that at the hazard level of 475 year of return period the performance of those two networks differs a lot. In the gas network the minor ($20\%\,CL$) and moderate ($50\%\,CL$) damage states would be certainly reached and for the extensive ($80\%\,CL$) damage state exists 44.4% probability of exceedence. On the other hand the electricity network is subjected to 6.2% probability of exceedence of minor damage state and 0% of probabilities of exceedence for $50\%\,CL$ and $80\%\,CL$.

How do we explain these results? In order to understand this phenomenon we have to examine the location and the role of the most vulnerable elements in gas and electricity networks.
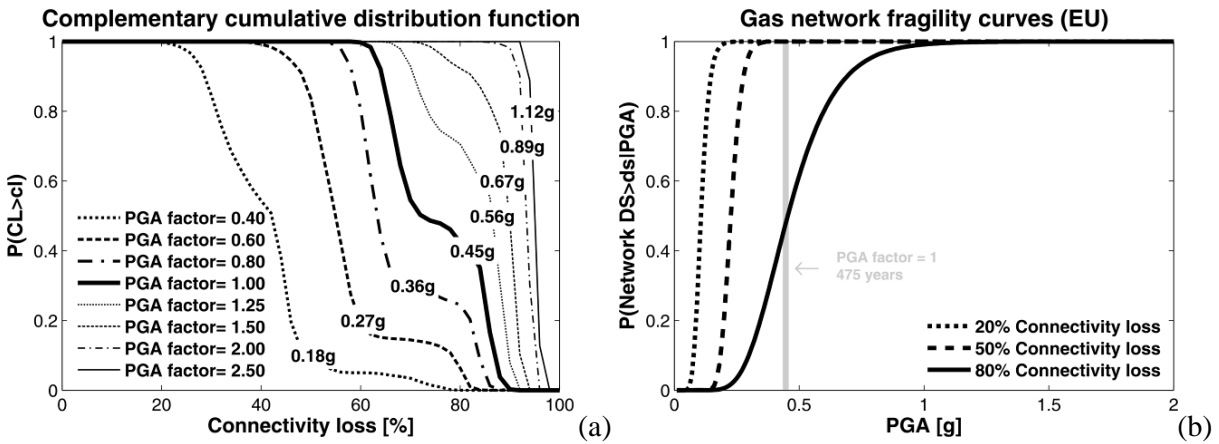

Figure 36: Results of Monte Carlo simulations in the case of European gas network presented for different hazard levels as complementary cumulative distribution function (a) and summarized in network fragility curves for different damage states (b).
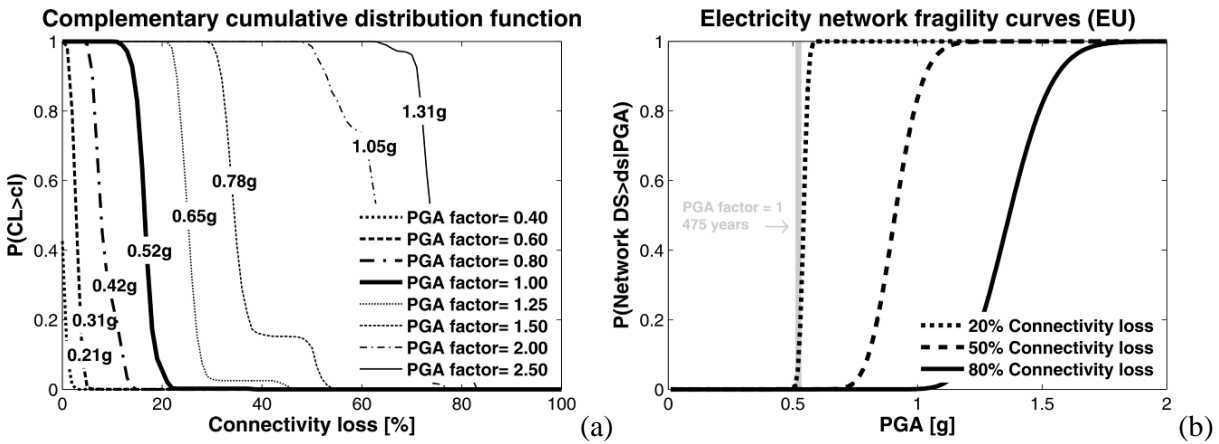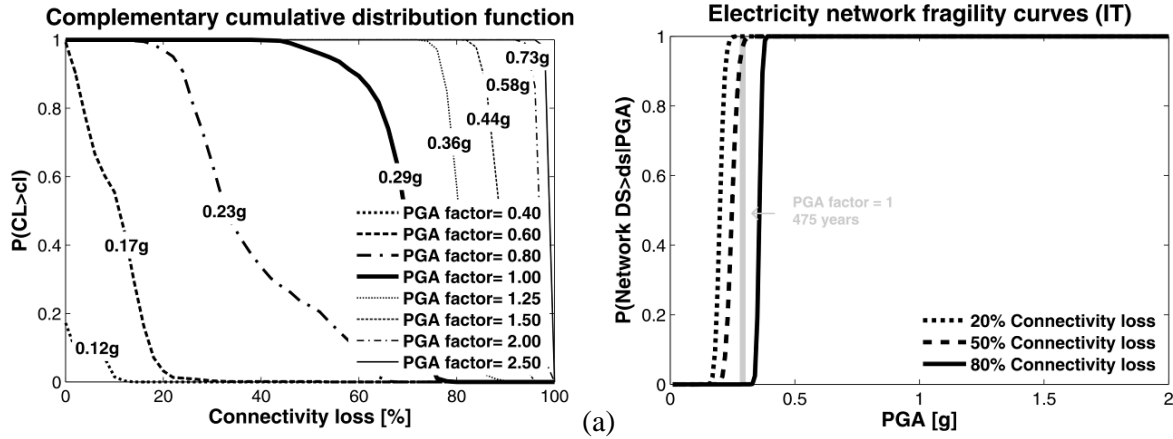

Figure 37: Results of Monte Carlo simulations in the case of European electricity network presented for different hazard levels as complementary cumulative distribution function (a) and summarized in network fragility curves for different damage states (b).

(b)

Figure 38: Results of Monte Carlo simulations in the case of electricity network of Italy presented for different hazard levels as complementary cumulative distribution function (a) and summarized in network fragility curves for different damage states (b).

The gas network has two types of vulnerable elements, gas pipelines (defined as arcs) and compressor stations (gas sources defined as vertices). Probabilities of failure of the vertex element are always a reflection of the seismic hazard map. This is because the fragility curves of the vertices are mostly dependent on the PGA of the vertex location. The higher the PGA the higher the probability of failure calculated from the fragility curves for the same type of facility. This is not the case with the arc element (pipeline), where the fragility is not only dependent on the PGA of the end vertices but also on the length of the arc. Therefore, the pipelines that are the most vulnerable to earthquake hazard do not appear only in the areas with the high PGA values but also in the source countries (Algeria, Turkey, and North See in Norway). This is because the majority of gas pipelines, which transport the gas directly from the gas fields to the areas of the high gas consumption are very long. In particular, the elimination of those connections in the damaged networks causes the fastest rise in the connectivity loss due to disconnection of the source vertices. Also we have that the gas fields vertices presents 87% of sources and the source vertices present only 5% of all the vertices in gas network. As such, gas fields play an important role by the network performance. Figure 39 of the gas network reveals that the probability of failure of arcs is actually very high already at the hazard level defined with 475 return period and, what is more, arcs are much more vulnerable than vertices.
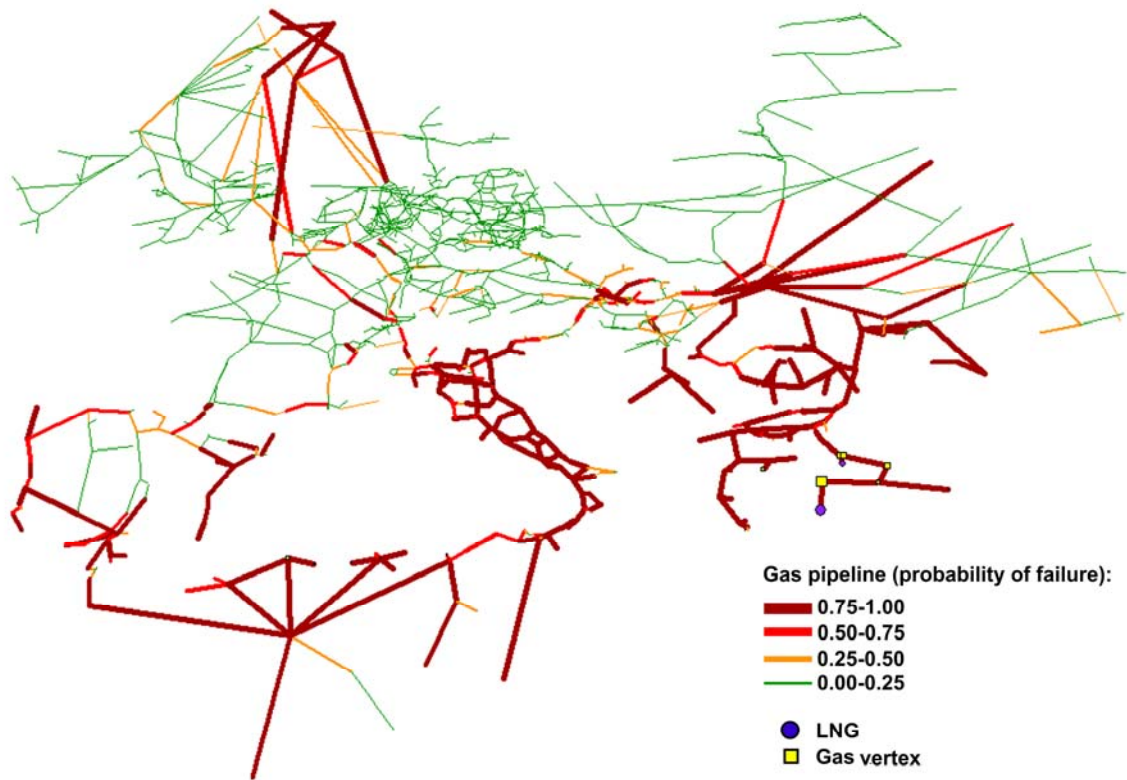
Figure 39: European gas network: the size of the vertices and the width of the lines correspond to the probability of failure according to 475 return period seismic hazard map.

On the other hand, in the electricity network only the vulnerability of vertices has been analyzed. Preliminary studies of this network's fragmentation shows that arc elimination is no more harmful than the vertex elimination. However, it is the length dependency of the arc fragility that becomes the issue in our situation. The probabilities of the arc (pipeline) failure could be much higher than those of vertex (e.g pumping station) failure, so that that higher network damage states are reached under the same hazard level. Furthermore, Figure 35 shows that the probabilities of failure of vertices are a reflection of PGA seismic hazard map. If we assume that the sources and the sinks are evenly distributed across Europe than the sinks within small PGA region will suffer much less connectivity loss than the sinks in the area with high values of PGA. The averaging effect in the final calculation of the connectivity loss (Equation (7)) as network characteristic displays the average damage state of the electricity network as whole.
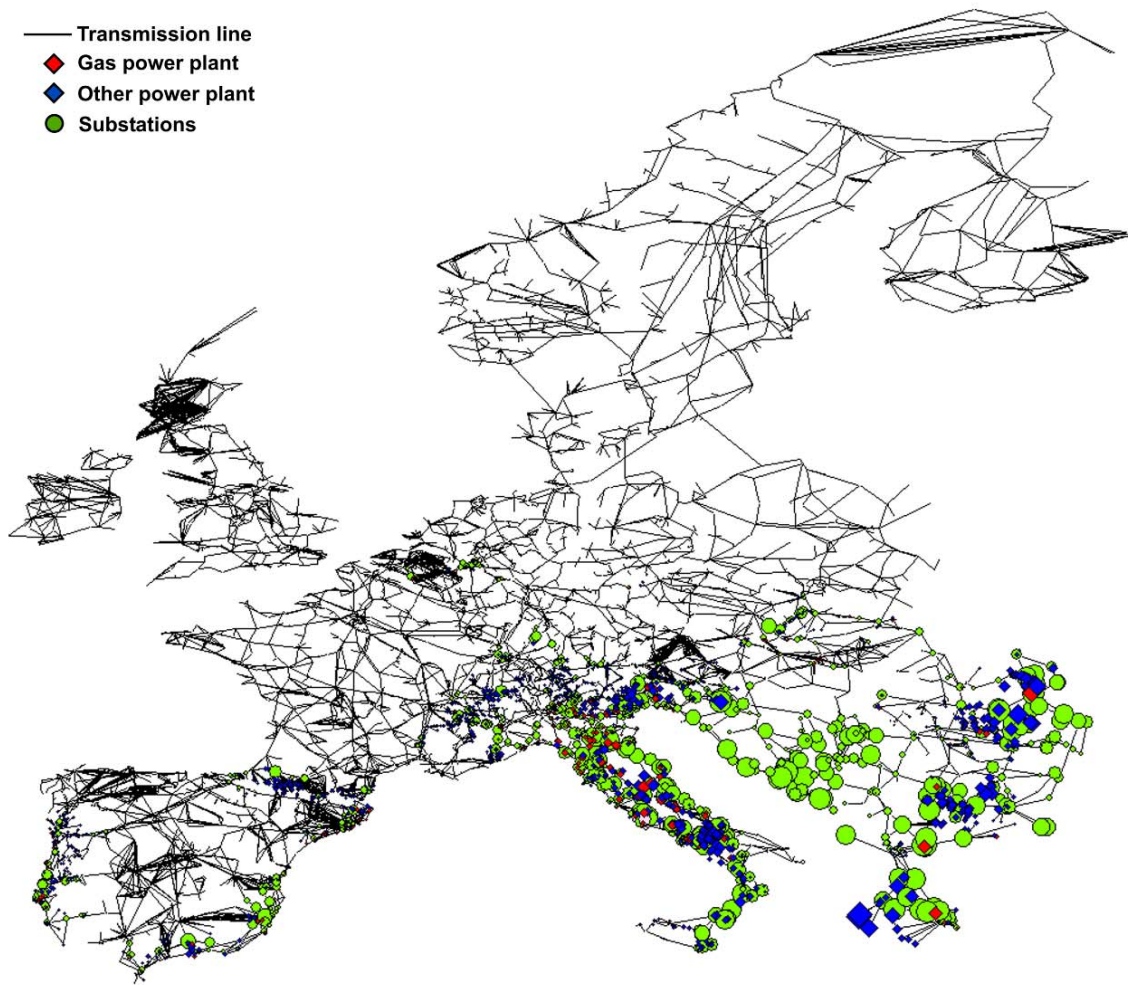
Figure 40: European electricity network: The sizes of the vertices correspond to the probability of failure according to 475 return period seismic hazard map.

However, countries in the area of high PGA would be subjected to higher connectivity loss if they would be treated individually. Building on these findings, we have, in addition, examined the electricity grid of Italy. It was extracted from EU electricity grid without considering the vertices adjacent to cross border connections as possible sinks or sources. The Italian electricity network has 1265 vertices, of those 662, 203 and 400 vertices are defined as sources, transmission vertices, and sinks. Besides, the portions of sources in both networks are very similar, 52.3% in Italian versus 51.2% in European electricity network. The results (Figure 38) of analysis of Italian electricity network confirm our premise. The vulnerability of Italian electricity grid is higher than that of the European grid as a whole. For Italy we have that the 475 year return period hazard level gives

100%, 97.7% and 0% probability of exceedence for $20\% CL$, $50\% CL$ and $80\% CL$, respectively. This could be an evidence to suggest that the network fragility curves are subjected to the effect of scaling (dependent on the number of vertices and arcs) mostly due to geographical variation of PGA.

8.2 Gas source supply stream fragility curves

So far, we have seen the results of the analysis of independent networks. In order to apply our interdependency model properly we shall now introduce the fragility curves of the gas source supply stream. They are defined for each gas vertex adjacent to gas power plant and present the vulnerability of these particular gas vertices to disability of gas distribution downstream to the gas power plant. Fragility curves of the gas source supply stream consider direct earthquake failure and disconnection from the gas sources because of the earthquake-induced failures of the other elements in the networks. Fragility curves presented in Figure 41 are a by-product of the analysis of the gas network. Through the Monte Carlo simulations the connectivity loss was measured for each of the gas vertex adjacent to gas power plant. Finally, we process the results in the same way as the calculation of the network fragility curves. The number of the gas source supply stream fragility curves equals the number of gas power plants (i.e. 998 in the European electricity network) because gas power plants are dependent on only one gas vertex and each of those gas vertices supply only one gas power plant.
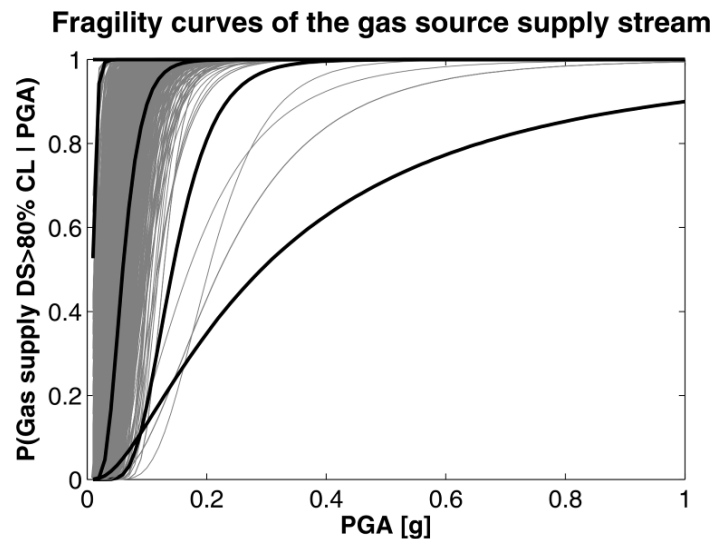

Figure 41: The gas source supply stream fragility curves for all gas power plants.
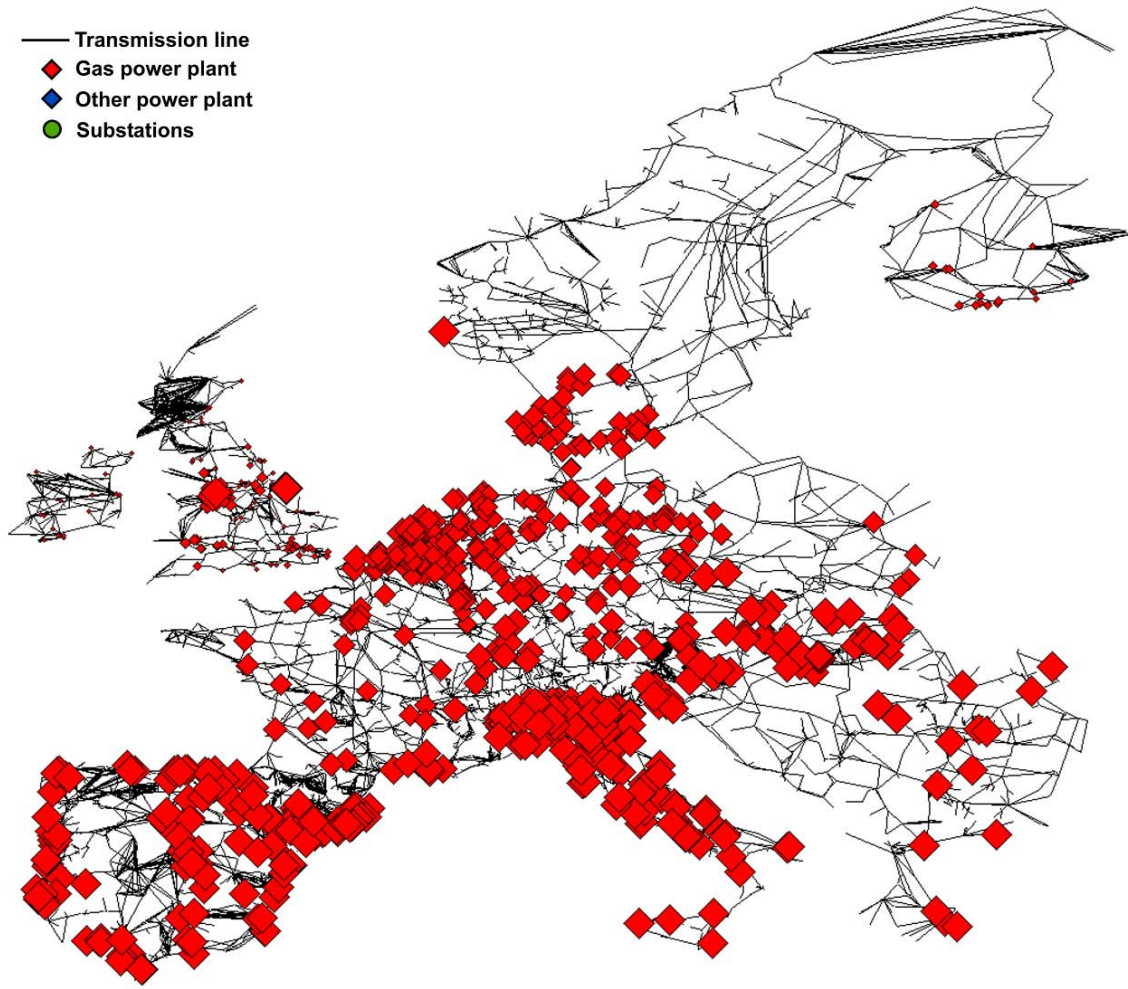
Figure 42: The probability of failure of gas vertices adjacent to gas power plants in the case of hazard level of 475 return period seismic hazard map.

Now, if we equate the gas source supply stream fragility curve of each gas vertex adjacent to the gas power plant at PGA of its location under the chosen hazard level, we calculate the probability of failure of the gas vertex due to direct seismic action combined with the disturbances in the downstream gas supply. Specifically, we have calculated the value of $P(G_i)$ that is in need for the evaluation of the probability of failure of the gas power plant due to gas disturbances $P(E_j^{dep})$ in Equation (18). We notice (Table 5) that the probabilities of failure of gas vertices adjacent to gas power plants are extremely high in comparison to the probability of failure due to structural damage of gas power plants caused by an earthquake. This is not surprising considering the high seismic

vulnerability of the gas network. How strongly do those high vulnerabilities of gas vertices affect the functionality of the gas power plants is regulated with the strength of coupling?

Table 5: Average probabilities of failure of gas power plants due to earthquake and of gas vertices adjacent to gas power plants.

	Average probability of failure (EU)	
	of gas power plants due to eartquake	of gas vertices adjacent to gas power plant
PGA factor	$P(E_j^{earth})$	$P(G_i)$
0.40	0.00	0.21
0.60	0.00	0.38
0.80	0.00	0.52
1.00	0.01	0.63
1.25	0.01	0.74
1.50	0.02	0.84
2.00	0.05	0.94
2.50	0.09	0.98
3.00	0.12	0.98

These additional vulnerabilities of gas power plants are introduced in the dependent network analysis using approach described in Chapter 7.3.

8.3 Dependant network vulnerability

The dependent network in our interconnected system is the electricity network. As in chapter 8.1, we analyze the electricity network of Europe and Italy. The plots in Figure 46 - Figure 48 and Figure 49 - Figure 51 introduce sets of dependent network fragility curves for Europe and Italy, respectively. We should notice the different range of PGA values on the abscissa but almost the same range of the PGA factors in the presented results for the Italian and European electricity networks. In the case of the electricity network, we study all three performance measures defined in Chapter 6.1 (connectivity loss, power loss and impact factor on population) and the influence of the coupling behaviour. Therefore, we first group the fragility curves according to the performance measures, then we sort them into three graphs according to the damage states and inside each graph

we can observe the influence of dependency, which is regulated by the strength of coupling. Considering the interdependency effect, we use the fragility curves of the gas source supply stream, which are calculated out of whole gas network, but which we extract according to the gas power plant under consideration. So, the set of fragility curves of the gas source supply stream is the same irrespective of the analyzed electricity network — Italian or European.

The plots inside one graph clearly show the consistent increase in system vulnerability as the strength of coupling grows. The extent of dependency effect is neither dependent on the damage state nor the performance measure.

Furthermore, considering the extent of the dependency effect, it is interesting to know the importance of gas as a fuel for electricity power generation. There are two aspects to its evaluation: first, how much electricity generation capacity is produced by gas power plants. in terms of ratios of total MW (i.e. to assess power loss), and the second is the ratio of the number of gas-fired plants (to assess connectivity loss). For the European electricity network we calculated that 19.5% of electricity generation capacity is obtained from gas power plants and 18.6% out of all power plants are fuelled by gas. Gas power plants are not the only one type power generation facilities in the electricity network but, rather, represent the minor part in the power generation capacity. Is it then wrong to expect that only disturbances in the gas supply cannot cause extensive network damage state of the electricity network? How can we prove this? Pretend to encounter the extreme case where we construct the damaged network with elimination of all gas power plants without asking ourselves what would be possible scenarios. Afterwards we execute one deterministic run of network analysis without applying the seismic load. Calculated values for connectivity loss, power loss and impact factor on population are 18.8%, 19.1% and 19.7%, respectively. Because the European electricity network is one strong component the values for the connectivity loss and power loss must equal above ratios of power plants and the electricity power generation dependent on gas. Nevertheless, there are some minor disconnected parts of electricity network, so you can notice the slight difference in the values of connectivity loss and power loss. As the characteristic of the whole network, they have not exceeded the minor network damage state in any of the categories of the performance measures. We must place a caveat on this conclusion, and that is that because we define loss in topological terms to the exclusion of other important functional characteristics. We should note that gas-fired power plants play a crucial role in the flexibility of electricity power generation and that in our analysis the robustness of functionality of the power sources is not considered.

Figure 43 and Figure 44 show the diversity of importance of the gas supply from country to country. We also note the variation between the share of electricity power generation capacity from gas power plants and the share of power plants fuelled by gas; for example, in Italy 43% of electricity generation capacity is covered by gas while only 24.3% of power plants are fuelled by gas in Europe as a whole. Performance measures of the network exposed to elimination of all gas power plants are 24.3%, 42.8% and 43.1% for connectivity loss, power loss and impact factor on population, respectively. Therefore, the Italian electricity network is more dependent on the gas fuel supply than the European electricity grid. The disturbances in gas supply could cause, in extreme situations, the exceedence of the minor network damage state. In the same manner we can draw similar conclusions for the other countries with similar gas-fired power ratios.
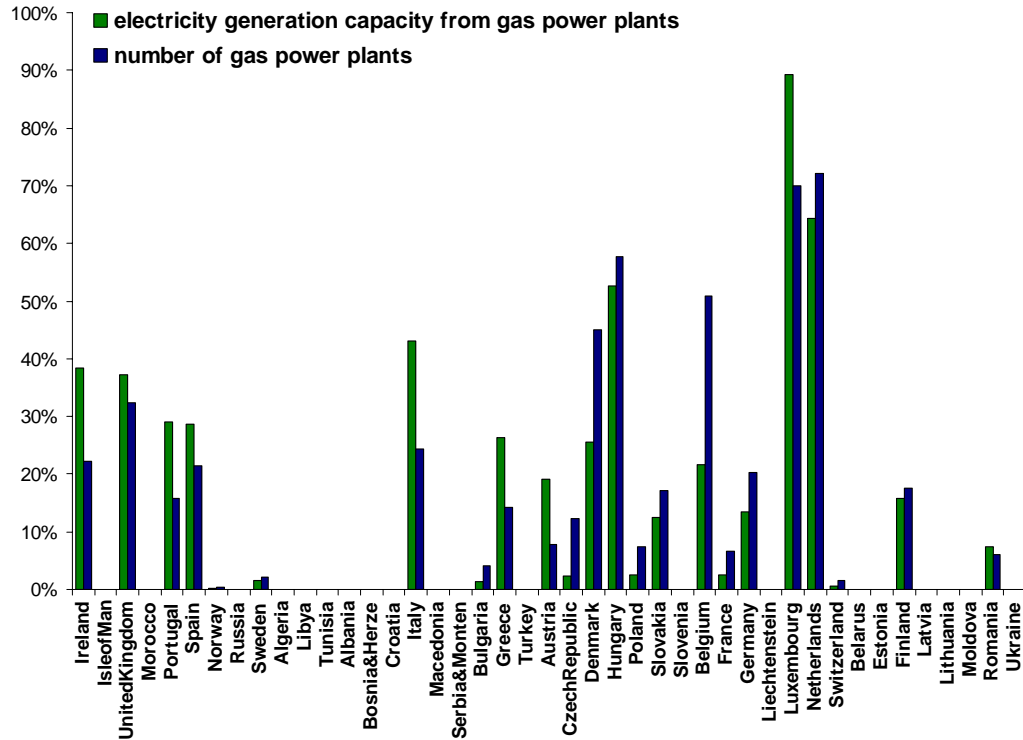

Figure 43: Share of gas power plants out of all power plants measured in electricity power generation capacity (green) and in number of facilities (blue) in percentage by the country.

The different performance measures seem to point at similar conclusions. Why do we encounter such similarity? Is it possible that 20% (50% or 80%) of connectivity loss more or less corresponds to 20% (50% or 80%) of power loss or 20% (50% or 80%) impact factor on population? Yes, if the

topology has a predominant influence on the calculated performance measure, while additional information introduced (nominal power of the power plants and the population assigned to each distribution substation) only contributes to the minor changes in the final value of the performance measures.

This could be due to the extremely skewed frequency distribution not only of the nominal power of the power plants but also of the extent of population assigned to each distribution substation (Figure 45). Almost 80% of power plants have the nominal power less then 100MW and almost 60% of distribution substations cover less than 100000 people. Therefore, such data cannot introduce noticeably higher diversity into the results.
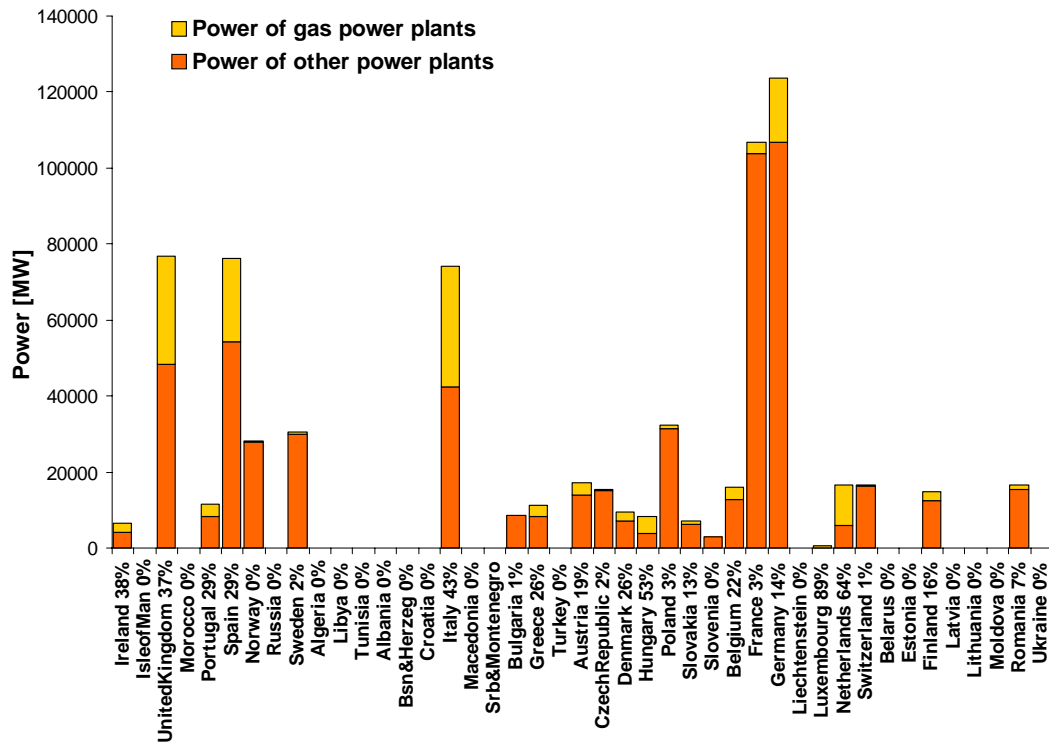
Figure 44: Electricity power generation from gas power plants and the other power plants presented as an absolute value in MW and as a share of electricity power generation covered by gas power plants in percentage by the country.
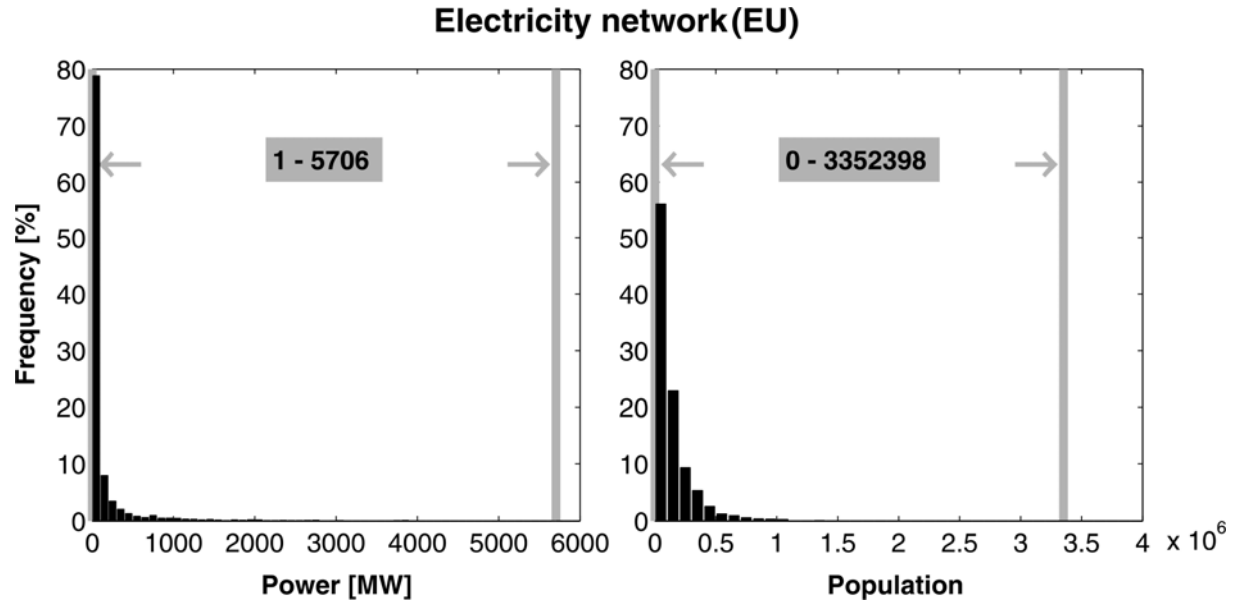
Figure 45: Frequency distribution of the nominal power of the power plants and the population assigned to the distribution substations in the European electricity network.

Extreme values in the tail of the frequency distribution are rare, and as such tend disappear in averaging process when calculating the network performance measure. However, if we would observe the performance measures at the local level (i.e. of each distribution substation), those extreme values can cause anomalies. For example, there are distribution substations with high power loss but low impact factor on the population if the demographics have a scattered geographical nature. Such discrepancies among different performance measures are therefore geographically dependent and we come across this phenomenon again in Chapter 8.4.
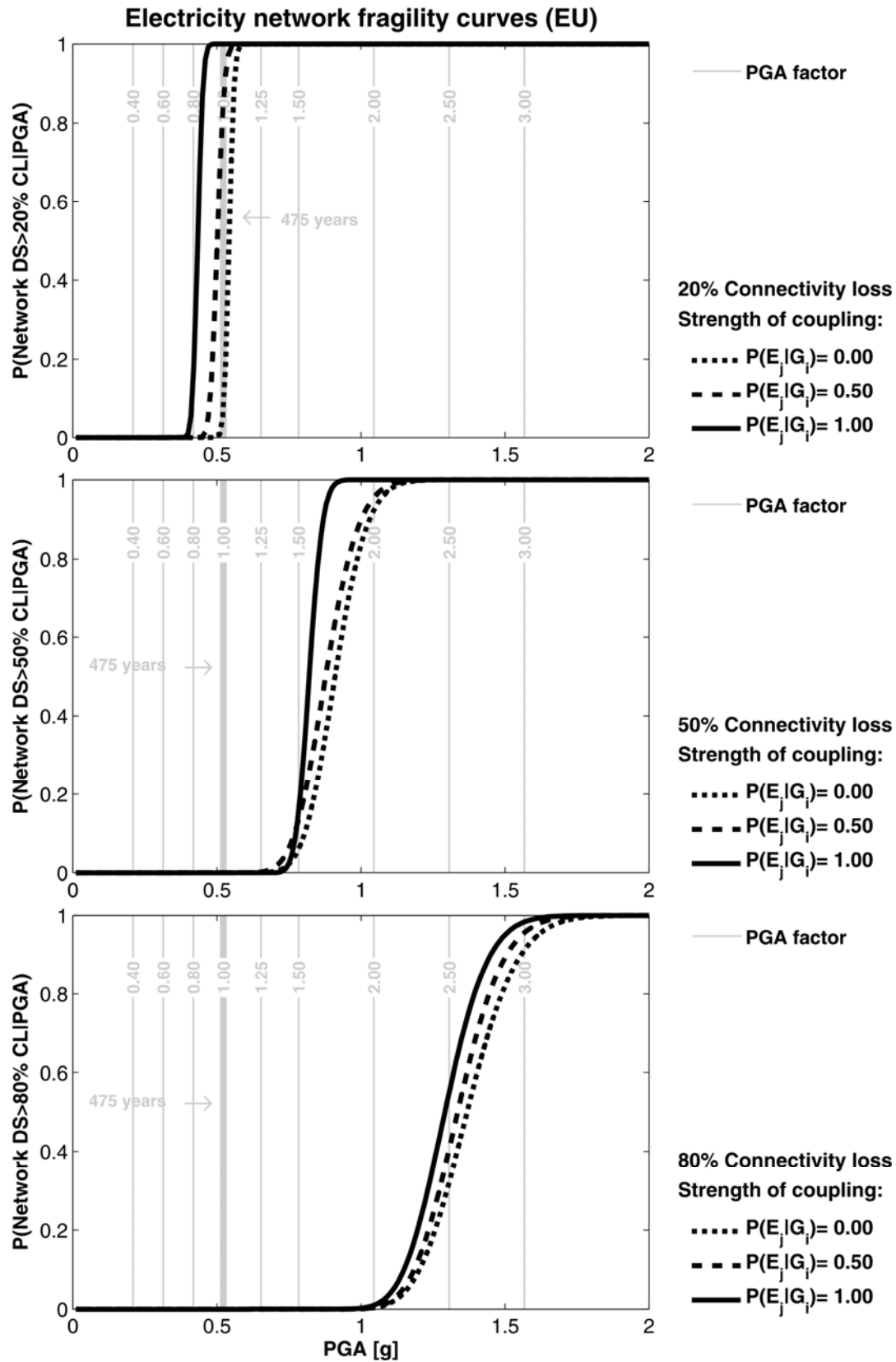
Figure 46: Dependent network fragility curves for EU electricity network at different damage states in terms of Connectivity loss as performance measure.
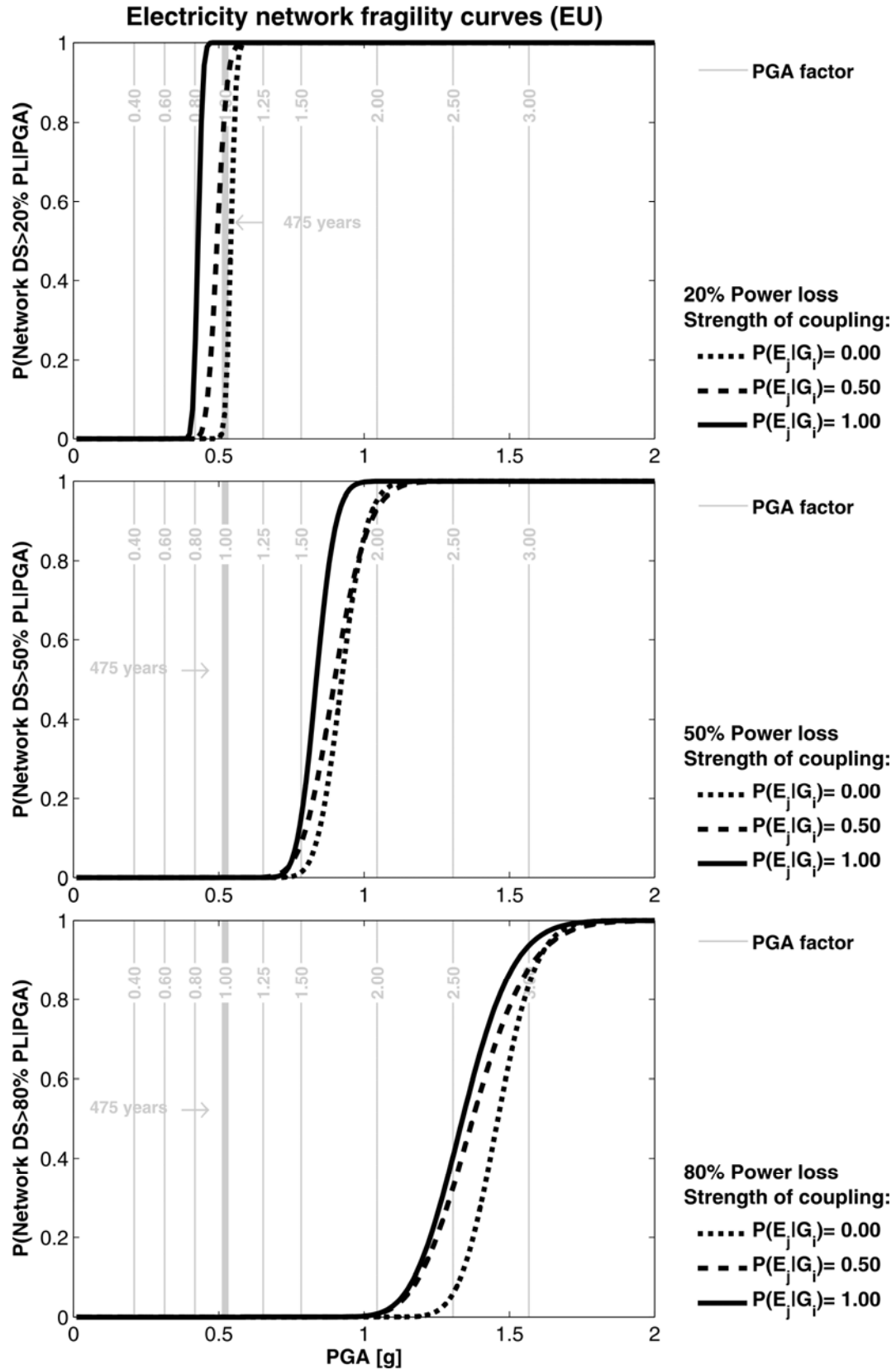
Figure 47: Dependent network fragility curves for EU electricity network and different damage states in terms of power loss as performance measure.
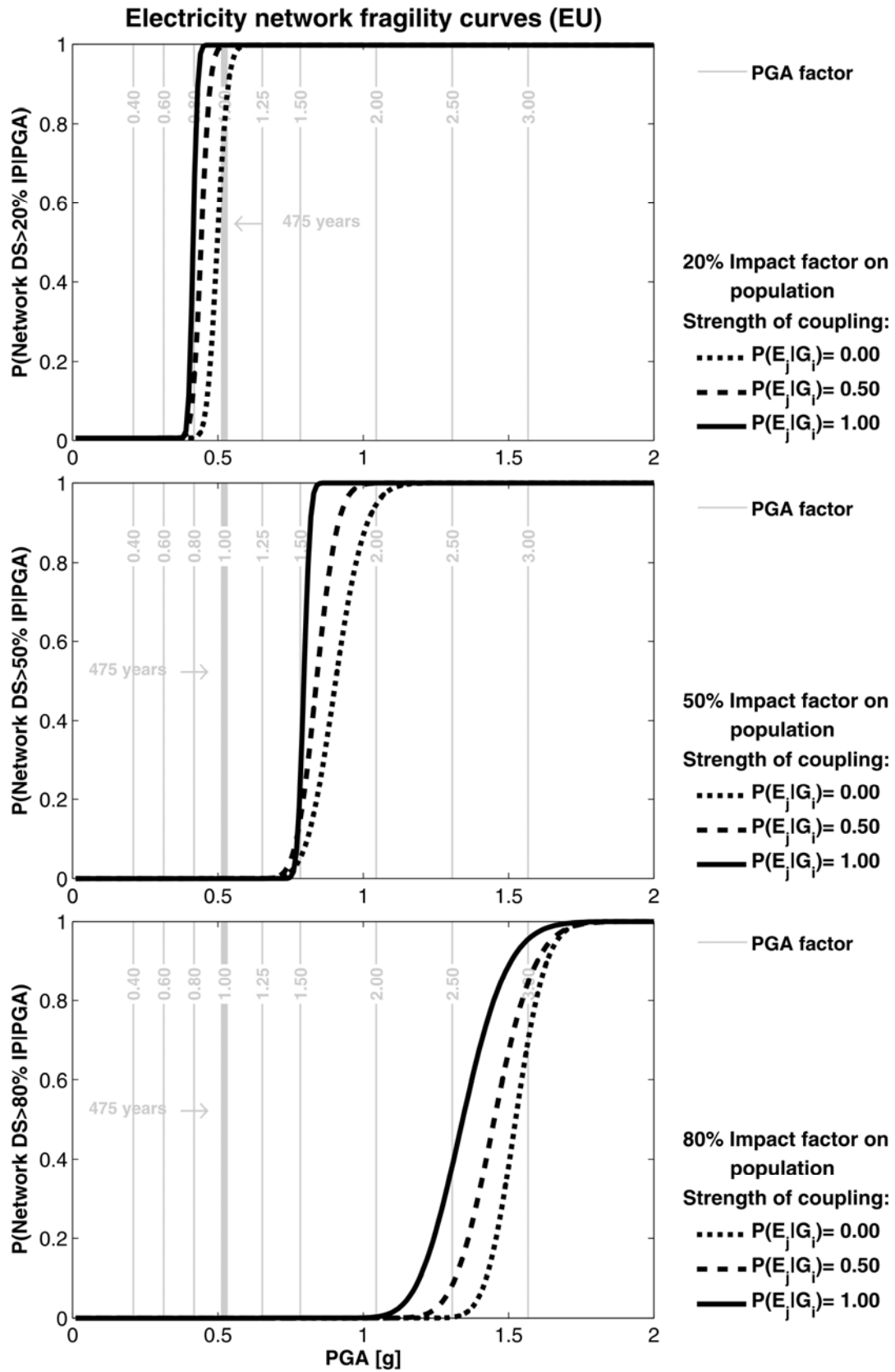
Figure 48: Dependent network fragility curves for EU electricity network and different damage states in terms of impact factor on population as performance measure.
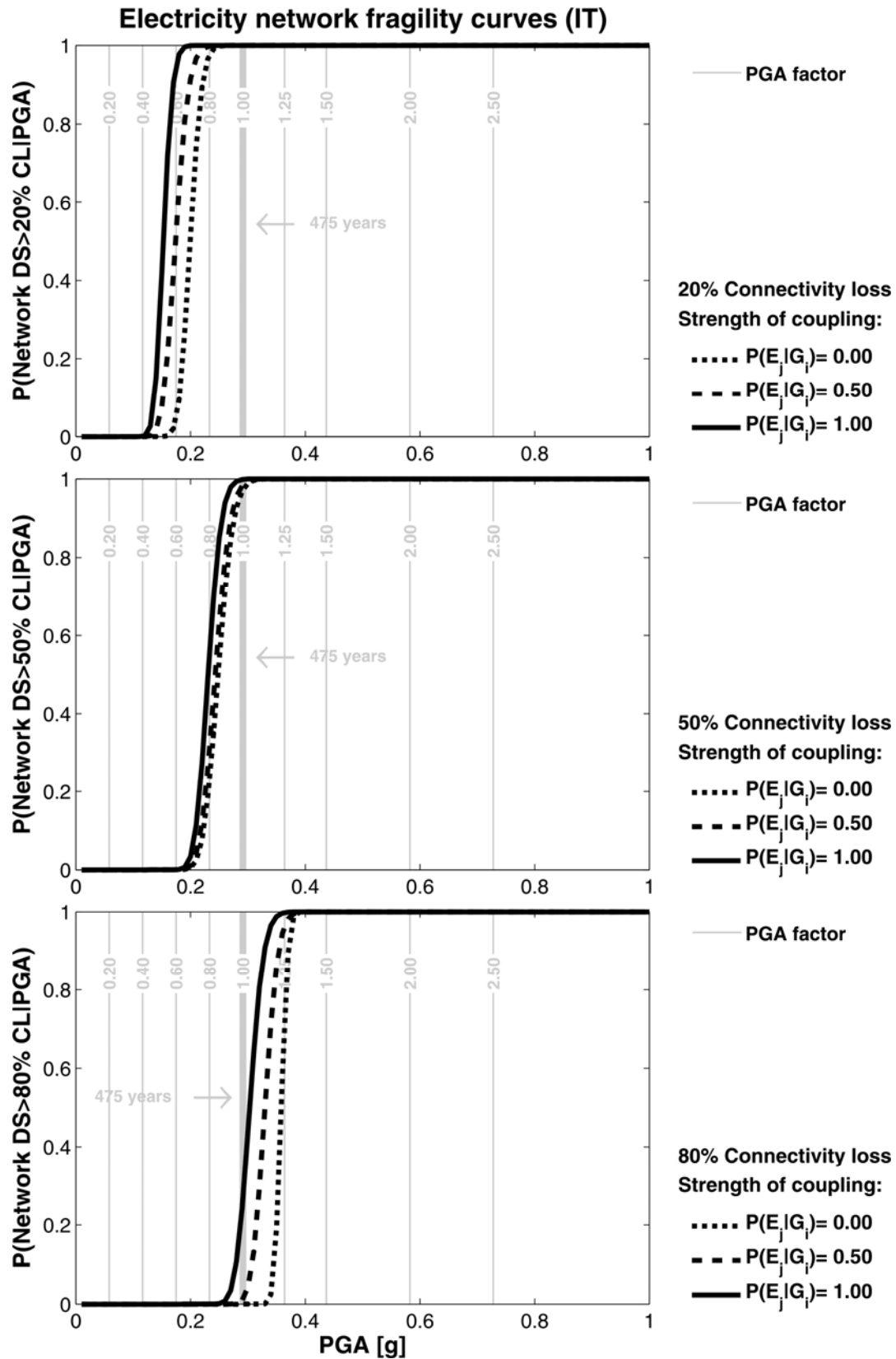
Figure 49: Dependent network fragility curves for IT electricity network and different damage states in terms of connectivity loss as performance measure.
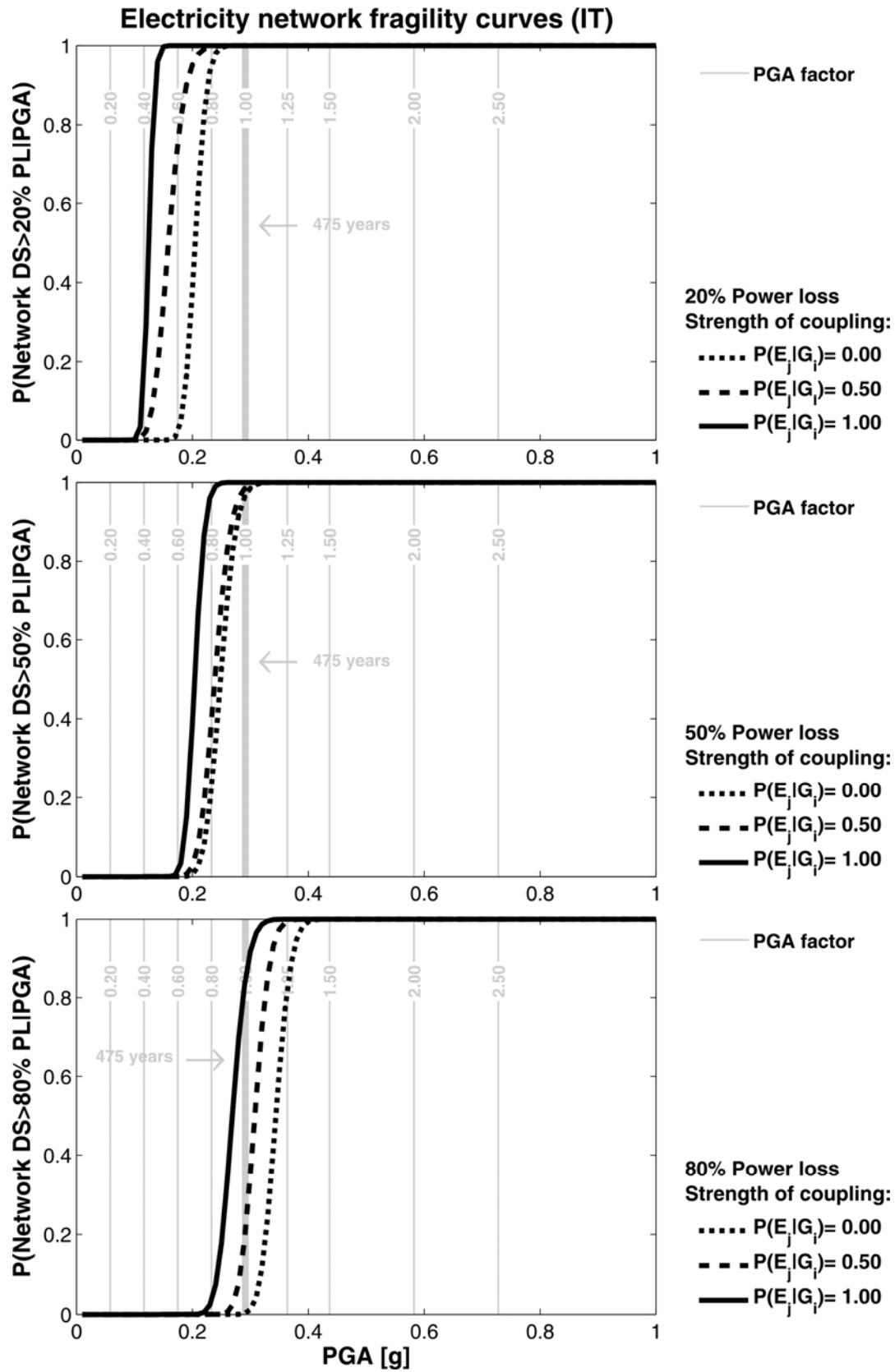
Figure 50: Dependent network fragility curves for IT electricity network and different damage states in terms of power loss as performance measure.
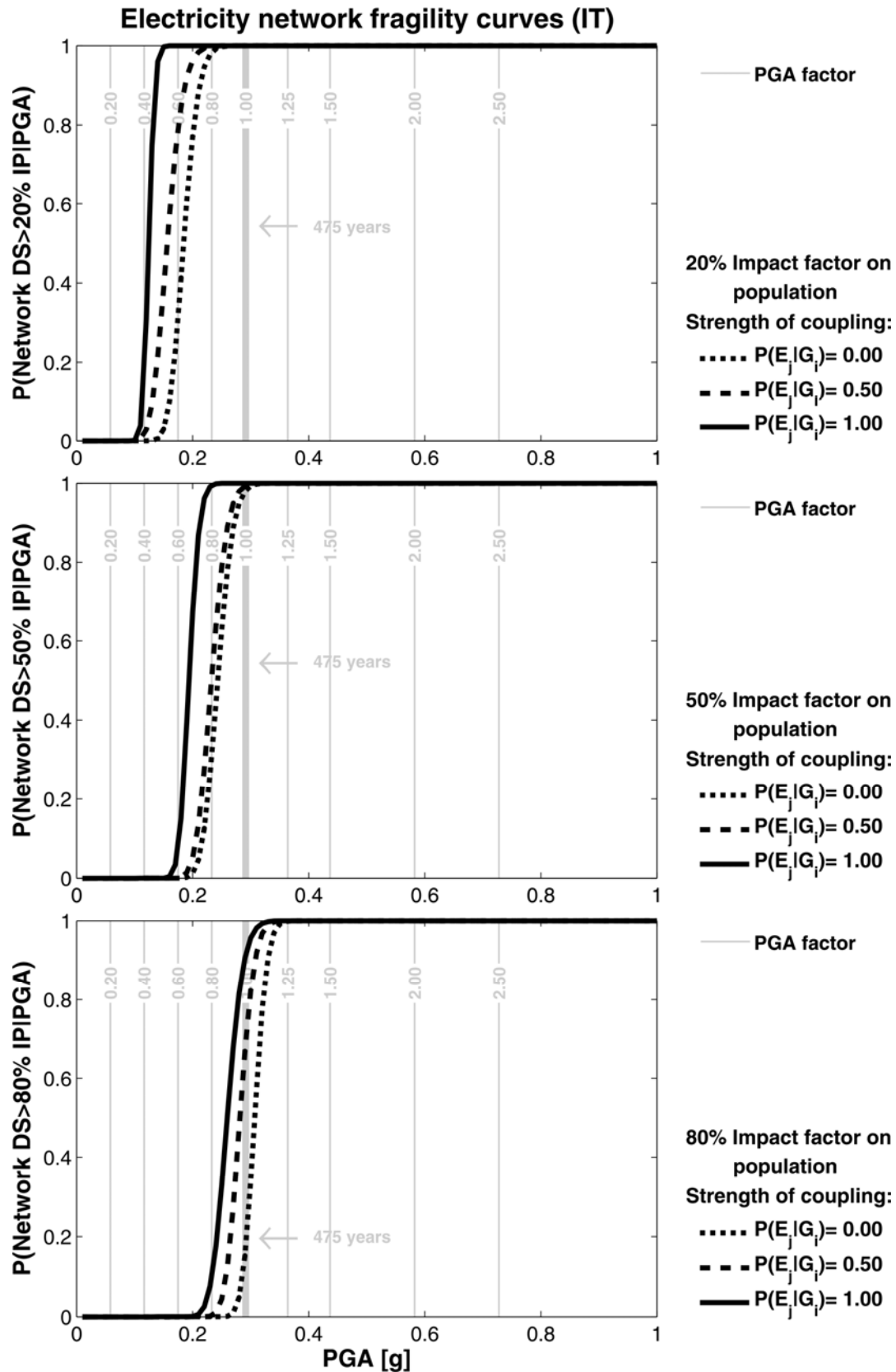
Figure 51: Dependent network fragility curves for IT electricity network and different damage states in terms of impact factor on population as performance measure.

8.3.1 Beetweenness centrality attack vs. seismic hazard and strength of coupling

Our work in chapter 8.3 began with an investigation of the dependency effect of gas network on electricity network. We found that the dependency effect introduces an extra vulnerability to the electricity network response under seismic hazard, but that this effect is relatively small. This finding raises an obvious question, why is this influence so small? To understand the phenomena better we must be aware that the response of the system is strongly dependent on the topology of the individual networks and modelling of the interdependency behaviour. There are probably more reasons for such results among which:

Physical interdependency: How intense is the propagation of earthquake-induced damage in the gas network on the electricity network? It would appear that it is certainly dependent on the quantity of the connection among the network. The larger the number of vertices whose functionality is closely dependent on the performance of the gas network, the faster is the spread of damage that can be seen in higher connectivity loss. In our case only the gas power plants suffer the disturbances in gas supply, which is dictated by the disconnection from the adjacent gas vertex. Such a one-to-one connection is typical for the physical dependency that is characterized by slow damage propagation. If we would define geographical interdependency, one vertex of independent network would influence more than one vertex in dependent network; in that case the propagation of damage would be faster and of cause more extensive damage.

Gas power plants are a minor part of source vertices: The problem of elimination of the sources from the network we have already encountered in the gas network. As we know, gas fields play a role in the gas network equivalent to the gas power plants in the electricity network, but their disconnections due to the high probability of failure of the long gas pipelines causes high connectivity loss. What is different in the electricity network? First gas fields in the gas network represent, as already mentioned, 87% of all the source vertices while gas power plants in European (Italian) electricity network represent only 18.6% (24.3%) of all source vertices. Besides, the sources in the gas network present only 5% of all the vertices, whereas sources in the European (Italian) electricity network represent 51.2% (52.3%) of all the vertices. The higher the portion of the sources in the network, the smaller is the effect of failure of one source on the connectivity loss.

Gas power plants are in general one-degree vertices: One-degree vertices have zero betweenness centrality. It is certainly true that the elimination of such vertice will not cause the fragmentation of the network in the sense of the increase in the number of components, but will raise the connectivity

loss. Since the connectivity loss measures the decrease in the number of sources reached by each sink, it is obvious that failure of one source out of 5318 will not cause a noticeable change. How about the vertex which has the highest betweenness centrality? Elimination of this vertex, which is on the path of many connections between the sources and the sinks can cause that certain sink nodes can be disconnected from more than one source at once. So, such an attack does not only quickly fragment the network but can also cause a large increase of the connectivity loss. In the case of the earthquake hazard, more than one vertex is bound to fail and, statistically, most of these will have a value of betwenness centrality closer zero (Figure 52). Therefore, the elimination of the electricity vertices due to earthquake failure can stifle the raise of the connectivity loss due to interdependency, i.e., the failure of gas power plant because of the disturbances in the gas supply.
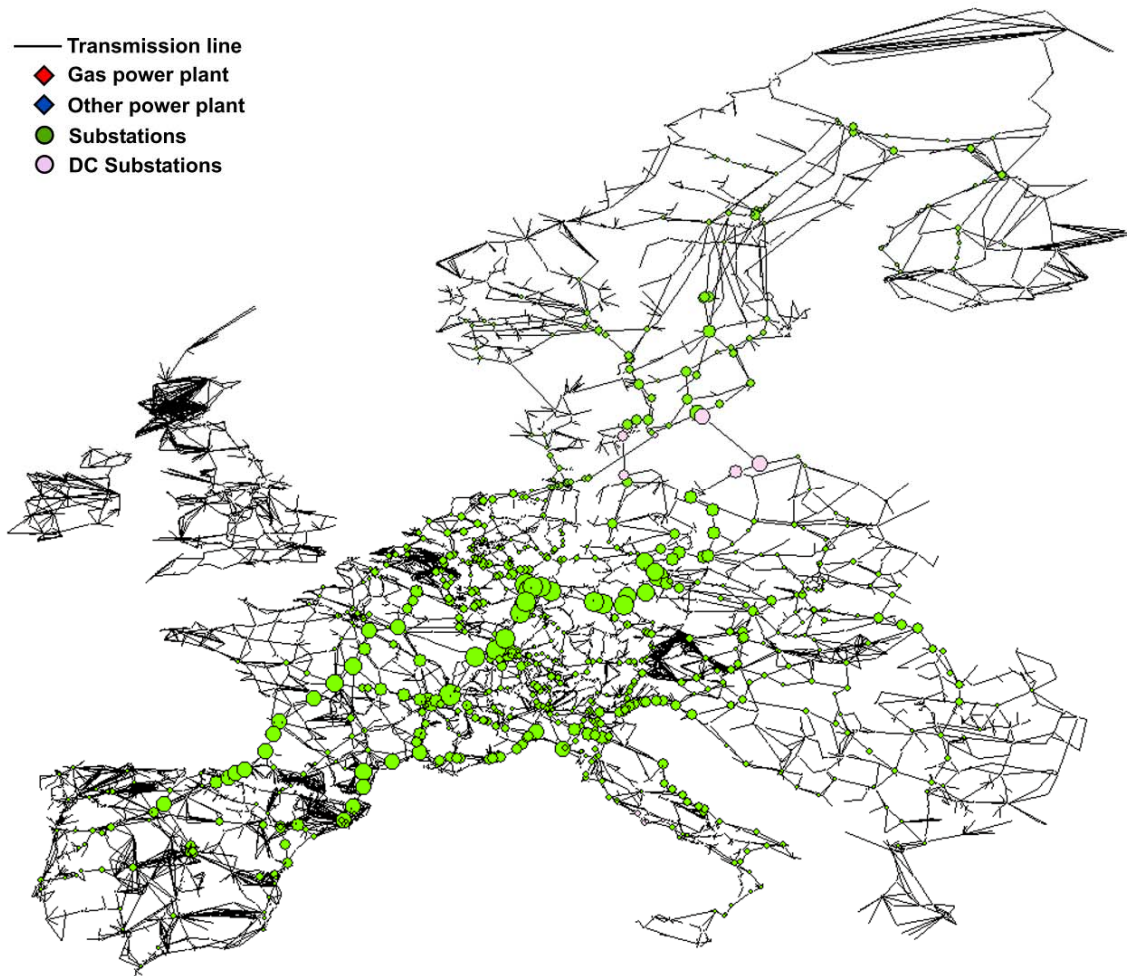

Figure 52: Vertex betweenness centrality in EU electricity network.

Next, we explore from a novel perspective the extensiveness of the response of the electricity network under earthquake hazard and interdependency effect. We will compare it to the response of the electricity network under betweenness centrality attack. This attack is defined as successive removal of the vertex with the highest betweenness centrality. Bewteenness centrality is recalculated for each new damaged network. The performance of the damaged network is, in both cases, measured with the connectivity loss. The only problem is that the betweenness centrality attack is a deterministic calculation while the response of electricity network under seismic hazard and interdependency effect is a probabilistic calculation. To overcome this discrepancy we compare only the average values of all the simulations in one series used in the probability approach.

Figure 53 and Figure 54 show the above described comparisons for the electricity network of Europe and Italy, respectively. In these graphs the connectivity loss is on the ordinate and the fraction of the removed vertices is on the abscissa; but note, we consider seismic hazard level and strength of coupling as the parameters of the third and the fourth dimension. In all the situations presented in the graphs, the connectivity loss is increasing with the fraction of the removed vertices. By far the fastest increase appears in the case of the betweenness centrality attack. Next, we can follow trends of connectivity loss along increasing parameter of hazard level or along the increasing parameter of the strength of coupling. Notice that the connectivity loss increases faster with the increasing hazard levels than with higher strength of couplings. Moreover, at the lower hazard levels the increasing strength of coupling causes higher increase in the connectivity loss than at the higher hazard level. Both of the above are only another argument of what was stated earlier, namely, that earthquake failures stifle the raise of the connectivity loss due to interdependency effect.

Next, there are some differences between the performance of the Italian and European electricity network. Their response under betweenness centrality attack is very similar. In the case of Italy 90% and 100%CL is reached after 0.018 and 0.477 of fraction of removed vertices, while in the case of Europe 90% and 100%CL is reached after 0.010 and 0.478 of removed vertices. On the other hand, the average response under the seismic hazard with the interdependency effect depends on the geographical extensiveness of the network. From this point of view the Italian electricity network is on average subjected to higher damage than European electricity under the same load. For example, at the PGA factor 1 and the strength of coupling 1 almost 20% and only 8% of vertices are eliminated while 77%CL and not more than 26%CL is reached in Italian and European electricity network, respectively.
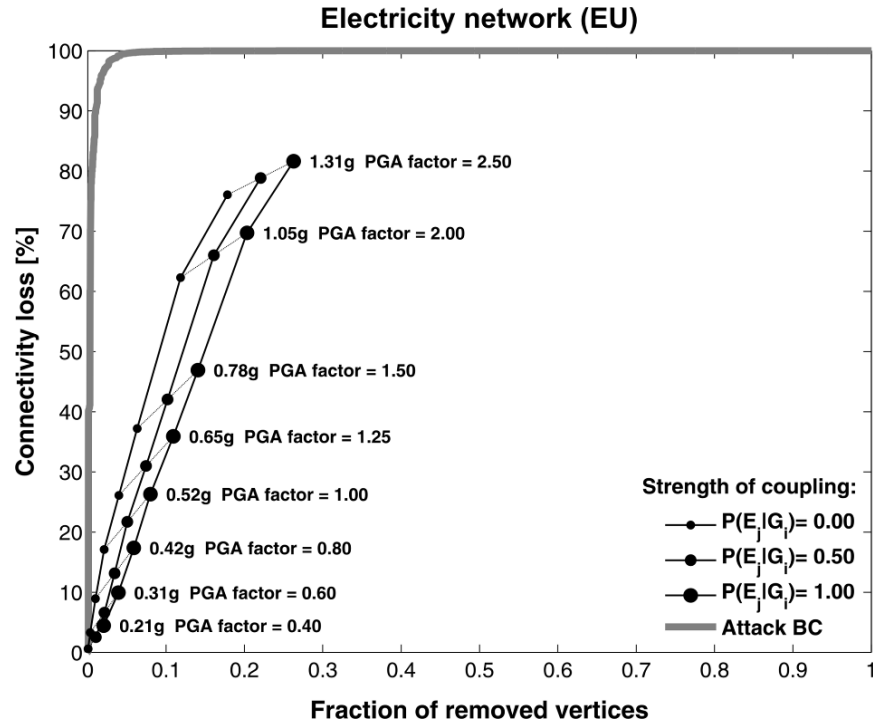
Figure 53: Comparison between the betweenness centrality attack and seismic hazard with different strength of coupling for the case of EU electricity grid.
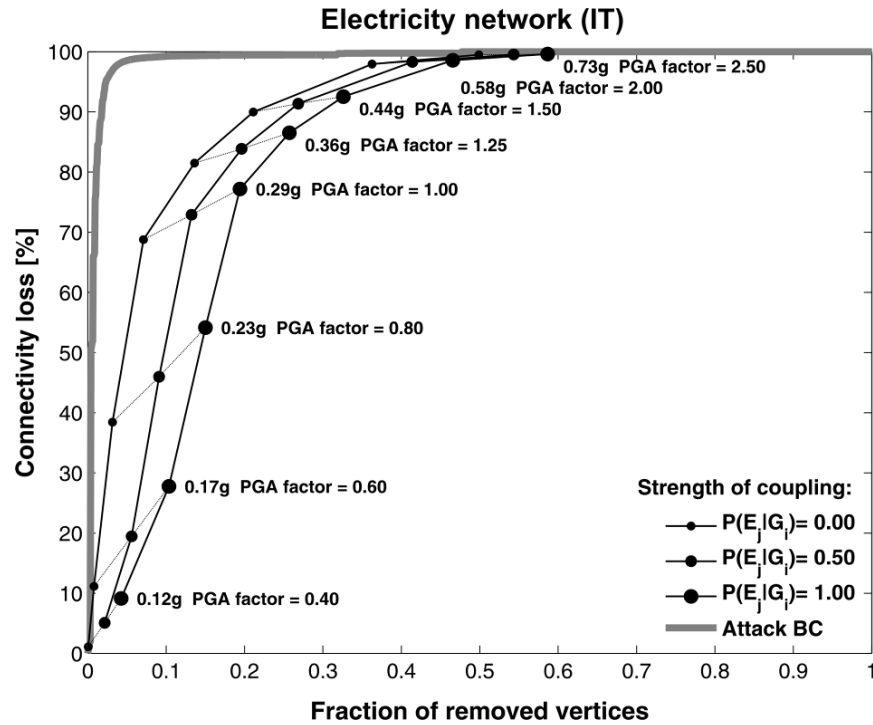

Figure 54: Comparison between the betweenness centrality attack and seismic hazard with different strength of coupling for the case of IT electricity grid.

Further observations are important only to keep the results of probabilistic reliability model under control. We can confirm that the average number of the removed vertices increases not only with the hazard levels but also with the strength of coupling.

8.4 Geographical spread of damage

Until now, we have observed the performance of the network as one macroscopic structure. We notice that the averaging procedure incorporated in the definitions of the performance measures suppresses extreme damage restricted to certain geographical locations. Therefore, we focus in this chapter on the Thiessen polygons as the final object of the analysis with defined geographical borders to which some characteristics can be assigned.

We calculated power loss for each of the distribution substation of the electricity network and we assigned its value (that ranges from 0-1) to the Thiessen polygon covered by each of the distribution substations. We have results for different hazard levels (Figure 55) and different strength of couplings (Figure 56 and Figure 57) but presented as the average value of all the simulations executed in one series. This way we can represent the probabilistic results on the map of Europe. Now we would like to calculate to what extent the population is affected by the hazard event. We have already related the population data to the area covered by each distribution substation. If we multiply the number of population in each area (Thiessen polygon) by the distribution substation's power loss, we get the absolute value of the population affected for each of the Thiessen polygons.

Finally, we obtained two damage measures, power loss of the distribution substations and affected population of the Thiessen polygons, that are geographically dependent and could be quantitatively and qualitatively presented in the map using the GIS tool.
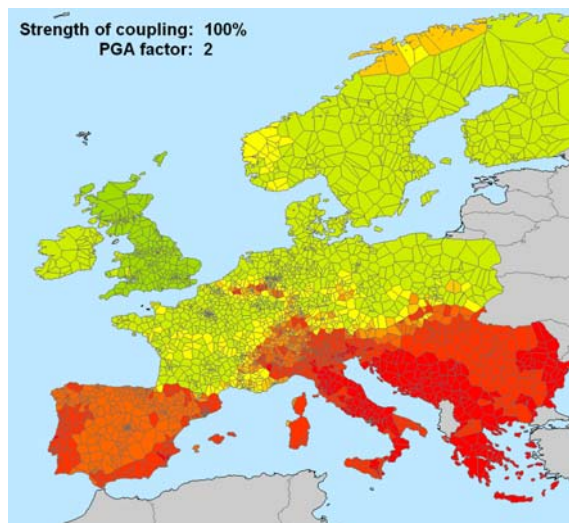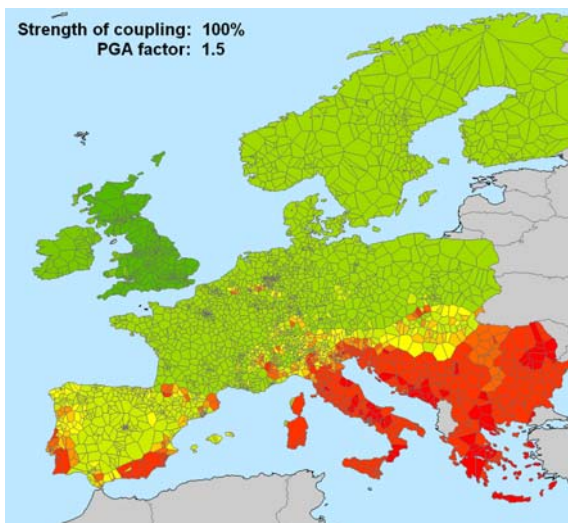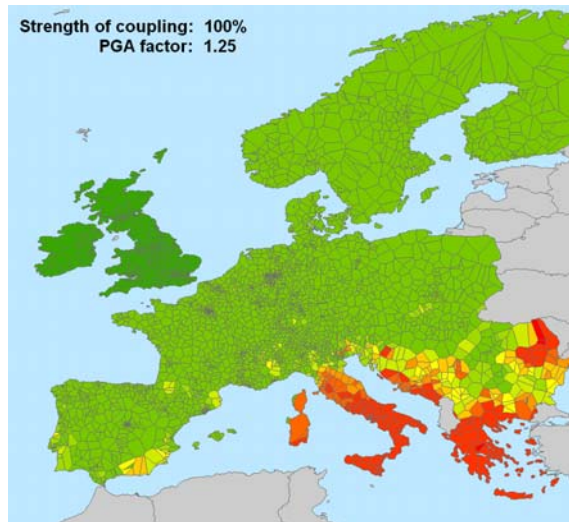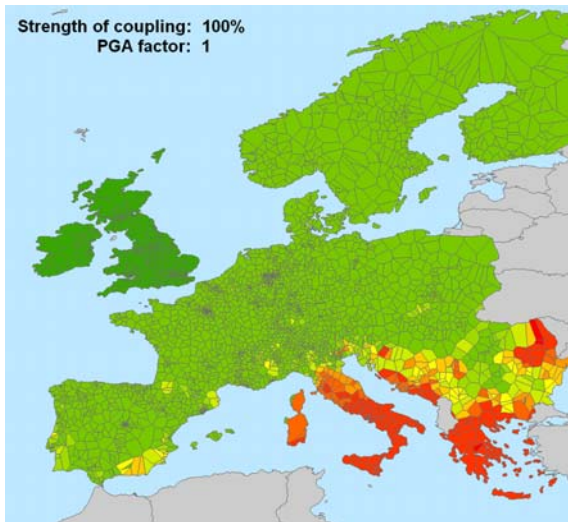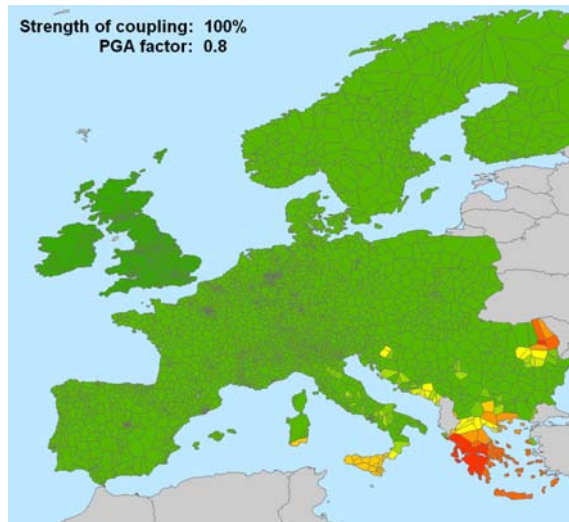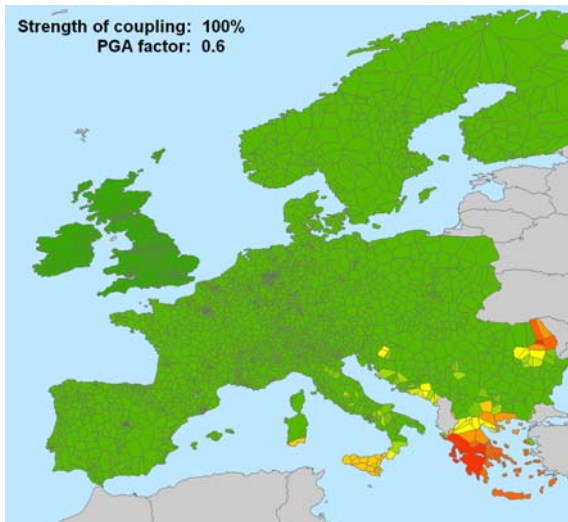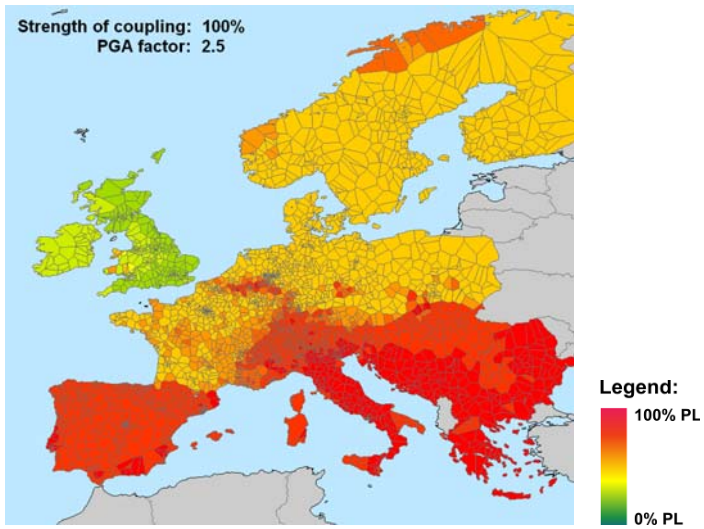
Figure 55: Geographical spread of power loss for 100% of strength of coupling and PGA factor from 0.8 – 2.5.
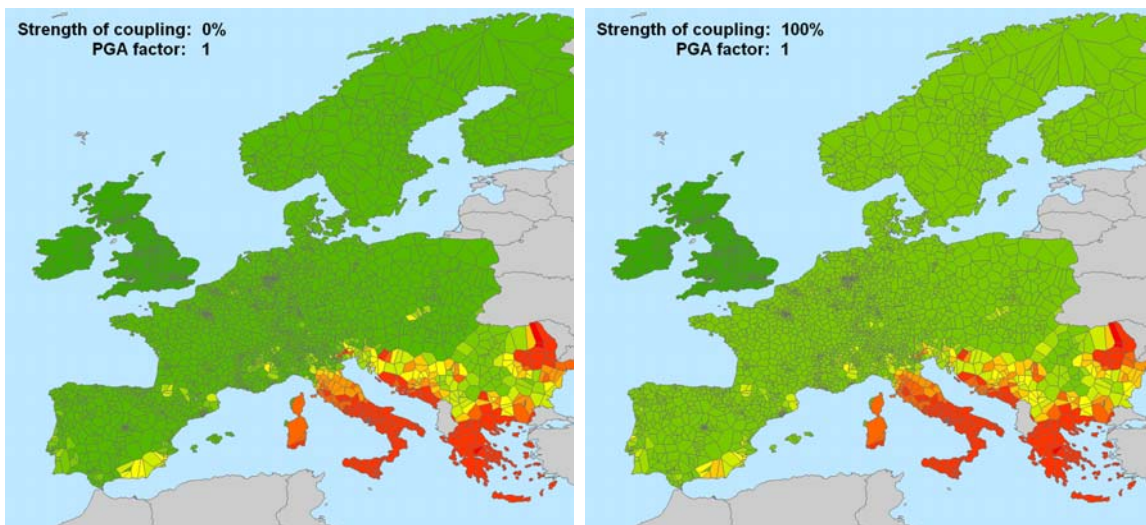

Figure 56: Comparison between the strength of coupling 0 and 100% at PGA factor 1.
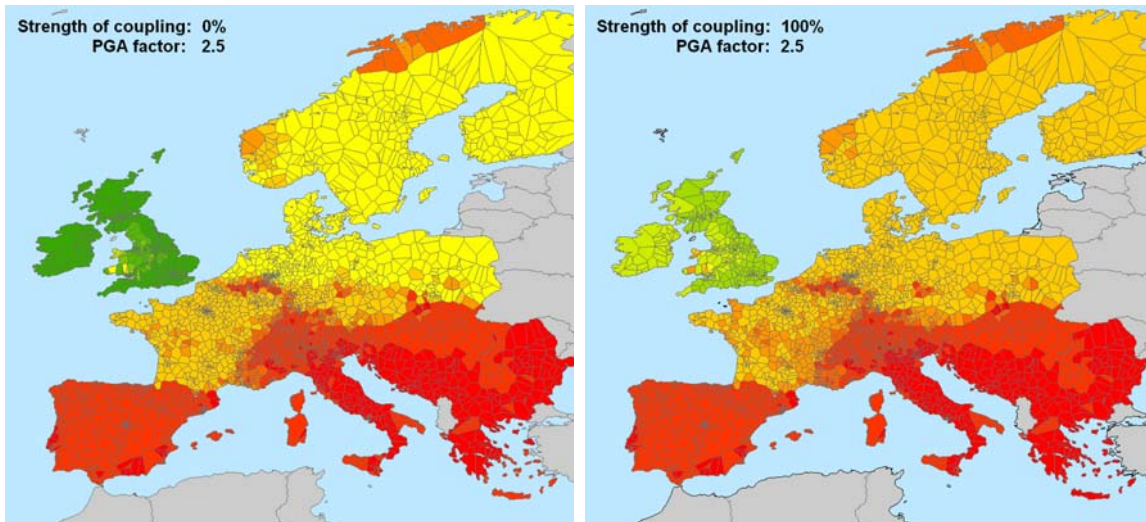
Figure 57: Comparison between the strength of coupling 0 and 100% at PGA factor 2.5.

The results for the affected population (Figure 58) is a combination of the population density, the size of the Thiessen polygons and all the factors that influence the power loss of certain distribution substation. We notice that extreme values for the affected population does not coincide with the highest values of the power losses. It appears, for example, in The Netherlands, where a locally not so branched electricity transmission network, generates a large Thiessen polygon of high population density but which is assigned to one distribution substation.
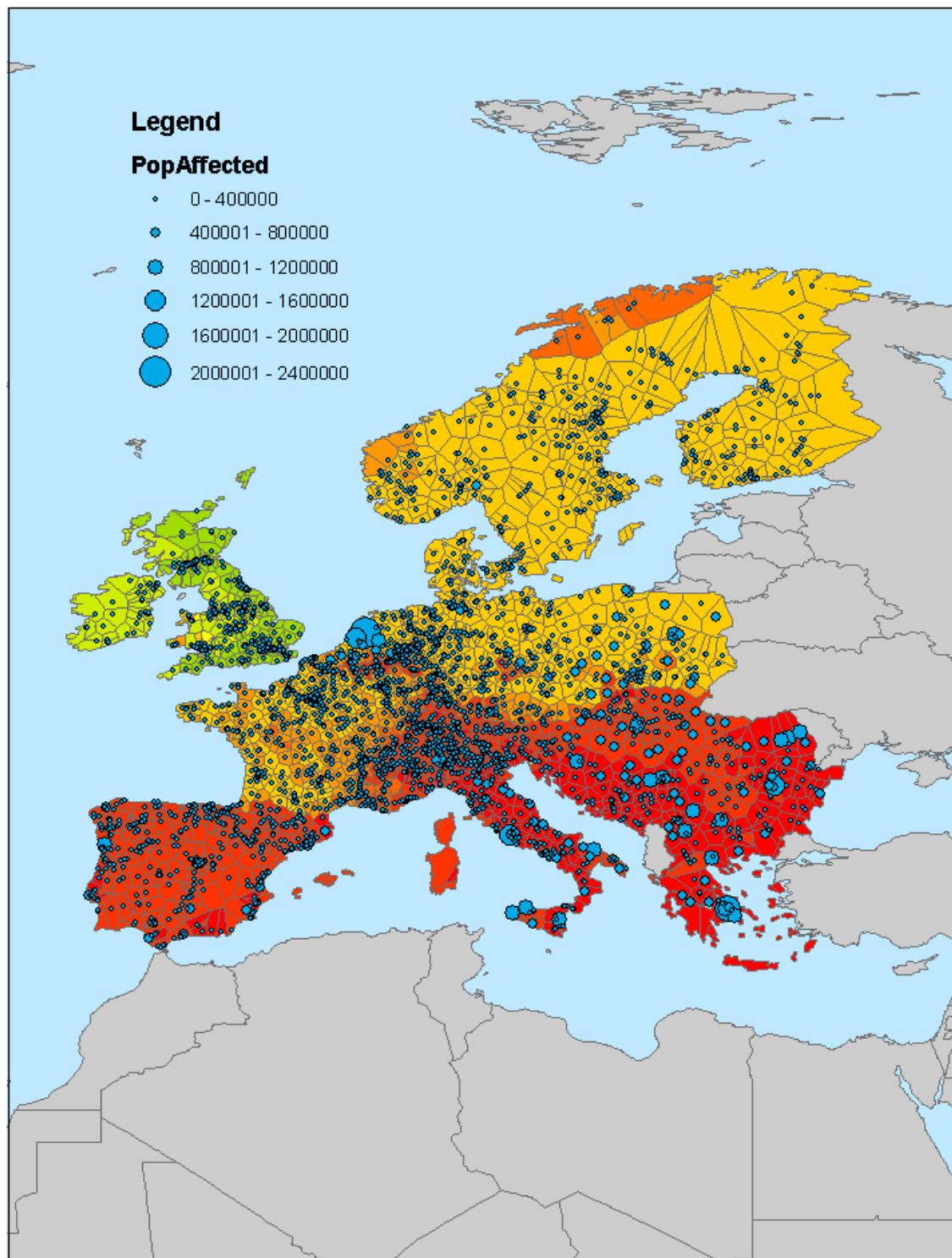
Figure 58: Affected population for the strength of coupling 100% and PGA factor 2.5.

9 Conclusions

A GIS-based probabilistic reliability model was developed in order to generate network fragility curves of spatially distributed interconnected network systems subjected to natural hazards. More specifically, we applied the concept of *structural fragility* curves to a network in such a manner that a network's vulnerability to a natural hazard can be expressed in probabilistic terms by an aggregate *network fragility* curve. The method was successfully employed to encompass the geographic distributions of both the infrastructure and the natural hazard; specifically, we analyzed the interconnected European gas and electricity transmission networks in such a manner that the gas-fired power plants form the physical connections between the two types of networks.

The network interdependency model manages to follow (in a topological sense) the propagation of failures resulting from seismic vulnerability of the gas network and how they affect the topology of the electricity network. The partial dependence of the electricity network on the gas transmission network introduces an additional (implicit) seismic vulnerability of the electricity network over and above the explicit structural seismic vulnerability of the components of the electricity network.

Network damage was measured in terms of connectivity loss, power loss and impact factor on the affected population. Damage was evaluated at both macroscopic (for the whole network) and at a local levels by examining the damage status of each and every electricity distribution substation in the electricity grid. The seismic vulnerability of gas and electricity networks having been condensed in the form of fragility curves of the independent and dependent systems is then represented geographical distributions of the damage at the European level on a GIS tool; showing, as expected that the highest direct damage in southeast Europe. However, this does not imply that the European electricity network is not vulnerable to seismic hazards, on the contrary, because the main network in Europe is one single system, it is not impossible to foresee how damage in a seismic area may propagate through the whole system far away from the original disturbance if the conditions are right. For example, recent major disruptions in the UCTE system, having starting in Germany at localised positions, propagated throughout the system far away from the original disruption source.

It is beyond the scope of assessing how the probability of failures in certain geographical locations can propagate thorough the system; so, whereas we have begun to analyse the vulnerability of the system in terms of seismic hazard, we have yet to assess the associated risk of cascading failures.

Whereas the influence of gas network on the fragility curves of the electricity network appears to relatively small (which would appear to be consistent with the moderate generation capacity of gas-fired power plants' capacity of circa 20% for Europe as a whole), we cannot conclude from our data that the apparent low vulnerability dependence of electricity on gas-fired generation is so clear cut. For example, the recent geopolitical crises between the Russia and Ukraine highlighted another coupling mechanism between the gas and electricity system, namely: the propensity of individuals to use electric heating at home if the gas supply is cut off. Such geopolitical vulnerabilities, although outside the scope of our structurally biased hazard analysis, can, in principle, be equally well studied using the same probabilistic and GIS techniques described above.

10 Bibliography

[1]   Albert R, Albert I, Nakarado GL. Structural vulnerability of the North American power grid. Physical Review E 2004; 69(2):025103, 4. DOI: 10.1103/PhysRevE.69.025103.

[2]   Ang A.H.S., Pires J., Villaverde R. (1993). Seismic reliability of electric power transmission systems. In Kussmaul (ed.).12th International Conference on Structural Mechanics in Reactor Technology. August 1993. Elsevier Publishers B.V.

[3]   Barabási A.-L., Albert R. (1999). Emergence of scaling in random networks. Science, 286:509-512.

[4]   Bono F., Work Package 2 – D2.4b Data sets containing the European energy interconnected network Revision 2.1, ManMade project Report, May, 5 2008

[5]   Buckle P., Marsh G., Smale S. Assessing Resilience & Vulnerability: Principles, Strategies & Actions Guidelines. Emergency Management Australia, May 2001.

[6]   Chen J., Kumar A.V S., Marathe A., Atkins K., Model Based Spatial Data Mining for Power Markets. Conference Paper, SIAM-DM 2006 Workshop on Spatial Data Mining.

[7]   Dorogovtsev S.N., J.F.F. Mendes. Evolution of networks.Advances in Physics (2001).

[8]   Dueñas-Osorio L., Craig J. I., Goodno B. J. (2007). Seismic response of critical interdependent networks. Earthquake Engineering & Structural Dynamics, 36 (2), Pages: 285-306.

[9]   Environmental agency of the Republic of Slovenia. http://www.arso.si.

[10]   Eurocode 8. CEN-prEN1998-1-1:2003.Design of structures for earthquake resistance. Part 1. General rules, seismic actions and rules for buildings.

[11]   FEMA. HAZUS-MH technical manual: earthquake model. Multi Hazard Loss Estimation Methodology. United States Department of Homeland Security, Federal Emergency Management Agency, Washington, DC, 2003.

[12]   Giardini D., Jimenez M.J., Grunthal G. (2003). European – Mediterranean seismic hazard map. European Seismological Commission. Internatioanal Geological Correlation Program. Project No. 382. SESAME.

[13] Giardini, D., Grünthal, G., Shedlock, K. M. and Zhang, P.: The GSHAP Global Seismic Hazard Map. In: Lee, W., Kanamori, H., Jennings, P. and Kisslinger, C. (eds.): International Handbook of Earthquake & Engineering Seismology, International Geophysics Series 81 B, Academic Press, Amsterdam, 1233-1239, 2003.

[14] LandScan™ Global Population Database. Oak Ridge, TN: Oak Ridge National Laboratory. Available at http://www.ornl.gov/landscan/

[15] LESSLOSS. Prediction of Ground Motion and Loss Scenarios for Selected Infrastructure Systems in European Urban Environments. Ed.: Faccioli E. Risk Mitigation for Earthquakes and Landslides. Report No. 2007/08.

[16] O'Rourke M, Ayala G. Pipeline damage due to wave propagation. J Geotechn Eng ASCE 1993;119(9):1490–8.

[17] O'Rourke T.D.. Critical infrastructure, interdependencies, and resilience. Bridge, NationalAcademy of Engineering, 37(1):22–29, 2007.

[18] Perrow, C. Normal accidents: Living with high risk technologies. New York: Basic Books, 1984

[19] Platts. http://www.platts.com.

[20] Rinaldi SM, Peerenboom JP, Kelly TK. Critical infrastructure interdependencies. IEEE Control Systems 2001; 21(6):11–25.

[21] Shinozuka M.,Cheng T.C., Feng M.Q., Mau S.T. (1997–1999).Seismic performance analysis of electric power systems, research progress and accomplishments. MCEER, 1999. p. 61–69.

[22] Tromans I. (2004). Behaviour of buried water supply pipelines in earthquake zones. PhD thesis. University of London.

[23] Wald, D. J., Quitoriano, V., Heaton, T. H., and Kanamori, H., 1999a. Relationships between peak ground acceleration, peak ground velocity, and modified Mercalli intensity in California, Earthquake Spectra 15, 557–564.

[24] Vanzi, I. (2000). Structural upgrading strategy for electric power networks under seismic action. Earthquake Engineering & Structural Dynamics 29(7). p:1053-1073.

[25] Watts, D.J.; Strogatz, S.H. (1998). Collective dynamics of 'small-world' networks. Nature 393 (6684): 409–10.